C.P. No. 935

C.P. No. 935

MINISTRY OF TECHNOLOGY

AERONAUTICAL RESEARCH COUNCIL

CURRENT PAPERS

Random and Systematic Factors in the Scatter of Creep Data

By

K. F A. Walles

LONDON: HER MAJESTY'S STATIONERY OFFICE
1967
PRICE 16s 0d NET

C.P. No. 935*

April, 1966

Random and Systematic Factors in the Scatter of Creep Data

-By-
K. F. A. Walles

SUMMARY

The study of scatter in creep is facilitated by using a previously developed formula to provide mean values of creep properties. Scatter can then be determined not only from the relatively few sets of tests repeated under identical conditions, but also from the far more numerous sets of tests performed under different conditions. Earlier studies suggested that scatter was, to a first approximation, distributed according to the Gaussian normal error form.

In the present study, it has been found that the distributions are often multimodal, and can be resolved into two or more component distributions each of which is Gaussian. Multimodal distributions show regularities in that, for a given composition, the standard deviation in temperature and the mean spacing in temperature between components is the same in each component distribution and in each cast.

The present study of Nimonics 80, 80A and 90, and of 18-12-Nb alloy supports the previous agreement of the formula with experimental data in finer detail and further validates the formula as a means of extrapolation. Multimodal scatter is identified as a problem of practical concern.

---

*Replaces N.G.T.E. NT.601 - A.R.C.28 326.

CONTENTS

CONTENTS (cont'd)

TABLES

APPENDICES

ILLUSTRATIONS

ILLUSTRATIONS (cont'd)

ILLUSTRATIONS (cont'd)

1.0 Introduction

A limited study of the scatter of experimental creep data was previously made[3] in order to assess the fit of a creep formula proposed by A. Graham[1,2A] and to establish the validity of the formula as a means of extrapolation on a statistical basis. This study suggested some interesting regularities and its extensions to cover a wider range of material in greater detail was undertaken. The results, summarised in Reference 36, are described in detail in the present Paper.

1.1 Creep formula

The creep formula proposed on the basis of experimental evidence and general considerations by A. Graham[1,2A] represents creep strain ε as the sum of a number of power law terms in stress σ, time t, and temperature T thus:

$$\varepsilon = C_1\sigma^{\beta_1}\phi_1^{k_1} + C_2\sigma^{\beta_2}\phi_2^{k_2} + \ldots C_r\sigma^{\beta_r}\phi_r^{k_r} \qquad \ldots.(1)$$

where the time-temperature parameter ϕ in each term takes the form*

$$\phi_r = t(T'_r - T)^{-20} \text{ when } T'_r > T$$

or

$$\phi_r = t(T - T'_r)^{20} \text{ when } T > T'$$

The exponents k and β are taken from the sequences:

$$k = \ldots\tfrac{1}{3},\ 1,\ 3,\ \ldots$$

$$\beta/k = 1,\ 2,\ 4,\ 8,\ 16\ \ldots$$

while the quantities C and T' are constants for a particular sample of material, being evaluated by fitting Equation (1) to the experimental data. From this formula, curves of log strain versus log time, log stress versus log time and log time versus temperature can readily be calculated. The formula can also be used[2] to represent rupture data. When the constants have been chosen to give the closest fit to a set of experimental data, the

*The parameter ϕ in the first form, with $T' > T$, was proposed[2] to represent the observed increases with temperature of the slope $(\partial \log t/\partial T)$ of some log time versus temperature graphs, an increase not represented by other parameters. It was convenient to use it[2A] in the second form for those other graphs whose slope decreased with temperature. In this second form it is indistinguishable in practice from the Dorn parameter $t \exp(^{-Q}/_{RT})$.

family of curves - described below as a fitted family - is considered to represent the mean properties of the material.

1.2 Previous comparison of individual sets of data with formula

In previous work, comparisons of fitted curves with experimental creep curves and their cross-plots indicated agreement to within the apparent scatter for 164 out of 178 sets of data referring to 50 different materials e.g., Nimonic alloys, stainless and low alloy steels and aluminium alloys. The remaining 14 sets are considered in Section 5.3. Much of this work was reported in Reference 2A but some of the more recent comparisons have not been reported.

For the few sets of data for which replicate tests were available a more precise indication of the agreement of the formula with results was obtained by a numerical comparison of the overall scatter of experimental points with the scatter of replicate tests. For this purpose the scatter was assumed to be Gaussian in log time and the comparison was made between the respective standard deviations. (The assumption is examined in detail in Section 2.1 below.)

The standard deviations, of which a sample is shown in Table II, agreed to within their statistical confidence limits. The comparison was extended[3,4] to tests of extrapolation, in which formula 1 was fitted to short time experimental data only and then compared with long time data. Figure 1 taken from Reference 3 is a sample of the results which show that scatter in the extrapolated region is no greater than in the directly fitted region.

In these analyses however some relatively small anomalies were noted which suggested that scatter was not simply Gaussian. For example, the scatter ogives A and C in Figure 1 appear to have a non-Gaussian tail. Such anomalies could not be effectively studied from replicate data alone, since there was too little of it. However, the agreement between the scatter determined from fitted curves and from replicate tests justified the use for this purpose of data containing no replicate tests, and so the range of materials and test conditions for which scatter could be studied was considerably increased.

1.3 Previous comparison of data from several casts of a single material with the formula - common family

Detailed comparisons between different casts of a single alloy were made possible by the observation that when Equation (1) was individually fitted to the data for different casts of any one Nimonic alloy, the fitted curves did not appear to differ significantly in shape, and it appeared possible to refer the data for all casts to a common family of fitted curves. Common families were therefore constructed by trial for all the alloys for which adequate data was readily available, namely 18-12-Nb steel, Nimonic 80, Nimonic 80A, Nimonic 90. Common families of log stress versus log time curves for rupture of the four alloys are presented in Figures 2 to 4; the corresponding families relating to the creep curves of the last three are in Figures 16 to 18 and 22 to 24.

While the common family may be considered to represent approximately the mean properties of the casts examined, no special attempt was made to find the precise mean of casts, since the family is used essentially as a datum to which each cast is separately referred. As a datum, it was expected to represent closely the trend of properties with stress and temperature, since it was generally derived from several hundred test results; as a mean of casts it had little statistical significance because of the small number (3 to 9) of casts from which results were drawn.

It appeared that the data for any one cast could be related to the corresponding common curve (whether for a component of creep or for rupture) merely by an overall displacement ΔT_c in temperature (where ΔT_c is the mean of the deviations of individual points from the common curve). The scatter about the displaced common family as measured by the standard deviation was no greater than the standard deviation about a family fitted individually to the particular set of data.

A few points were discrepant whether referred to the common or the individually fitted family, and were provisionally attributed (Reference 3 Section 5.2) to multimodal creep.

These earlier comparisons of scatter have not been presented in detail because they are largely superseded by the results of the present study, but they served to establish the common families shown in Figures 2 to 4, both as representing the mean properties of a material and as a promising basis for detailed analysis of scatter.

1.4 Scope of present Note

The present report examines the results of the previous work in greater detail by means of a detailed study of scatter and its departures from a simple Gaussian form. It considers 26 casts of the four alloys mentioned above together with a single cast of 18-12-Mo steel. Each cast of the four was compared with the appropriate common family, but for 18-12-Mo steel only the individually fitted family for the single cast was available. The study has both indicated regularities in the scatter and provided additional evidence of the agreement of the scatter from fitted curves with that from replicate tests. The agreement of formula 1 with experimental data and the validity of common families are thereby supported more closely.

2.0 Expression and analysis of scatter

In the previous studies, scatter (cf. Section 2.2) was assumed without detailed study to be both uniform in log time and distributed according to the Gaussian law. Moreover, no distinction was made between the different stages of creep. It is now appropriate to examine these assumptions in some detail.

2.1 Choice of variables

When three of the experimental variables - stress, strain, time and temperature - are specified, the deviation of experimental points from the fitted curves can be expressed in terms of the fourth variable. If the

deviation is to be uniform, the fourth variable must be chosen so that, for the widest possible range of data, its average deviation is independent of the values of the other three.

It is desirable to use a common measure for creep curves and for rupture, hence the quantities stress, time, and temperature are to be preferred to strain. A choice is also possible between the absolute deviation δx and the relative deviation $\delta x/x$ or $\delta(\log x)$. The range of stress and time is sufficiently large to reveal significant differences between absolute and relative deviations, but the range of temperature is much smaller. Hence a choice must be made between five quantities which may be denoted δt, $\delta\sigma$, δT, $\frac{\delta t}{t}$, $\frac{\delta\sigma}{\sigma}$. A cursory examination of creep data is sufficient to reject δt, since, for example, a deviation of 10 hr would be far too large for tests of 10 hr duration or less, but far too small for tests of 10,000 hr. A choice between $\delta\sigma$, $\frac{\delta t}{t}$, and $\frac{\delta\sigma}{\sigma}$ involves some study of the more extensive sets of data e.g., that in Figure 5. This data, for the creep rupture behaviour of S.590 alloy, has been fitted with a family of curves, and the deviations of individual points from the curves measured, in terms of each quantity. The data has been arbitrarily divided into five regions covering the stresses 1·1 to 4·5, 4·6 to 11·1, 11·2 to 22, 23 to 31, 32 to 45 t.s.i. In each region the algebraic sum of the deviations was substantially zero (confirming that the curves represented average properties), but the deviations averaged without regard to sign varied from one stress range to another, see inset Table in Figure 5. Inspection of the Table indicates a systematic change with stress for both $\delta\sigma$ and $\delta\sigma/\sigma$, but the variations of $\frac{\delta t}{t}$ are not systematic and are small enough to be statistically insignificant: thus the scatter in these data may be considered uniform in $\frac{\delta t}{t}$ or in $\delta(\log \text{time})$. The final choice between log time and temperature is less easily made, since according to the formula

$$\frac{\partial \log t}{\partial T} = -\frac{20}{\left[T' - T\right]} \qquad \ldots.(2)$$

and this ratio does not change rapidly unless the testing temperature T approaches T'. In the present report the set of data in Reference 25 is the only one that provides definitive evidence. In this set tests at 1000°C are only 16°C from the T': this data favours a constant deviation in temperature. None of the other sets of data deny it.

Thus in the analysis that follows, deviations in temperature are generally reported. As data for replicate tests is more immediately available in terms of log time, it has for convenience been plotted in this way. From Equation (2), since replicate tests are all at the same temperature, the ratio between deviations in log time and deviations in temperature is constant.

2.2 Resolution of creep curves

Since an experimental creep curve may lie to one side of the fitted curve at short times, cross it at some intermediate time, and lie to the other side at long times, the scatter of an experimental creep curve cannot be expressed by a single number. However, any creep curve can be represented by formula 1 which, for constant stress and temperature, reduces for the materials considered below to

$$\varepsilon - \varepsilon_0 = \left(\frac{t}{t_{\frac{1}{3}}}\right)^{\frac{1}{3}} + \left(\frac{t}{t_1}\right) + \left(\frac{t}{t_3}\right)^3 \qquad \ldots.(3)$$

Equation (3) with individually chosen values of $t_{\frac{1}{3}}$, t_1 and t_3 fits the experimental creep curves concerned with an error substantially less than the difference between repeated tests. It follows that the scatter of experimental creep curves may be adequately represented by the scatter of the quantities $t_{\frac{1}{3}}$, t_1 and t_3. Each of these quantities can be plotted against stress and temperature in the same way as rupture times, and its scatter in temperature about the fitted curve, which is the estimated mean curve, determined.

2.3 Homogeneous sets of data studied

A group of test specimens is regarded as homogeneous when there is no known difference, prior to testing, between them. Groups in which some specimens had a markedly different heat treatment from others, or in which specimens were from different casts, or from significantly different locations in a cast or forging, were not considered homogeneous in the present analysis.

The scatter values obtained from a homogeneous group of specimens for any one of the quantities $t_{\frac{1}{3}}$, t_1, t_3 or rupture time are regarded as a homogeneous set of values characteristic of the cast from which the specimens were taken. Homogeneous sets that were sufficiently extensive to be statistically significant have been analysed in the manner of Sections 2.4 and 2.5 below.

The number of casts studied was 1 of 18-12-Mo steel, 4 of 18-12-Nb steel, 4 of Nimonic 80, 8 of Nimonic 80A and 10 of Nimonic 90, a total of 27.* For the first two materials only rupture data were available. For the latter three, 9 casts provided either creep families or rupture data and the remaining 13 provided both. In principle each family of creep curves would be expected to provide three sets of scatter data, one for each of the quantities $t_{\frac{1}{3}}$, t_1 and t_3 in Equation (3); however 3 families were so small that they defined only t_3, and 1 family defined only $t_{\frac{1}{3}}$ and t_3. For one cast[28,29] two families of creep curves were available from independent tests at two laboratories. Thus the 27 casts provided 74 independent homogeneous sets of scatter data.

2.4 Graphical presentation of the distribution of scatter within a homogeneous set

Deviations of individual points from the datum curves of a common family (cf. Section 1.3) may be summarised in a graph of frequency of

*The data quoted for these materials, and particularly for Nimonic 80A and and Nimonic 90, is old and of significantly lower order than that of current production.

occurrence of deviation versus magnitude of deviation in the form of a histogram Figure 6A in which the scale of deviation is divided into intervals of arbitrary width, and all values within an interval are represented by a single ordinate of frequency.

An alternative presentation is a graph of cumulative frequency against deviation in the form of an ogive Figure 6B which is effectively the integral of the histogram. It is however convenient for subsequent calculations to use arithmetic probability scales e.g., in Figure 6C, upon which a Gaussian distribution is represented by a straight line whose slope is proportional to the standard deviation. In the particular application of this method here used (Appendix II), it is not necessary to divide the data into intervals, since each point on the ogive can be plotted at its observed deviation. The method is more efficient for small samples of data.

2.5 Method of analysing the scatter distribution within a homogeneous set

Examination of the histograms for individual homogeneous sets showed that some sets e.g., that in Figure 6A had only a single most probable value or "mode", with the frequency diminishing on either side, and that the histograms could be represented by the Gaussian "normal error" distribution. Other sets (e.g., that of Figure 7A) clearly had two "modes", and appeared to be composed of two Gaussian distributions superposed. The remaining sets (e.g., Figure 8A) were too irregular, or formed too small a sample, for the nature of the distribution to be clear from the histogram.

Examination of graphs like Figure 6C suggested a general method (Appendix II) of analysing multimodal distributions. When this method was applied to distributions like that of Figure 8A it resolved them into two or more components, each represented on the graph by a straight line i.e., each component was of Gaussian form. When the method was applied to ogives Figure 6C and 7B corresponding to the definitive histograms Figure 6A and 7A, it resolved the distributions into one and two straight lines respectively, in agreement with the indications of the histograms. In view of this agreement, and the greater resolving power of analysis based on the ogive, the method of Appendix II has been adopted for all subsequent analysis.

2.6 Common value of standard deviation for a single homogeneous set

Of the 74 sets of scatter data plotted in the manner of Section 2.4, 21 could be fitted by a single straight line as in Figure 6C indicating that only one Gaussian distribution was present. Of the remaining 53, 9 sets were found to be sufficiently extensive to distinguish lines corresponding to the component distributions of multimodal scatter and also to define the slopes of at least two of the lines as in Figure 7B. For 8 of these 9 the slopes were the same and for the ninth the apparent difference in slope between its two components did not prove to be significant (cf. Section 4.3.1, Table VII). In each of the remaining 44 smaller sets, only one of the component distributions contained enough observations to establish a

slope, but the slope was accepted by the points for the remaining component or components of the set.

Thus, for each set of data, whether for rupture or for the $t_{\frac{1}{3}}$, t_1 or t_3 component of creep in any one of the 27 casts examined, the standard deviations of all components appeared to be the same.

Each of the terms in Equation (3) was assumed to have a different standard deviation, as also was the time to rupture: the separate values are conveniently denoted $S_{\frac{1}{3}}$, S_1, S_3 and S_r. Observed values of these quantities given in Tables IV to VIII, range from 1·4°C to 24°C.

2.7 Deviations of each mode of a distribution

For a unimodal set of data compared with its own best fitting curves, the deviation of the mode is, by definition, zero. When the same data are referred to the common family as a datum, the deviation is not zero but takes the value ΔT_c as in Section 1.3, where ΔT_c is regarded as a constant specific to the cast. For a multimodal set of data the deviation of each mode from the common family depends upon the scatter distribution as well as the cast; it is denoted by ΔT_d.

The values of ΔT_d are readily obtained from the lines for individual components of the ogive: e.g., in Figure 7B.

3.0 Further regularities observed in scatter, illustrated from rupture data

The following Sections 3.1 and 3.2 illustrate from rupture data the regularities observed cf. Sections 4.0 to 4.5 in the data as a whole. The illustration in Section 3.2 is confined to 18-12-Nb steel.

3.1 Regular relations between different casts of a single alloy

Cast to cast regularities have been found in data for the four alloys 18-12-Nb steel, Nimonic 80, Nimonic 80A and Nimonic 90. Although the discussion that follows is limited for convenience to rupture data, similar regularities occur in creep families where indeed they were first observed.

The data for each cast were separately compared with the appropriate common family (cf. Section 1.3) and their scatter about this family analysed after the manner of Section 2.5. The analysis provided both the common value of standard deviation S_r (cf. Section 2.6) and the displacement ΔT_d (Section 2.7) of the mean of each distribution from the common family. The data for 18-12-Nb is presented in Figure 9 and Tables III, IV.

The values of s.d. and spacing presented in Table III were indistinguishable from those obtained by referring each of the three casts to an individually-fitted family. For the fourth cast, references to the common family gave larger values of s.d. and the cast has therefore been referred (cf. Table IV) to its own individually-fitted family. The difference

between the fourth cast and the other three is attributed in Section 4.1 to a large difference in heat treatment that was observed[10] to change both metallographic structure and creep properties.

In the three Nimonic alloys the heat treatment variations were less marked, and all sets for each could be satisfactorily referred to their common family (see Sections 4.2 and 4.3).

For each of the four alloys, Tables III and V show that the different casts had the same spacing between the component distribution to within the estimated confidence limits. The standard deviations S_r of Nimonics 80A and 90 varied systematically cf. Figure 10 with date of testing (e.g., for Nimonic 90 from 5·8 ±1·1°C in 1951 to 1·4 ±0·1°C in 1963), but corresponding evidence for 18-12-Nb steel and Nimonic 80 was not available because the several casts were tested at about the same time. At any one time the s.d. does not seem to vary between one cast and another, or between one testing laboratory and another.

Some of the values of S_r relate to unimodal data (denoted U in Figure 10) others to multimodal (M) data - it is apparent that both fit the same curve to within the confidence limits. The relative numbers of test specimens falling into one distribution rather than another appeared to vary from cast to cast, but different casts were tested under somewhat different stresses and temperatures. Since (cf. Section 3.2) the relative numbers also vary with stress and temperature, the limited data available was not sufficient to establish that the variation would still occur if different casts had been tested under the same conditions.

3.2 Effect of stress and temperature on scatter

Where as in Figure 9 the several component distributions barely overlap, each individual point can be assigned with reasonable confidence to one distribution or another. Experimental points in the log stress versus log time graph can be coded to indicate to which distribution they belong. For example, in Figure 11, which presents the rupture data analysed at the top of Figure 9, experimental points falling into the low-temperature component-distribution of Figure 9 are denoted by filled circles, those in the intermediate component by half-filled, and those in the high temperature component by open circles.

Figure 11 which relates to 18-12-Nb steel shows rather clearly an effect which can also be discerned (Sections 4.2.2 and 4.3.2) in the other alloys. The proportion of low, medium and high points varies with stress and temperature: in particular, points for the low temperature component occupy a wedge-shaped region around 10 t.s.i., with points for the high temperature component around its boundary.

For any one component, the displacement of individual points from the family of curves does not vary systematically with either stress or temperature, as is readily seen by inspection of the intermediate temperature points whose mean displacement is almost zero: these half-filled points are seen to scatter randomly about the curves. The absence of any systematic trend with stress or temperature within a component is further evidence of the validity of the common family.

4.0 More extensive analysis of results

This section continues the discussion of Section 3.0 on rupture data in greater detail, and extends it to the corresponding features of creep data. Specific features shown by individual alloys and casts are briefly discussed.

4.1 Four sets of rupture data for a British 18-12-Nb steel

Of four sets of rupture data[7,8,9] each referring to a single sample of material, it was found that three could be referred (Figures 11, 13 and 14) to the single common family of Figure 2.

As indicated in Section 3.1, the three sets show the typical regularities of a group, namely a common family (Figure 2), common s.d., and common spacing between the distributions (see Figures 11A, 13A and 14A): the only difference between them was in the relative numbers of results in the three distributions (see Table III, Column 2). The scatter of the fourth set of data about the common family (5·9°C) was significantly greater than the average for the three (3·2°C), moreover the individual deviations varied systematically with stress (contrast Section 3.2). Since the set deviated systematically from the common family it was provided with an individually-fitted family in Figure 15. Comparison with the common family (shown as broken lines in Figure 15) shows at any one temperature a difference in the average slope of the log stress versus log time curve. The scatter of the fourth set about its own best-fitting curves, appeared (see Table IV, Figure 15A) to have the same standard deviation and the same spacing between distributions as the scatter of the other three sets about the common family.

A discussion of the data in Reference 10 indicates that this fourth set, which refers to material cut from a steam pipe rather than from superheater tube or bar, had effectively a different heat treatment to the other three, and showed a lower ductility in creep and a different distribution of niobium carbide precipitates.

4.1.1 Distribution of multiple modes over stress and temperature in three of the four sets

The previous discussion of Section 3.2 indicates that multimodal creep in the data of Reference 7 tends to occur in a particular range of stress and temperature, namely in a wedge-shaped region around 10 t.s.i. (see Figure 11). Comparison with mean ductility values for the alloy obtained from Reference 11 and transferred to Figure 11 as broken lines suggested a close correspondence between the region of low (<6 per cent) ductility and that of multimodal creep.

The remaining two of the three sets of data are plotted in Figures 13 and 14, in which the curves are again from the common family of Figure 2. The number of points is too few for detailed analysis, but inspection suggests that multi-valued creep is distributed in the same general pattern as Figure 11 but at somewhat different stresses, suggesting that the stress

for multi-valued creep (unlike the several quantities common to the casts, Section 4.1 above) is affected by cast to cast variations. Thus the chance of a test result falling into a long or short-time distribution varies markedly with stress, to some extent with temperature and apparently also with the cast.

4.2 Creep and rupture data for Nimonic 80 and Nimonic 80A

For Nimonic 80 (Table VI) four sets of creep curves and two sets of rupture times, and for Nimonic 80A (Table VII) seven sets of creep curves and five sets of rupture times, were available. Three of the seven sets[18,19,20] are of limited extent and do not define the quantities $t_{\frac{1}{3}}$ and t_1 sufficiently for analysis; and one[16] has such a small contribution from the second term in Equation (3) that the quantity t_1 is insufficiently defined.

The two alloys were found to have features in common, and are conveniently considered together. Thus all casts from both alloys can be referred with appropriate displacements ΔT_d to the same common families, Figures 16 to 19. Figures 16 to 18 are graphs of stress versus the creep-curve quantities $t_{\frac{1}{3}}$, t_1 and t_3, Figure 19 is a graph of stress versus rupture times, the curves being repeated from Figure 3. The points in these Figures refer to a typical single cast of Nimonic 80 (data from Reference 13). The distribution of scatter in temperature of the points for this cast about these common graphs is given in Figure 20. The scatter analysis for all twelve casts is summarised in Tables VI and VII and is represented diagrammatically in Figure 21. The Tables indicate, for each of the quantities $t_{\frac{1}{3}}$, t_1 and t_3, the number of tests in each distribution, the standard deviation $S_{\frac{1}{3}}$, S_1, S_3 or S_r (as defined in Section 2.6), and the observed value of ΔT_d. Confidence limits, calculated by dividing the standard deviation by the square root of the number of tests, are given for S_r, ΔT_d, and for the spacing which is the difference of the ΔT_d values.

For these two alloys the $S_{\frac{1}{3}}$, S_1 and S_3 do not change significantly with date of testing (cf. Table VI) and they have therefore been separately averaged for each alloy. Similarly, the spacings do not change systematically with date of testing, and these also have been averaged. If the two alloys are compared, each of the quantities S_1 and S_3 are seen to be common to both to within the confidence limits (as also cf. Table V is the S_r for rupture), but the $S_{\frac{1}{3}}$ of $4{\cdot}5 \pm 0{\cdot}5^{\circ}C$ for Nimonic 80 is significantly less than that of $11{\cdot}6 \pm 0{\cdot}9^{\circ}C$ for Nimonic 80A. Comparison of spacings for the two alloys suggests no significant difference for t_1, t_3 and t_r, but the spacing in the $t_{\frac{1}{3}}$ term for Nimonic 80A is twice that for Nimonic 80.

Values of spacing occur of about twice the mean (e.g., for the t_3 term of References 19 and 22 in Table VII): it appears reasonable to attribute these to the absence of an intermediate distribution.

The main difference between the alloys is that the individual values of ΔT_d are in general, negative for casts of Nimonic 80, and positive for Nimonic 80A, in agreement with the ability of Nimonic 80A to bear a given stress at a higher temperature than Nimonic 80.

4.2.1 Details of individual casts

For the four casts of Nimonic 80 none of the 14 individual values of s.d. or 15 values of spacing deviated from the mean by more than their 95 per cent confidence limits, and most were within the 64 per cent confidence limits: it thus appears that the four casts had both common values of $S_{\frac{1}{3}}$, S_1, S_3 and S_r and common values of the corresponding spacings.

For Nimonic 80A however, one value of standard deviation for the t_3 term (S_3 = 11·2 ±1·3) fell above the 99·99 per cent confidence limits and one (S_3 = 2·3 ±0·4) fell below them. The former set of data refers to sheet material. The larger scatter of this sheet data may correspond to an early stage in sheet manufacture, since a subsequent set of sheet data[23] has a normal value of s.d., namely 4·4 ±0·9°C; no reason can be offered for the low s.d. and low value of spacing in the bar data of Reference 17.

As in Section 3.1 no significant difference is found between the standard deviation of a unimodal set and an individual distribution of a multimodal set.

4.2.2 Distribution of multiple modes over stress and temperature

No single set of bar data for Nimonics 80 and 80A (nor cf. Section 4.3.2 for Nimonic 90) defines a region of multimodal behaviour as clearly as the set of data for 18-12-Nb steel in Figure 11. The available rupture data for Nimonics 80 and 80A bar has therefore been aggregated in Figure 30, and compared with the common graph. Each cast is identified by a tag while the three distributions are identified, as in Figure 11, by filled circles for the low ΔT_d, half-filled for the medium ΔT_d, and open for the high ΔT_d distribution. Since in Table V no more than two distributions were present in each sample of bar material (contrast Table IV), the most numerous distribution has been taken as the medium ΔT_d distribution.

The displacement ΔT_d is a function of cast as well as of distribution. If attention is given to the proportion of points that are either filled or open this is seen to be greatest in the region between 16 and 28 t.s.i. at temperatures between 600 and 700°C i.e., a similar stress range but a lower temperature to the region observed (Section 4.3.2) in Nimonic 90. The distribution of multiple values in the two sets of sheet data is more complex and cannot be fully resolved from the evidence at present available, and so it has not been reported here.

4.3 Creep and rupture data for Nimonic 90

Most of the discussion of Section 4.2 above applies also to Nimonic 90, for which nine sets of rupture data and ten sets of creep curves were considered. The common graphs are presented in Figures 22 to 25, the experimental points referring to the data of Reference 27. The scatter data for this cast is shown in Figure 26; the scatter of all 11 casts is summarised in Figure 27. The $S_{\frac{1}{3}}$, S_1 and S_3 decrease systematically with date of testing (see Table VIII and Figure 28). With two exceptions noted in Sections 4.3.1 the s.d. of the various casts whether unimodal or

multimodal do not deviate by more than the 95 per cent confidence limit from the line of s.d. versus date of testing in Figure 28; similarly the spacings deviate no further from their respective means. The mean values of spacing are significantly different from those for Nimonics 80 and 80A.

4.3.1 Details of individual casts

Deviations beyond the 95 per cent confidence limit occurred only in the t_1 and t_3 terms for a set of sheet data[34] to which the remarks of Section 4.2.1 apply. Unimodal and multimodal sets have, cf. Sections 4.1 and 4.2.1, similar values of standard deviation. One set (from Reference 22) appeared to have different values of standard deviation for its two $t_{\frac{1}{3}}$ components, namely 13°C and 9·5°C, but (cf. Table VII) the statistical uncertainty of 2°C on each is sufficient to account for the apparent difference.

4.3.2 Distribution of multiple modes over stress and temperature

The available rupture data for Nimonic 90 covering the five different casts of bar material which were tested at a range of stress and temperature has been aggregated in Figure 29, and compared with the common graph as in Section 4.2.2. Since each cast has its own overall displacement, it may happen that, for example, the short-time distribution of one cast overlaps the medium time distribution of another. However, if the overall displacement ΔT_d of each cast is disregarded, it is seen that short and long-time points tend to occur together mainly between 20 and 30 t.s.i. and around 700°C; a few long-time points also occur amongst the medium time points at times in excess of 7000 hr. The concentration around 700°C may correspond to the region of low ductility.

Similar graphs have been constructed for the quantities $t_{\frac{1}{3}}$, t_1 and t_3, and multimodal creep appears to predominate in particular regions of stress, but no correlation has been found with ductility. The graphs have not been presented.

4.4 Single extensive set of rupture data for 18-12-Mo steel

The largest available set of data upon a single sample of material, that of Reference 6, comprises groups of six repeated tests at twenty-two different stresses distributed over three temperatures; no other set had substantial numbers of both repeated tests and tests at different conditions on the same sample. The scatter of this data was analysed by its authors using standard techniques of determining the mean of each group and its variance, and combining the variances for the several groups at each testing temperature. They reported the scatter in log time as being 0·050 and 0·048 at 1500 and 1300°F (815°C and 704°C) respectively, but 0·174 at 1100°F (593°C).

The present author re-analysed the data by the procedure of Section 4.1 above, namely by fitting log stress versus log time curves to the data and determining the scatter about the curves. For convenience of comparison the measure chosen was log time. The ogives (Figure 12A) at 1500 and 1300°F were bimodal, each having one major and one minor mode; the

standard deviations S_r of 0·052 ±0·008 and 0·040 ±0·006 correspond closely to the directly determined values of 0·050 and 0·048. This result suggests that the mean values from the fitted formula correspond very closely to directly determined mean values.

At the third temperature of 1100°F analysis (see worked example in Appendix II) of the ogive Figure 12C suggested three major and two minor modes. The standard deviation 0·052 ±0·010 of the component distributions at 1100°F in Figure 12B is indistinguishable from that at 1300 and 1500°F, so that the apparently anomalous s.d. at 1100°F can be attributed to markedly multimodal creep. The distribution of experimental points between the major distributions is indicated in Figure 12 (the minor modes have been ignored because the few results involved might have been due to experimental variations); it appears that values at 1500 and 1300°F are essentially unimodal and fall into distribution A with mean deviations substantially zero (i.e., the points fall evenly on either side of the calculated curve) but those at 1100°F are only unimodal at the lowest stress where they fall into distribution A. At the next four higher stresses a substantial number of values fall into distribution B and C, which are displaced towards shorter times. At the highest stress most values again fall into distribution A.

5.0 Discussion

5.1 Comparison with previous analyses

Tables IX, X and XI offer a comparison between the results of analysis of data according to the present principles with overall analyses in the manner of References 3 and 4, i.e., without resolution of multimodal distributions into components. Comparison is made between the common values S of s.d. (defined in Section 2.6) and the overall s.d. denoted S', and between the component displacements ΔT_d and the overall displacements ΔT_c.

The overall distributions are not in general of Gaussian form, and hence the estimated value of the overall s.d. depends somewhat on the method of estimation. The values previously taken in References 3 and 4 are approximately equivalent to those obtained by setting a straight line through the unresolved scatter ogive (e.g., the broken line in Figure 8B) and from it reading off a standard deviation. This method has been used to provide values of overall s.d. in the Tables.

The S' for multimodal sets of data are seen to be significantly greater than the S. In Tables IX, X and XI the S and S' have been separately averaged for unimodal and multimodal sets whenever both are available and it will be observed (cf. Sections 3.1, 5.2.1 above) that while unimodal and multimodal values of S do not differ significantly, the multimodal S' is about twice the unimodal S'.

A further comparison is made in Figure 31, in which S' has been plotted against date of testing for Nimonic 80A and Nimonic 90 rupture. It is particularly apparent for Nimonic 90 that multimodal values of S', unlike those of S, lie considerably above the line through the unimodal values, (contrast Figure 31 with Figure 10).

Comparison between the displacements ΔT_d of individual distributions and the overall displacement ΔT_c from the common family in Tables IX to XI indicates that while in general none of the ΔT_d are exactly equivalent to the ΔT_c unless the cast is unimodal, the ΔT_d for the most frequently occurring distribution is usually approximately equivalent to the ΔT_c.

The regularities of standard deviation and spacing which appear only after the data has been resolved into its component distributions provide considerable support for the validity of the resolution.

The regular relations between S for different casts of the same alloy make possible a more precise comparison of the scatter of replicate and non-replicate tests. In previous work (e.g., Reference 3) comparisons could only be made within a single cast, and the number of replicate tests available for a cast that had also been tested over a range of temperatures was small. Thus cf. Table IIB the largest number of replicate tests for a cast of Nimonic 90 was 8 - the total for three casts being only 16 - and the statistical uncertainty in the s.d. (S') for replicate data was therefore relatively large, with 64 per cent confidence limits of 8 $\pm 2^{\circ}C$.

The data from References 33 and 35 contains large numbers (40 and 200) of replicate tests, which establish the replicate scatter closely (S_r = 2·1 $\pm 0{\cdot}3^{\circ}C$ and S_r = 1·4 $\pm 0{\cdot}1^{\circ}C$) while other sets of data contain many tests at different stresses and temperatures which closely establish the scatter about the fitted family. The replicate scatter of one cast, and the scatter about the family of another is indicated by Figures 10, 28 to agree to within the rather small statistical uncertainty. This agreement suggests that any departure of the fitted families from the "true" mean properties of the alloy is significantly smaller than the uncertainty of a single test: in the largest and most reproducible sets of data, the departure appears on average to be less than $1^{\circ}C$.

The only set of data (that of Section 4.4) for which adequate numbers of both replicate tests and tests at different conditions are available on the same casts also indicates a close agreement between replicate and fitted scatter and directly supports the formula to the same degree of precision.

5.2 Possible further regularities

Some possible further regularities in the differences between the ΔT_d are suggested by the data for Nimonics 80 and 80A in Tables VI, VII and for Nimonic 90 in Table VIII. Thus for Nimonic 80A the mean spacings of the $t_{\frac{1}{3}}$ and t_1 terms (11·6 $\pm 0{\cdot}9$ and 13 $\pm 1{\cdot}2$ respectively) do not differ significantly; nor comparing Table VII with Table V do the spacings for t_3 and for rupture times. The Nimonic 80 data is similar except that the t_1 spacing appears twice the $t_{\frac{1}{3}}$ spacing. The data for each of these two alloys suggest one "quantum" of spacing for $t_{\frac{1}{3}}$ and t_1 terms, and another for t_3 and rupture. For Nimonic 90 the $t_{\frac{1}{3}}$ spacings of Reference 29 appear anomalously high, and of References 33 and 34 anomalously low: all but the last can however be accounted for by a "quantum" of $38^{\circ}C$, and this is in close agreement with the spacing of the t_1 term. Similarly the t_3 and rupture times might accept a quantum of about $10^{\circ}C$ for their spacing.

The evidence thus suggests the possibility of further regularities in the scatter of experimental data, but is not adequate to establish them.

5.3 Apparently discrepant data

The 14 sets of data to which Equation (1) could not be directly applied included several sets tested over such a wide range of temperature that metallurgical changes are either known to occur (*e.g.*, from ferrite to austenite in FV.448 around 800°C) or may be suspected. All 14 sets of data could be fitted up to the stage of log time versus temperature crossplots, but one of the crossplots showed either a discontinuity or a change of slope at some critical temperature. Thus *e.g.*, for FV.448 data covering a range of 500 to 1000°C the rupture crossplot for slope $-\frac{1}{4}$ had a marked discontinuity at 800°C, with an entirely different value of C and T' above the discontinuity to that below it. There was apparently no discontinuity in the other crossplots.

In all 14 sets, if the data were divided into parts at the discontinuity, each of the parts could be fitted to within the estimated scatter by the formula.

It is possible that the discontinuities involving change of C and T' may be multimodal creep in a more extreme form, but data presently available appears inadequate to confirm or deny the possibility.

5.4 Summary of results

For the four alloys 18-12-Nb, Nimonic 80, Nimonic 80A and Nimonic 90 the agreement of Equation (1) with experimental data has been confirmed to within the confidence limits of the present scatter analysis; for the best sets of rupture data, these limits do not exceed ±1°C. The validity of common families has been confirmed to the same degree of accuracy - the only cast (one of 18-12-Nb) for which a common family was not appropriate was one which had been given a markedly different heat-treatment to the others. Scatter has been evaluated, and the form of its distribution shown to be basically Gaussian, but generally with more than one mode. Resolution has been made of multimodal distributions into their components. The quantities defining the scatter have displayed regularities, in that to within confidence limits the standard deviation of a component distribution appears to be common both to all distributions in a cast and, at any one time, to all casts of an alloy, (it tends to diminish from earlier to later casts presumably as the alloy is developed); also the spacing between distributions is common to all distributions and all casts. The regularities apply equally to rupture data and to the three terms of Equation (3) into which families of creep curves may be resolved.

Hence the common family, and the spacing between distributions, appear to be properties of the alloy, and the standard deviation to be typical of the alloy at a particular date; the deviation ΔT_d of a particular cast from the common family is a specific property of the cast. The relative number of tests falling into one distribution rather than another varies with stress and temperature; there appear to be certain regions of stress and temperature where multimodal creep is common, others where it is

not. The limited information available suggests that regions of multimodal creep correspond to regions of low ductility and of unsatisfactory behaviour in service. The relative numbers appear to vary from cast to cast. Apart from this connection of multimodality (with both unusually long, and unusually short, rupture times) with ductility troughs, no clear correlation was found between the time to rupture and the strain at rupture.

Although supporting evidence for other alloys would be desirable, it appears probable that the creep properties of an alloy could be economically established by testing a single cast over a wide range of stress and temperature, thus establishing a representative family of curves, followed by determination of the mean displacement ΔT_d for individual casts by a few tests of short duration. The tests that establish the family should also establish the current standard deviation and the spacing between distributions, together with the presence and probable location of multimodal creep regions. They generally need not extend to the same length as the service life, since it would appear[3] that an adequate defined set of creep data can be extrapolated without significant error by up to 10/1 in time. The mean properties of any one cast are then obtained by displacing the representative family by the amount ΔT_d.

If design stresses fall outside any multimodal regions, the displaced representative family and the standard deviation may be used to calculate stresses and temperatures for a given chance of failure: if however they fall within such regions, not only must the mean properties be referred to the lowest-temperature distribution, but also a risk of premature failure should be allowed for.

6.0 Conclusion

The regularities observed in the scatter of creep and creep-rupture data have proved amenable to an analysis similar to that previously used to estimate mean properties. The previously derived creep formula is found to represent mean creep properties for Nimonics 80, 80A and 90, and for 18-12-Nb steel, to well within the statistical uncertainty of a single test. Its use for extrapolation has been supported to within uncertainties of similar magnitude. Analysis by means of the formula has been shown to provide reliable values of standard deviation without replicate tests and to indicate the presence or absence of multimodal creep. It is apparent that the individual properties of several casts of any one of these alloys could have been determined by extensive tests on a single cast to establish the common family, together with brief calibration tests on each of the others to determine its individual displacement, ΔT_d. Limited studies of other Nimonic alloys suggest that common families may be equally valid for these also, and there is no apparent reason why such families should not be used for stainless and low steels when the compositions and heat treatments are adequately controlled.

For alloys for which common families prove valid, it appears that design information can be obtained, with only a moderate testing effort, in sufficient detail to specify the entire course of the creep curve and its scatter and thus provide a basis for detailed mechanical design.

It is hoped that this study of creep data and its regularities may also provide some guidance to the alloy developer.

REFERENCES

No.	Author(s)	Title, etc.
1	A. Graham	Phenomenological theories of creep "The Engineer" 8th and 15th February, 1952.
2	A. Graham	Regularities in creep and hot-fatigue data, Part I, A.R.C. Current Paper - CP.379, December, 1956.
2A	K. F. A. Walles A. Graham	Regularities in creep and hot-fatigue data, Part II, A.R.C. Current Paper - CP.380, December, 1956.
3	K. F. A. Walles A. Graham	On the extrapolation and scatter of creep data, A.R.C. Current Paper - CP.680, 1961.
4	K. F. A. Walles A. Graham	An analysis of data from the 1960 Dusseldorf Conference on creep and of related data. Unpublished work at N.G.T.E.
5	N. J. Grant A. G. Bucklin	On the extrapolation of short-time stress rupture data Trans. A.S.M. Vol. 42, p.720, 1950.
6	F. Garofalo R. W. Whitmore W. F. Domis F. von Gemmingen	Creep and creep rupture relationship in an austenitic stainless steel Trans. Met. Soc., AIME Vol. 221, p.310 April, 1961.
7	H. W. Kirkby R. J. Truman	Further data on the elevated temperature behaviour of 18-8-Nb type austenitic steel. Paper presented at Dusseldorf Conference 1960.
8	K. L. Irvine J. D. Murray F. B. Pickering	The effect of heat-treatment and microstructure on the high temperature ductility of 18-Cr-12-Ni-1Nb steels. Journal Iron and Steel Inst. October, 1960.
9	E. A. Jenkinson M. F. Day A. I. Smith L. M. T. Hopkin	The long-term creep properties of an 18-Cr-12-Ni-1Nb steel steam pipe and superheater tube. Journal Iron and Steel Inst., p.1011. December, 1962.

REFERENCES (cont'd)

No.	Author(s)	Title, etc.
10	R. J. Truman	Discussion, Structural processes in creep p.348 Symposium of Iron and Steel Institute and the Institute of Metals, London May, 1961
11	W. H. Bailey N. G. Gemmill H. W. Kirkby J. D. Murray E. A. Jenkinson A. I. Smith	Creep properties of austenitic nickel chromium steels containing niobium Proc.I.Mech.E. Vol. 171, 1957, p.911
12	National Physical Laboratory	Creep data on an early heat OKW of Nimonic 80 Private communication
13	R. W. Ridley G. R. Tremain	A summary of the creep and fatigue properties of a supply of Nimonic 80 at 600, 650, 700 and 750°C N.P.L. Engineering Division No. 471/50
14	International Nickel (Mond)	Creep data upon heat MRL of Nimonic 80. Private communication
15	K. F. A. Walles A. Graham	Unpublished M.O.A. Report.
16	R. W. Ridley B. S. W. Mann G. R. Tremain	The creep properties of Nimonic 80A at 700, 750 and 815°C and the fatigue properties at 750°C for periods up to 2000 hours N.P.L. Engineering Division No. 477/51
17	International Nickel (Mond)	Creep data upon heat Z88 of Nimonic 80A. Private communication
18	International Nickel (Mond)	Creep data upon a heat MRM of Nimonic 80A. Private communication
19	International Nickel (Mond)	Creep data upon a heat MRP of Nimonic 80A. Private communication
20	International Nickel (Mond)	Creep data upon a heat MRS of Nimonic 80A. Private communication
21	E. G. Webster	Replicate rupture tests on Nimonic 80A. Private communication

REFERENCES (cont'd)

No.	Author(s)	Title, etc.
22	A. K. Cruden W. A. Potter	The creep properties of Nimonic 80 in sheet form. Joseph Lucas Research Laboratories. Report No. B45,929, 1960
23	Joseph Lucas Research Laboratories	Creep properties of another sample of Nimonic 80. Private communication
24	R. W. Ridley B. S. W. Mann G. R. Tremain	The creep and fatigue properties of Nimonic 90 at 700, 750 and 815°C N.P.L. high temperature mechanical properties section HT.3/51
25	R. W. Ridley	The creep properties of Nimonic 90 bar material at 850, 900, 950 and 1000°C for periods up to 1000 hours N.P.L. high temperature mechanical properties section HT.35/53
26	International Nickel (Mond)	Creep data upon heat NFH of Nimonic 90. Private communication
27	International Nickel (Mond)	Creep data upon heat NFK of Nimonic 90. Private communication
28	International Nickel (Mond)	Creep data upon heat ABDA of Nimonic 90. Private communication
29	K. F. A. Walles B. Bonner	Unpublished M.O.A. Report.
30	Bristol Aero-Engines	Unpublished data upon Nimonic 90
31	A. Graham G. J. Bates	An analysis of the scatter in creep of an alloy of Nimonic 90 type N.G.T.E. Report No. R.231. A.R.C.21 108 March, 1959
32	E. G. Webster	Replicate rupture tests on Nimonic 90. Private communication
33	E. G. Webster	Creep tests on Nimonic 90 material A.I.D. Test Report No. M.3127
34	A. K. Cruden W. A. Potter	The creep properties of Nimonic 90 in sheet form Joseph Lucas Research Laboratories Report No. B.45,964, 1960

REFERENCES (cont'd)

No.	Author(s)	Title, etc.
35		Repeated rupture tests on Nimonic 90 Private communication
36	K. F. A. Walles	Random and systematic factors in the scatter of creep data. N.G.T.E. Report No. R.280. July, 1966.

TABLE I

Creep and rupture data fitted by formula in present report

Alloy	No. of sets fitted	Typical composition - main constituents											
		Fe	Ni	Cr	Co	Ti	Aℓ	Cu	Mo	Nb	C	Mn	Other
Nimonic 80	2	0.4	76	20	-	2.5	0.6	-	-	-	0.05	0.5	-
Nimonic 80A	5	0.3	77	19	-	2.4	1.2	-	-	-	0.08	0.5	-
Nimonic 90	8	0.4	56	20	20	2.5	1.2	-	-	-	0.05	0.3	-
Red Fox 36	1	67	12	18	-	-	-	-	-	1	0.10	2.0	-
18-12-Nb	4	69	12	18	-	-	-	-	-	1	0.1	-	-
18-8	1	73	9	18	-	-	-	-	-	-	0.06	0.5	-
18-12-Mo	1	64	12	18	-	-	-	-	2	-	-	2	-
S816	1	3	20	20	44	3.0	-	-	4	4	0.4	1.5	W = 3.8
S590	1	25	20	21	19	-	-	-	4	4	0.4	1.5	W = 4

TABLE II

Scatter about mean curves compared with scatter of replicate tests
Scatter data from Reference 3

Standard deviations in log time except where otherwise indicated

(a) creep rupture

Material		Number of pairs of repeated tests	Scatter between repeated tests s.d.	Scatter of data about mean curve s.d.
Group I† Nimonic 80A		4	0.04	0.04
Group I† Nimonic 90		1	0.36	0.11
Group I† Red Fox 36		1	0.06	0.12
Weighted mean scatter	log time		0.10 ±0.04*	0.09 ±0.01
	temp. °C		4 ±1.7	3.7 ±0.4
Group II† 18-8		1	0.40	0.16
Group II† S8-16		3	0.45	0.22
Group II† S590		2	0.05	0.32
Weighted mean scatter	log time		0.31 ±0.12*	0.23 ±0.02
	temp. °C		13 ±5°C	10 ±1°C

*Confidence limits of s.d. from six observations

†Group I materials rupture during tertiary (t^3) creep
Group II during secondary (t^1) creep

(b) creep curves

Material	Number of pairs of repeated tests	Scatter between repeated tests s.d.	Scatter of data about mean curve s.d.
Nimonic 80A	2	0.05	0.14
Nimonic 80A	2	0.18	0.27
Nimonic 90	8	0.15	0.18
Nimonic 90	6	0.27	0.15
Nimonic 90	2	0.19	0.25
Weighted mean scatter log time		0.18 ±0.04†	0.20 ±0.02
temp. °C		7 ±1.7°C	8 ±0.8°C
Nimonic 90 only: mean scatter log time		0.20 ±0.05	0.20 ±0.02
temp. °C		8 ±2°C	8 ±0.8°C

†Confidence limit of s.d. from twenty observations

TABLE III

Standard deviations and deviations of means in degrees C for rupture of three individual casts of 18-12-Nb steel referred to the common family of Figure 2

Data from Reference	No. of results in component distributions	Standard deviation S_r	Deviation of mean °C ΔT_d	Spacing between component distributions °C
7	4	3.1 ±0.5	13.4 ±1.5	14 ±1.6
	27		-0.5 ±0.6	11 ±1.2
	10		11.8 ±1.0	
8	2	3.3 ±0.7	2.5 ±2.3	12 ±2.5
	19		-9.3 ±0.8	11 ±2.2
	3		-20.8 ±1.9	
9	10	3.4 ±0.7	-4 ±1.1	12 ±1.6
	10		-16 ±1.1	13 ±2.6
	2		-29 ±2.4	
Average		3.2 ±0.3		12.2 ±0.7

TABLE IV

Standard deviations and deviations of means in degrees C for one cast of 18-12-Nb steel referred to own fitted family

Data from Reference	No. of results in component distributions	Standard deviation S_r	Deviation of mean °C ΔT_d	Spacing between component distributions °C
9	11	3.2 ±0.6	3 ±1.0	8 ±1.5
	16		-5 ±0.8	
	4		-19 ±1.6	13 ±1.8

TABLE V

Standard deviations and deviations of mean in degrees C for rupture of individual casts of Nimonic alloys referred to the appropriate common family

NIMONIC 80 referred to Figure 3

(Old data; lower than that of current production)

Data from Reference	No. of results in component distributions	Standard deviation S_r	Deviations of distributions ΔT_d	Spacing between component distributions
12	7	4.7 ±1.2	-38 ±1.9 -27 ±1.5	11 ±2.3
13	11	3.4 ±0.7	-5.5 ±0.7	-
Mean for Nimonic 80		4.0 ±0.6		11 ±2.3

NIMONIC 80A referred to Figure 3

16	16 4	4.9 ±1.2	26 ±1.3 38 ±2.5	12 ±3
17	28	4.5 ±0.9	12.2 ±0.9	-
21	5 17	3.3 ±0.7	12 ±1.5 22 ±0.8	10 ±1.8
22 (Sheet material)	7 13 11 10 4 7	3.5 ±0.5	-39 ±1.3 -27 ±1.0 -16 ±1.0 0 ±1.0 12 ±1.7 25 ±1.3	12 ±1.8 13 ±1.5 16 ±1.5 12 ±2.0 13 ±2.2
23 (Sheet material)	5 9 9	2.7 ±0.7	-7 ±1.2 6 ±0.9 18 ±0.9	13 ±1.7 12 ±1.4
Mean for Nimonic 80A		3.8 ±0.3		12.5 ±0.7

TABLE V (cont'd)

NIMONIC 90 referred to Figure 4

(Data lower than that of current production)

Data from Reference	No. of tests in component distributions	Standard deviation S_r	Deviations of distributions ΔT_d	Spacing between component distributions
24	7 18	5.8 ±1.1	-13 ±2.2 6 ±1.3	19 ±2.6
25	17	5.6 ±1.3	17 ±1.3	-
27	33 8	4.2 ±0.7	-4.6 ±0.7 12 ±1.5	16.6 ±1.8
28	11 3	3.5 ±0.9	0 ±1.0 20 ±2	20 ±2.5
30	5 10	4.9 ±1.3	-22 ±2.2 -2 ±1.5	20 -3
32	11	3.0 ±1.0	4 ±1.0	-
33	41	2.1 ±0.4	-2.5 ±0.4	-
34	3 32 9	5 ±0.8	-37 ±3 -19.5 ±0.9 0 ±1.7	17.5 ±3.3 19.5 ±2.1
35	2 210 8	1.4 ±0.1	15 ±1 11 ±0.1 5 ±0.5	4 ±1 6 ±0.6
Mean spacing for Nimonic 90, ignoring Reference 35				18.8 ±1.0

TABLE VI

Standard deviations and deviations of means in degrees C for creep of individual casts of Nimonic 80, referred to appropriate common families

Data from Ref.	$t_{\frac{1}{3}}$ referred to Figure 16					t_1 referred to Figure 17				t_3 referred to Figure 18			
	$N_{\frac{1}{3}}$	$S_{\frac{1}{3}}$	ΔT_d		Diff. of ΔT_d	N_1	S_1	ΔT_d	Diff. of ΔT_d	N_3	S_3	ΔT_d	Diff. of ΔT_d
12	14	6.5 ±1.5	-42	±1.7	21 ±3.7	2	9 ±3	-61 ±6	30 ±7	10	2.5 ±0.7	-34 ±0.8	12 ±1.4
	4		-21	±3.3		7		-31 ±3.4		4		-22 ±1.2	
13	10	3.9 ±0.8	-34.2	±1.2	18 ±1.6	25	15 ±3	-24 ±3	-	12	4.1 ±0.9	-23 ±1.2	16 ±1.7
	12		-16.4	±1.1	21 ±3					11		-7 ±1.2	
	2		4.5	±2.8									
14	3	3.5 ±1.3	-53	±2	26 ±2.7	5	11.5 ±4.7	-63 ±5	40 ±13	5	3.1 ±1.1	-30 ±1.4	10 ±2.3
	4		-27	±1.8		1		-13 ±12		3		-20 ±1.8	
	2		-15	±3									
15	7	4.4 ±1.0	4.7	±1.7	20 ±3.5	19	9.8 ±2.2	-4 ±2.2	-	3	3.2 ±0.7	-11 ±1.8	14 ±2.0
	6		24.5	±1.8	20 ±2.5					13		2.6 ±0.9	
	4		37	±2.2	13 ±2.8					3		11 ±1.8	8 ±2.0
Averages		4.5 ±0.5			20 ±1.0		11.3 ±1.5		33 ±5		3.2 ±0.4		12 ±0.8

$N_{\frac{1}{3}}$, N_1, N_3 indicate number of results in each $t_{\frac{1}{3}}$, t_1, t_3 distribution respectively

TABLE VII

Standard deviations and deviations of means in degrees C
for creep of individual casts of Nimonic 80A

Data from Ref.	$t_{\frac{1}{3}}$ referred to Figure 16				t_1 referred to Figure 17				t_3 referred to Figure 18			
	$N_{\frac{1}{3}}$	$S_{\frac{1}{3}}$	ΔT_d	Diff. of ΔT_d	N_1	S_1	ΔT_d	Diff. of ΔT_d	N_3	S_3	ΔT_d	Diff. of ΔT_d
16	20	12.5 ±2.7	30 ±2.8	71 ±10	-		-	-	22	4.4 ±0.9	27 ±0.9	-
	2		101 ±9									
	7		-29 ±3.2	28 ±3.8					6		6.4 ±0.9	9 ±1.1
17	17	8.5 ±1.5	-1 ±2.0		17	17 ±6	-51 ±17	64 ±18	19	2.3 ±0.4	15.3 ±0.5	9 ±1.1
	6		55 ±3.4	56 ±3.9			13 ±6		5		24 ±1.0	
									1		-1 ±4.4	12 ±5
18	-	-	-	-	-	-	-	-	3	4.4 ±1.8	10.5 ±2.5	16 ±3.4
									4		26.5 ±2.2	
19	-	-	-	-	-	-	-	-	2	-	5	29 ±4
									3		34	
									1		-4 ±3.4	16 ±4
20	-	-	-	-	-	-	-	-	3	3.4 ±2.0	12 ±2.3	16 ±4
									1		28 ±3.4	
21	NO CREEP DATA											
	35	13 ±2.2	-18.5 ±2.2		25				48		-10 ±1.6	
22	30	9.5 ±1.7	20 ±1.7	38 ±2.8	50	12 ±1.4	-57 ±2.8	41 ±3.2	21		2 ±2.4	12 ±2.9
							-16 ±1.8		6	11.2 ±1.3	25 ±4.5	23 ±5.1

TABLE VII (cont'd)

Standard deviations and deviations of means in degrees C for creep of individual casts of Nimonic 80A

Data from Ref.	$N_{\frac{1}{3}}$	$S_{\frac{1}{3}}$	$t_{\frac{1}{3}}$ ΔT_d	Diff. of ΔT_d	N_1	S_1	t_1 ΔT_d	Diff. of ΔT_d	N_s	S_s	t_s ΔT_d	Diff. of ΔT_d
23	16 11	14.5 ±2.9	-36 ±3.6 4 ±4.4	40 ±5.8	19 5	12 ±2.5	-35 ±2.8 3 ±5	38 ±6	5 15 3	4.4 ±0.9	-14 ±2.0 1 ±1.1 16 ±2.5	15 ±2.3 15 ±2.5
Averages		11.6 ±0.9		40 ±1.8		13 ±1.2		42 ±2.8		4.2* ±0.6		14† ±1.1

*Omitting s.d. from References 17 and 22

†Omitting spacing from Reference 17

TABLE VIII

Standard deviations and deviations of means in degrees C for creep of individual casts of Nimonic 90

Data from Ref.	$t_{\frac{1}{3}}$ referred to Figure 22 $N_{\frac{1}{3}}$	$S_{\frac{1}{3}}$	ΔT_d	Diff. of ΔT_d	t_1 referred to Figure 23 N_1	S_1	ΔT_d	Diff. of ΔT_d	t_s referred to Figure 24 N_s	S_s	ΔT_d	Diff. of ΔT_d
24	31	21 ±3.8	24 ±3.8	-	13	17 ±4.7	32 ±4.7	-	2 25	3.9 ±0.7	-13 ±2.8 6 ±0.8	19 ±3
25	10 6	19 ±4.7	6 ±6 72 ±8	66 ±10	12	11 ±3.2	6 ±3.2	-	2 10	4.5 ±1.3	2 ±3.2 20 ±1.4	18 ±3.5
26	6	24 ±10	31 ±10	-	2 3	13 ±6	-17 ±9 36 ±8	53 ±12	4	-	5 ±2	-

TABLE VIII (cont'd)

Standard deviations and deviations of means in degrees C for creep of individual casts of Nimonic 90

Data from Ref.	$t_{\frac{1}{3}}$ $N_{\frac{1}{3}}$	$S_{\frac{1}{3}}$	ΔT_d	Diff. of ΔT_d	t_1 N_1	S_1	ΔT_d	Diff. of ΔT_d	t_3 N_3	S_3	ΔT_d	Diff. of ΔT_d
27	38 3	21 ±3.3	−10 ±3.4 71 ±12	81 ±13	35	13 ±2.3	−10 ±2.3	–	35	6.8 ±1.1	−11 ±1.1	–
28	23	15 ±3.1	61 ±3.1	–	23	9.5 ±2.0	−6 ±2.0	–	7 11 6	2.5 ±0.5	−11 ±0.9 −1 ±0.8 +12 ±1.0	10 ±1.2 13 ±1.3
29	8 20	16 ±3.0	−78 ±6 +21 ±4	109 ±7	16 4	11 ±2.5	−29 ±2.8 3 ±5.5	32 ±6	10 3	4.3 ±1.2	−11 ±1.4 8 ±2.5	19 ±3
30	1 9 2	9 ±2.7	−56 ±9 12 ±3 85 ±6	68 ±10 73 ±7	8	6 ±2.3	−15 ±2.3	–	1 4	3.2 ±1.6	−35 ±3 −7 ±1.6	28 ±3.5
31	4 8 1	15 ±4.3	−35 ±8 49 ±5 124 ±15	84 ±9 75 ±16	8	4 ±1.4	−10 ±1.4	–	3 4	–	−46 ±2 −5 ±2	41 ±3
32	NO CREEP DATA											
33	40 5	11.2 ±1.7	35 ±1.8 79 ±5	34 ±6	44	4.2 ±0.6	−26 ±0.6	–	30	2.5 ±0.4	−7 ±0.4	–
34	36 5	16 ±2.5	−28 ±2.7 30 ±7	58 ±7	41	18 ±2.8	−35 ±2.8		3 26 10	6 ±1	−48 ±3.4 −21 ±1.2 −2 ±1.9	27 ±2.8 19 ±2.3
Average spacing				76 ±3				39 ±5				22 ±0.9

TABLE IX

Comparisons of s.d. and deviations of mean before and after resolution into components (see Section 6.1)

Nimonic 80

Ref.	$t_{\frac{1}{3}}$ term					t_1 term					t_3 term					Rupture			
	$S_{\frac{1}{3}}$	$S'_{\frac{1}{3}}$	ΔT_d*		ΔT_c	S_1	S'_1	ΔT_d*	ΔT_c	S_3	S'_3	ΔT_d*	ΔT_c	S_r	S'_r	ΔT_d*	ΔT_c
12	6.5	11	-42,	-21	-38	9	15	-61, -31	-40	2.5	6	-34, -22	-30	4.7	7	-38, -27	-33
13	3.9	14	-34, 4	-16	-22	15	15	-24	-24	4.1	8.2	-23, -7	-11	3.4	3.4	-5	-5
14	3.5	16	-53,	-27	-42	12	24	-63, -13	-57	3.1	6.8	-30, -20	-27	-		-	
15	4.4	18	-15, 24,	5 37	14	10	10	-4	-4	3.2	8	-11, 11	3	2	-		-	
Averages (Unimodal						12.5	12.5							3.4	3.4		
Averages (Multimodal						10.5	19.5							4.7	7		

*A single entry of ΔT_d indicates the material is unimodal in this term - more than one entry indicates multimodality.

TABLE X

Comparisons of s.d. and deviations of mean before and after resolution into components

Nimonic 80A

Ref.	$t_{\frac{1}{3}}$ term				t_1 term				t_3 term				Rupture			
	$S_{\frac{1}{3}}$	$S'_{\frac{1}{3}}$	ΔT_d*	ΔT_c	S_1	S'_1	ΔT_d*	ΔT_c	S_3	S'_3	ΔT_d*	ΔT_c	S_r	S'_r	ΔT_d*	ΔT_c
16	12.5	25	30, 101	33	-	-	-	-	4.4	4.4	27	27	4.9	7.5	26, 38	28
17	8.5	29	-29, -1, 55	4	17	26	-51, 13	5	2.3	5.2	6, 15, 24	15	4.5	4.5	12	12
18	-	-	-	-	-	-	-	-	4.4	11	-1, 11, 27	14	-	-	-	-
19	-	-	-	-	-	-	-	-	-	-	5, 34	22	-	-	-	-
20	-	-	-	-	-	-	-	-	3.4	10	-4, 12, 28	12	-	-	-	-
21	-	-	-	-	-	-	-	-	-	-	-	-	3.3	6	12, 22	22
22	11	21	-18,20	-2	12	23	-57, -16	-30	11.2	19	-10, 2, 25	-1	3.5	18	-39, -27, -16, 0, 12, 25	-13
23	14.5	23	-36, 4	-20	12	21	-35, 3	-28	4.4	10.6	-14, 1, 16	0	2.7	10	-7, 6, 18	
Unimodal									4.4	4.4			4.5	4.5		
Multimodal } neglecting data of Reference 22									4.2	9.2			.8	7.8		

*A single entry of ΔT_d indicates the material is unimodal in this term - more than one entry indicates multimodality.

TABLE XI

Comparisons of s.d. and deviations of mean before and after resolution into components

Nimonic 90

Ref.	$t_{\frac{1}{3}}$ term				t_1 term				t_3 term				Rupture			
	$S_{\frac{1}{3}}$	$S'_{\frac{1}{3}}$	ΔT_d	ΔT_c	S_1	S'_1	ΔT_d	ΔT_c	S_3	S'_3	ΔT_d	ΔT_c	S_r	S'_r	ΔT_d	ΔT_c
24	21	21	24	24	17	17	32	32	3.9	7	-13, 6	5	5.8	12	-13, 6	1
25	19	30	6, 72	31	11	11	6	6	4.5	7.5	2, 20	17	5.6	5.6	17	17
26	24	24	31	31	13	30	-17, 36	15	-	-	5	5	-	-	-	-
27	21	30	-10, 71	-6	13	13	-10	-10	6.8	6.8	-11	-11	4.2	7.2	-5, 12	-1
28	15	15	61	61	9.5	9.5	-6	-6	2.5	5.4	-11, -1, 12	-1	3.5	9	0, 20	3
29	16	44	-78, 21	-7	11	17	-29, 3	-29	4.3	10	-11, 8	-7	-	-	-	-
30	9	27	-56, 12 85	13	6	6	-15	-15	3.2	5.6	-35, -7	-12	4.9	10	-22, -2	-9
31	15	48	-35, 49 124	28	4	4	-10	-10	-	-	-46, -5	-23	-	-	-	-
32	-	-	-	-	-	-	-	-	-	-	-	-	3	3	4	4
33	11	24	35, 79	40	4.2	4.2	-26	-26	2.5	2.5	-7	-7	2.1	2.1	-2.5	-2.5
34*	16	28	-28, 30	-20	18	18	-35	-35	6	14	-48, -21 -2	-18	5	10	-37, -20 0	-17
35	-	-	-	-	-	-	-	-	-	-	-	-	1.4	2.5	5, 11, 15	11

*Sheet data

APPENDIX I

List of symbols

Symbol	Definition	Units
ε	Natural strain $\equiv \log_e \ell/\ell_o$: equivalent to engineering strain $(\ell - \ell_o)/\ell_o$ up to about 5 per cent ℓ and ℓ_o are current and original lengths of test section of specimen.	Non-dimensional - per cent
C	Constant in each term of formula, but different from term to term.	Complex but generally irrelevant.
σ	Natural stress $\equiv L/A$, where L is the load and A the current cross-sectional area. Approximately equal to engineering stress L/A_o where A_o is original area, up to 5 per cent strain.	t.s.i. or p.s.i.
β	Exponent of stress. Takes predetermined values defined by the series $\frac{\beta}{k} = 1, 2, 4 \ldots 2^n$.	Non-dimensional.
ϕ	A time temperature parameter, defined as $\phi = t(T' - T)^{-20} \quad (T' > T)$ or $\phi = t(T - T')^{20} \quad (T > T')$.	Seconds or hours.
t	Time.	Seconds or hours.
T	Temperature of testing.	^oC.
T'	Reference temperature, constant in any one term but different in different terms.	^oC.
k	Exponent of ϕ or of t. Takes values from sequence. $\ldots \frac{1}{3}, 1, 3, \ldots$	Non-dimensional.
Fitted family	A series of curves calculated from Equation (1) after the constants have been chosen to fit a set of experimental data. Commonly curves of log stress versus log time for several different values of temperature.	

APPENDIX I (cont'd)

Symbol	Definition	Units
Common family	A family of curves that has been fitted, not to a single set of data, but to a number of different sets of data for the same alloy.	
ΔT_c	Average displacement of data for a single cast from common family.	°C.
Homogeneous set of data	Data obtained by testing a group of specimens for which there is no known difference prior to testing - e.g., specimens from the same cast taken at random (cf. Section 2.3).	
Multimodal	Having several peaks with regions of lesser probability between them.	
Component distribution	Set of scatter values which conforms to the Gaussian law, extracted by analysis from a multimodal distribution.	
ΔT_d	Mean deviation of a component distribution from the common family.	
S_r	Standard deviation for single component distribution of rupture data.	log time or °C.
$S_{\frac{1}{3}}$	Standard deviation for single component distribution of $\left(\frac{t}{t_{\frac{1}{3}}}\right)^{\frac{1}{3}}$ term of Equation (3).	
S_1	Standard deviation for single component distribution of $\left(\frac{t}{t_1}\right)$ term of Equation (3).	
S_3	Standard deviation for single component distribution of $\left(\frac{t}{t_3}\right)^3$ term of Equation (3).	
$t_{\frac{1}{3}}$	Time in which the term $\left(\frac{t}{t_{\frac{1}{3}}}\right)^{\frac{1}{3}}$ of Equation (3) contributes a constant arbitrary strain (typically 0.1 per cent) to the overall strain.	Seconds or hours.

APPENDIX I (cont'd)

Symbol	Definition	Units
t_1, t_3	Corresponding times for terms $\left(\frac{t}{t_1}\right)$ and $\left(\frac{t}{t_3}\right)^3$.	Seconds or hours.
ε_o	A component of strain which does not vary significantly with time. Commonly used either (a) for any "plastic" strain on loading loading not accounted for by the time dependent terms, or (b) for correcting any error in the estimated elastic strain on loading.	Non-dimensional.
S'	Apparent standard deviation obtained by fitting Gaussian law to multimodal data without prior resolution into component distributions.	Log t or T^oC.

APPENDIX II

Method for resolving a multimodal distribution into its components

The value of ΔT for each experimental point is determined by comparing it with the fitted family of log stress versus log time curves, using linear interpolation to establish the ΔT. The observed values of ΔT are then entered as marks on the linear axis of a probability graph e.g., Figure 32. If the total number of marks is N, the number below a particular ΔT is n, and the number at the value is m, then the corresponding point on the probability graph is plotted at a cumulative probability of

$$\frac{n + \frac{m}{2}}{N} \times 100\% \qquad \ldots.A1$$

The graph thus obtained is the unresolved ogive.

Resolution into components proceeds by trial and error. Often the first indication is given by the distribution of the marks: thus in Figure 7 of the text where a histogram based on the marks is shown, the two components are approximately equal in number of points, and have a clearly defined minimum. In such a case the data is divided at the minimum value of ΔT yielding two sets with total numbers N_1 and N_2 (where $N_1 + N_2 = N$) and each set is then replotted in accordance with Equation A1, but putting N_1 or N_2 in place of N. The final division of points between the two ogives is made on the basis of the fit of the lines to the points.

The process of dividing up the data is however better illustrated by examples for which the histogram provides less evidence. For this purpose two examples in the test, Figures 11(a) and 12(b), are presented as worked examples.

The data of Figure 11(a) is reproduced as Figure 32, with the marks, and the values of n and of $n + \frac{1}{2}m$, entered on the left hand side. The crosses have been plotted from the latter values. At first sight the full line appeared a reasonable fit to the crosses, but closer examination showed that the departures were systematic. Thus, in the central region of the graph individual departures were significantly larger than the uncertainty $\pm(n + \frac{1}{2}m)^{\frac{1}{2}}$, (a few typical values of uncertainty are indicated by bars). The broken line was clearly a much closer fit than the full line in this region, but deviated markedly at extreme values of ΔT - thus the values of ΔT at which a single result would on average be expected are $+10^{\circ}C$ and $-13^{\circ}C$. These are indicated by horizontal broken lines.

The next step was to assume that all values between these limits belonged to a medium ΔT distribution, and all above or below to high or low ΔT distributions respectively. In Figure 33 the data has been renormalized on this assumption, each distribution being plotted separately, and the three sets fitted with parallel lines. Examination of the graph around $\Delta T = 10^{\circ}C$ indicated an excess of values in the central distribution (e.g., at $\Delta T = 12^{\circ}C$ the line predicted 3 per cent rather than 10.5 per cent), and a

deficit in the low ΔT distribution: a similar effect was found around +8°C. A further approximation was therefore made in which the dividing lines between distributions were brought closer together, and thus by successive approximation the graph of Figure 11(a) was obtained.

The other example, that of Figure 12(b) replotted as Figure 34, is interesting because of the unusually large number of distributions involved. The unresolved ogive does not at first sight deviate far from a straight line, but the distribution of marks is unusual in that there is an absence of values around Δ log t = 0.15 just where they would be expected to be most numerous. The corresponding histogram, if plotted, would show a minimum where a maximum would be expected. The data was therefore divided into two distributions, but division of the data at this value of log t provides (Figure 35) distributions which are clearly not of Gaussian form. Each was therefore further analysed with the results shown in Figure 12(b) and Figure 36.

The degree of division of a distribution that can be considered meaningful depends not only on the magnitude of the deviations of the points from the straight lines, but also on the statistical uncertainty of each point. Thus in Figure 36 it can be seen that the residual discrepancies are not significant, whereas the discrepancies in Figure 34 although apparently no greater are significant. These considerations were used to determine the degree of resolution appropriate to each set of data - their general correctness can best be assessed by the correlations to which they lead.

Determination of standard deviations

The quantity S' (Section 5.1) was determined from the line through the unresolved distribution, as the difference in the ΔT for 50 per cent and for 17 per cent cumulative frequency. Thus in Figure 32 S' = -1.5 - (-9.5) = 80°C, and in Figure 34 S' = -0.19 - (-0.41) = 0.22 in log time. The S were similarly obtained from one of the parallel lines through the resolved distribution. Thus in Figure 36 the S was -0.032 - (-0.100) = 0.068 in log time.

FIG. 1.

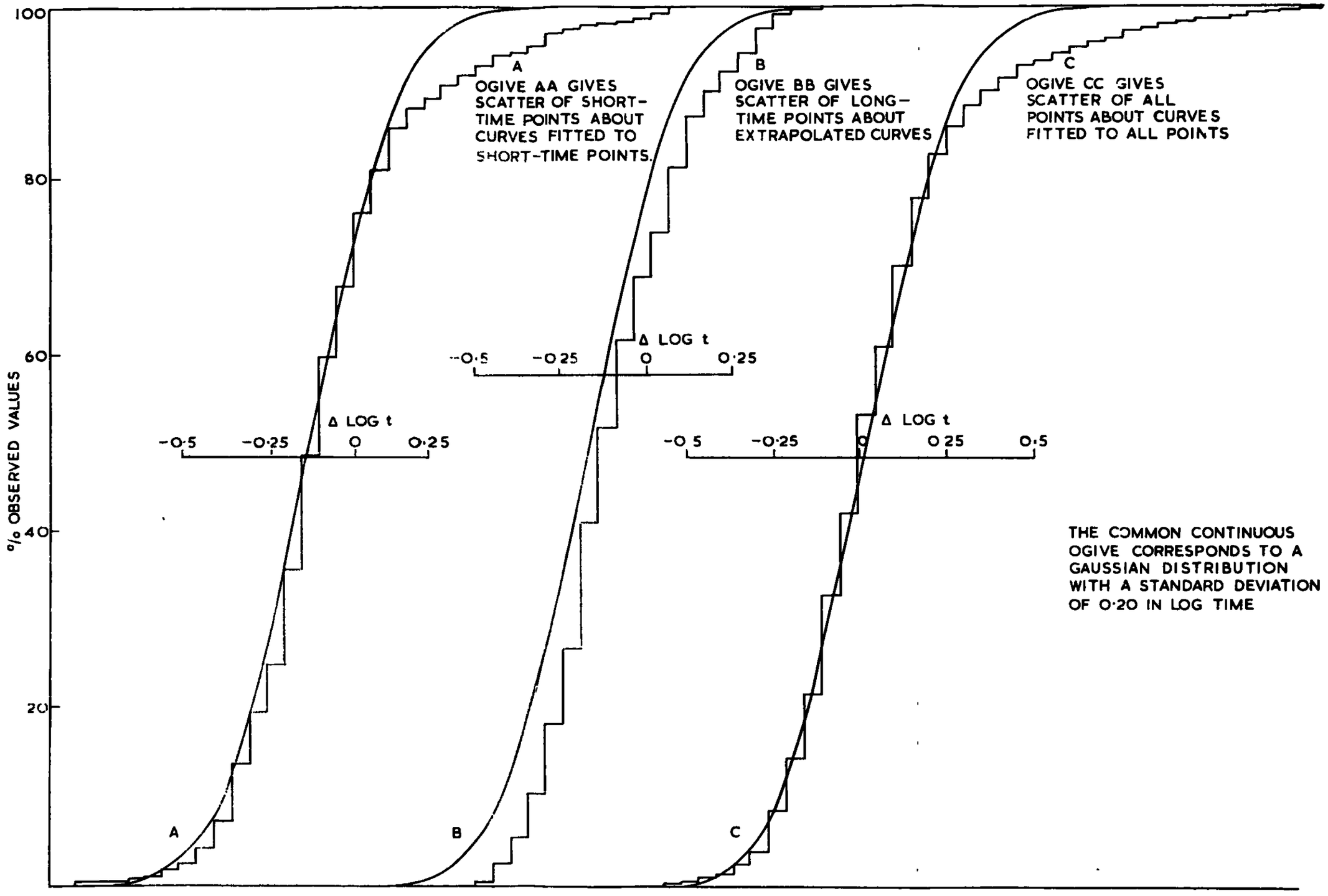

SAMPLE OF EVIDENCE INDICATING SCATTER IN EXTRAPOLATION TO BE NO GREATER THAN IN DIRECT FITTING.

FIG. 2

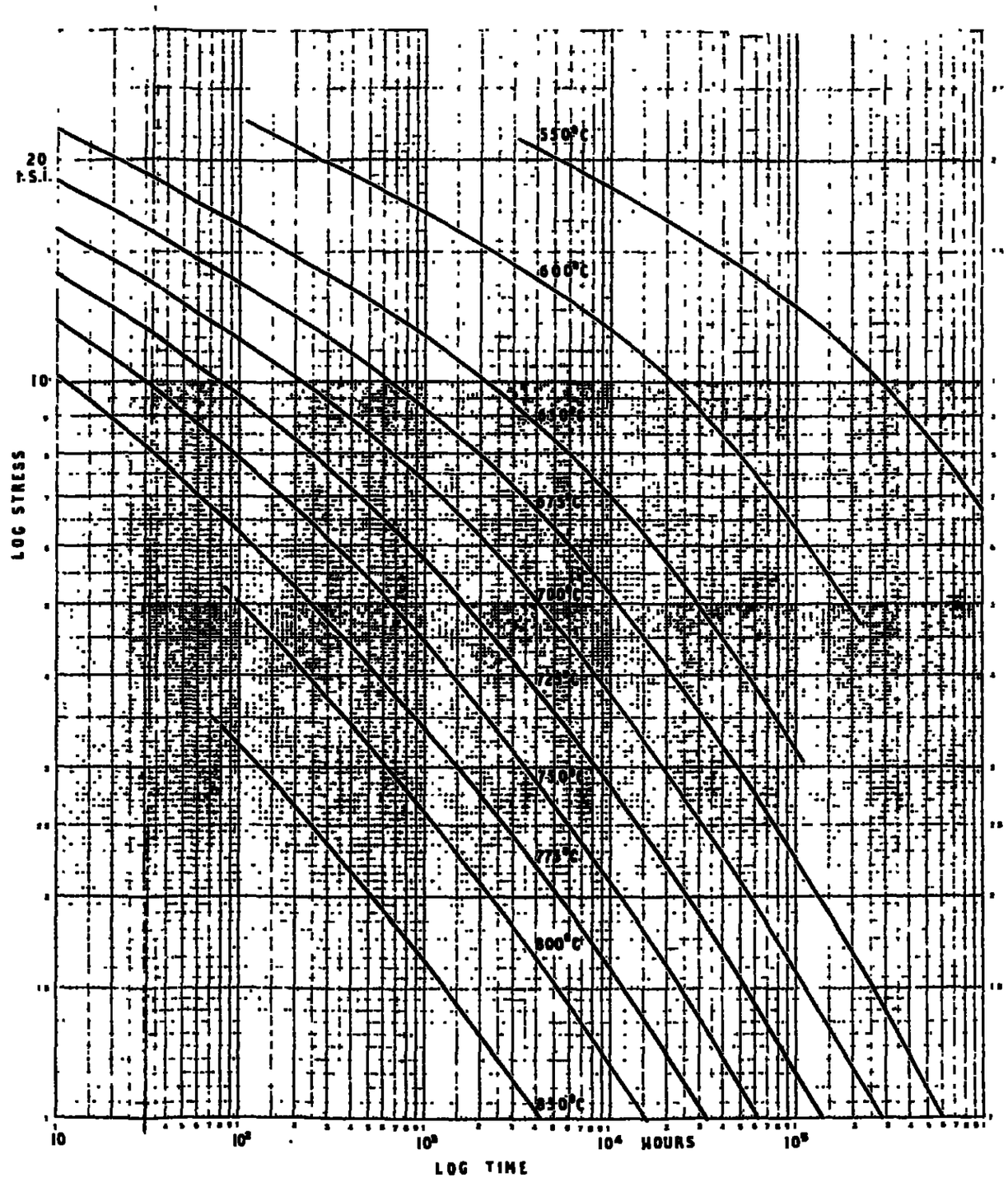

COMMON FAMILY FOR RUPTURE OF 18-12-NbSTEEL.

FIG.3

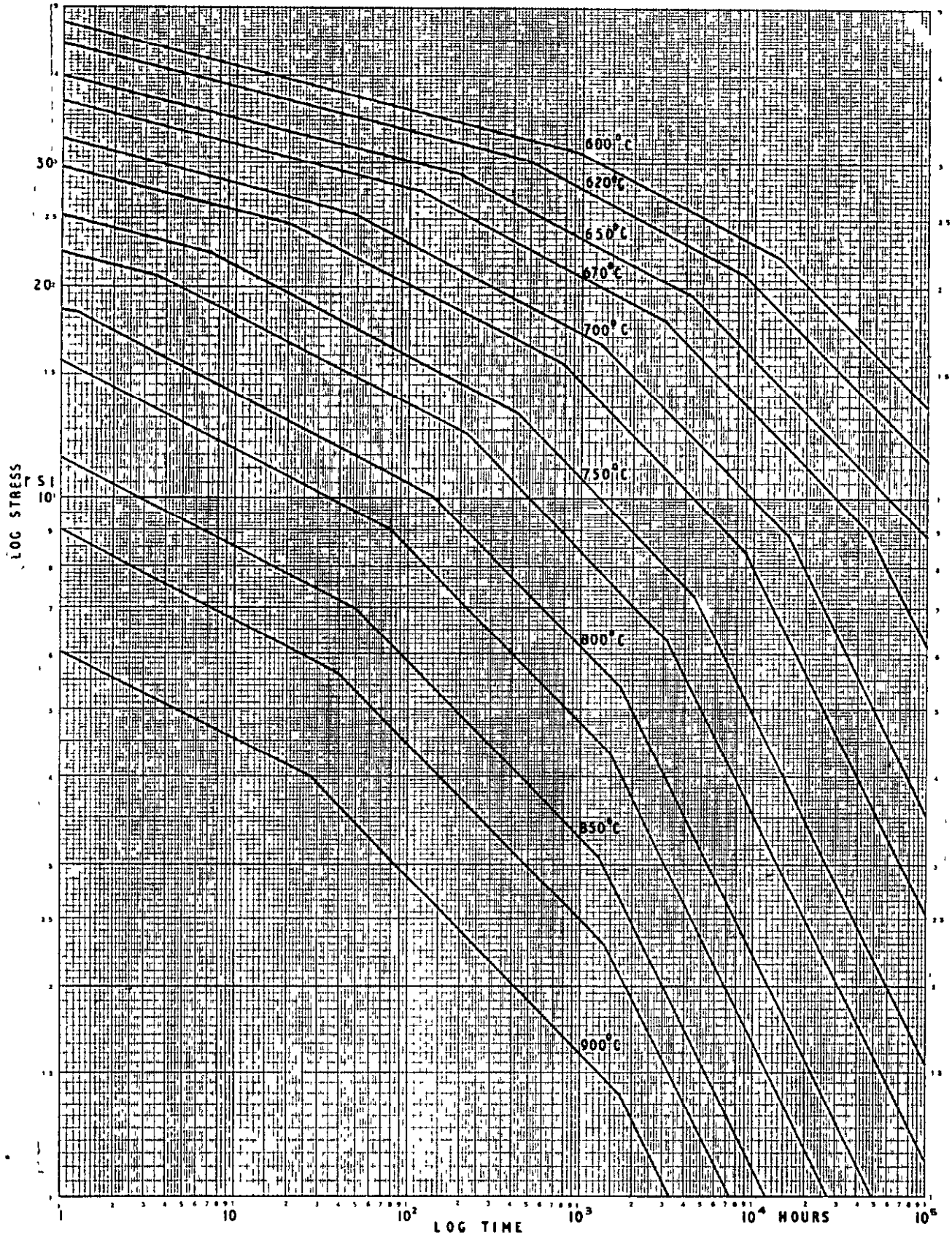

COMMON FAMILY FOR RUPTURE OF NIMONIC 80 AND NIMONIC 80A

FIG.4

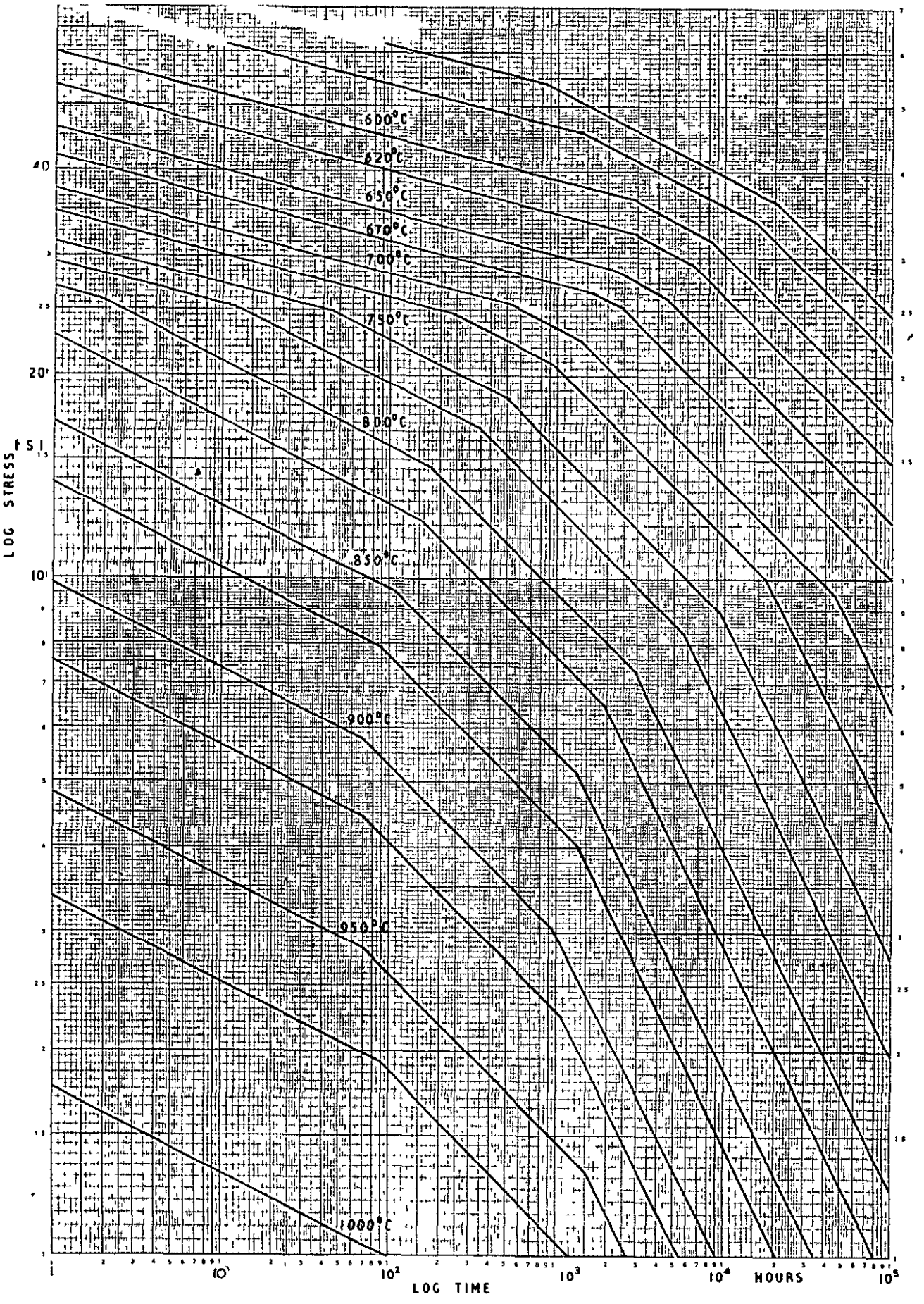

COMMON FAMILY FOR RUPTURE OF NIMONIC 90

FIG. 5

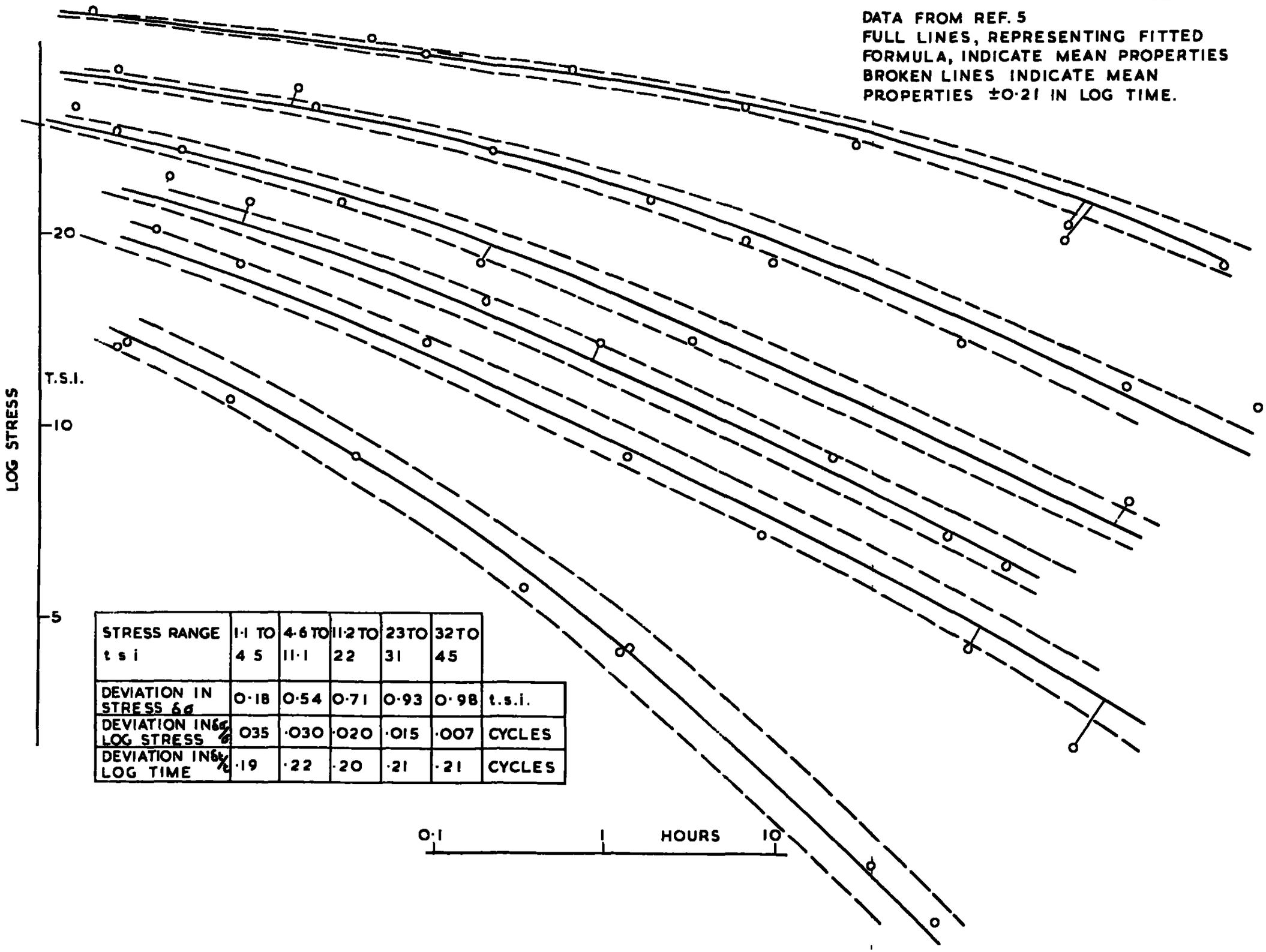

STRESS RANGE t s i	1·1 TO 4 5	4·6 TO 11·1	11·2 TO 22	23 TO 31	32 TO 45	
DEVIATION IN STRESS $\delta\sigma$	0·18	0·54	0·71	0·93	0·98	t.s.i.
DEVIATION IN LOG STRESS $\frac{\delta\sigma}{\sigma}$	035	·030	·020	·015	·007	CYCLES
DEVIATION IN $\frac{\delta t}{t}$ LOG TIME	·19	·22	·20	·21	·21	CYCLES

SAMPLE CREEP RUPTURE GRAPH SUGGESTING SCATTER MORE UNIFORM IN LOG TIME THAN LOG STRESS OR STRESS

FIG. 6

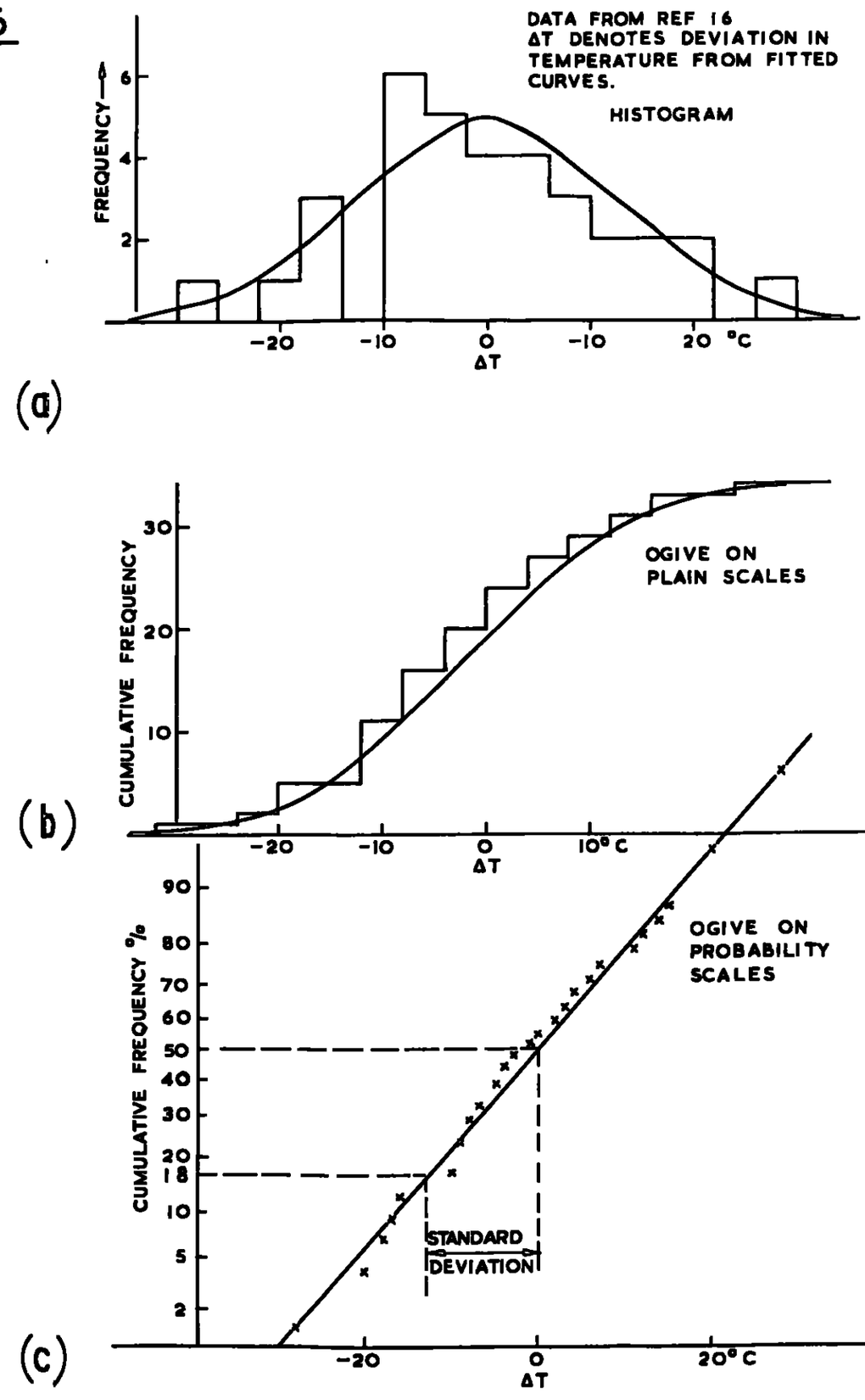

EXAMPLE OF SCATTER DATA SHOWING NORMAL DISTRIBUTION.

FIG. 7 (a)

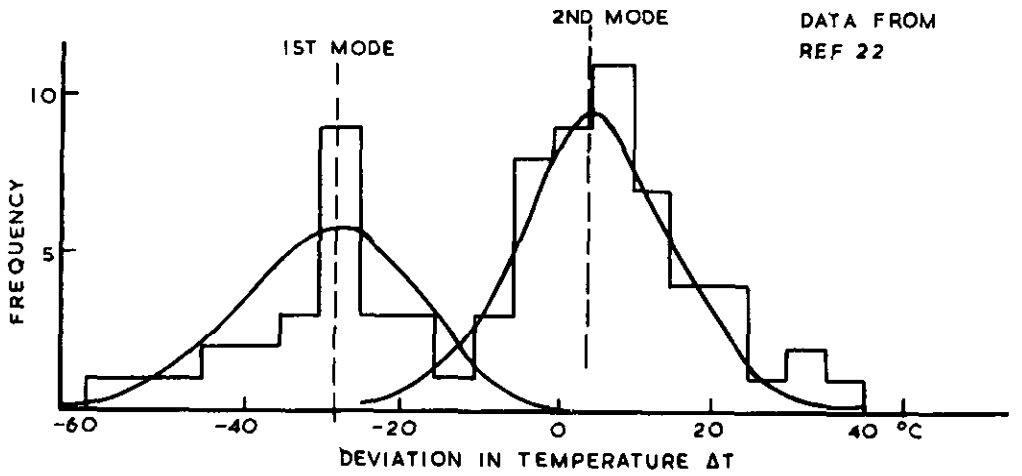

FIG. 7 (b)

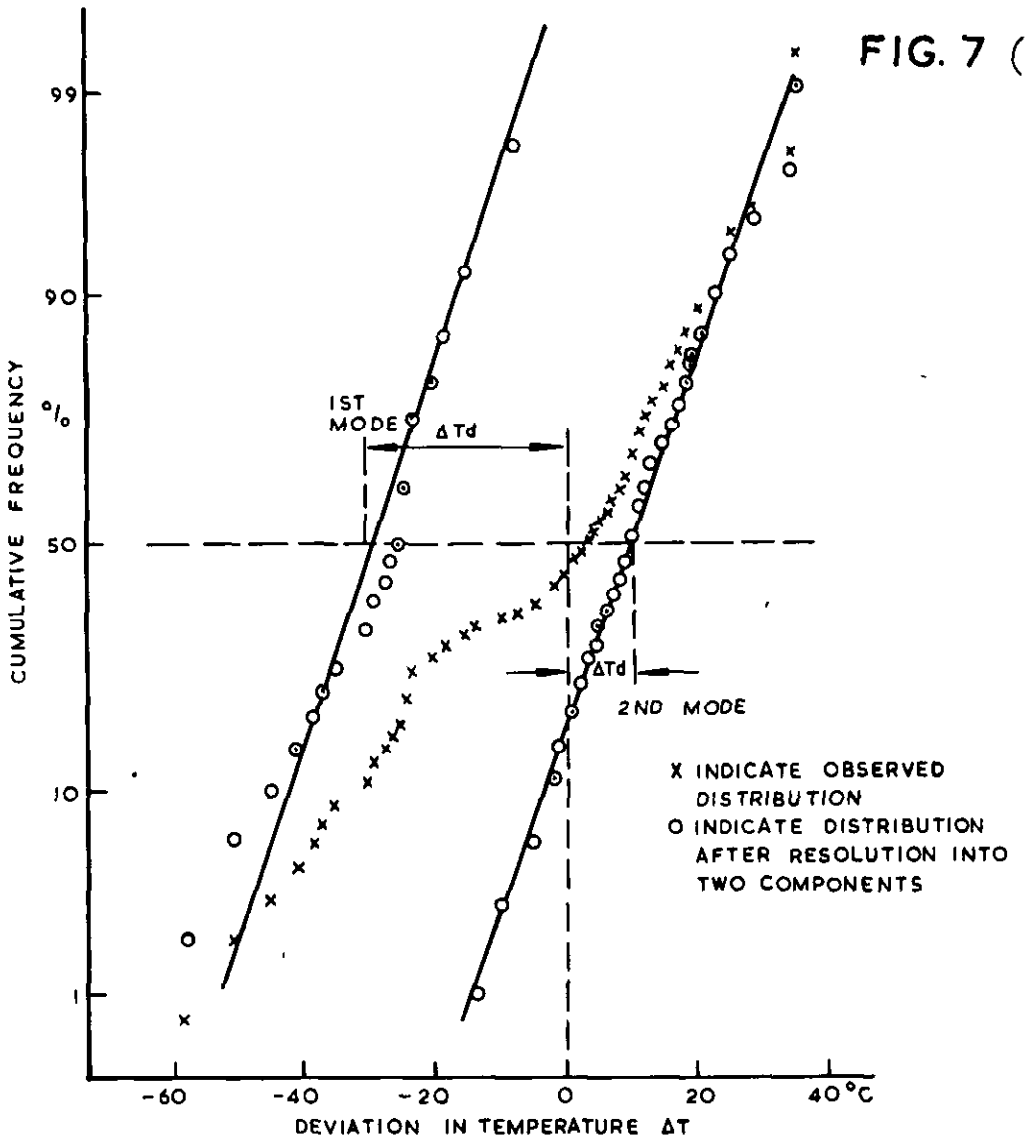

EXAMPLE OF DATA SHOWING BIMODAL DISTRIBUTION.

FIGS. 8 (a & b)

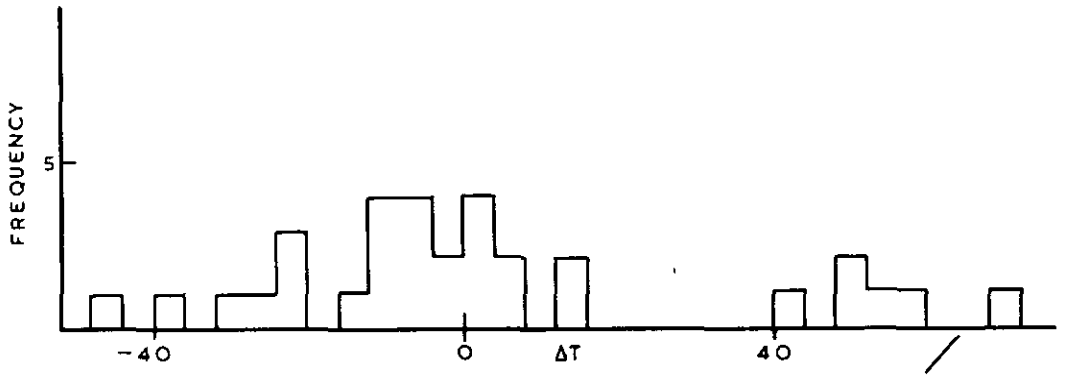

FIG. 8 (a)

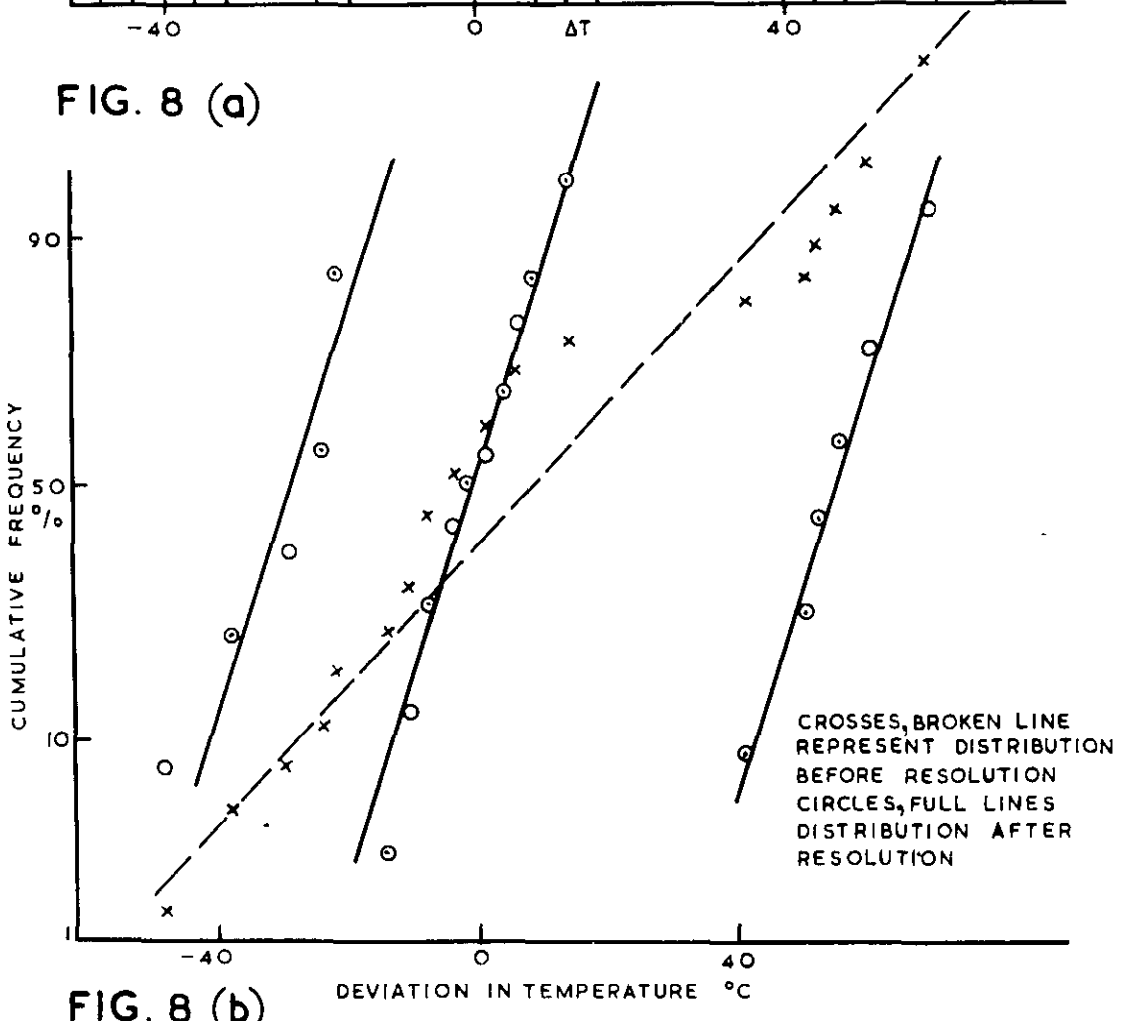

FIG. 8 (b)

EXAMPLE OF DATA SHOWING APPARENTLY IRREGULAR SCATTER.

FIG 9

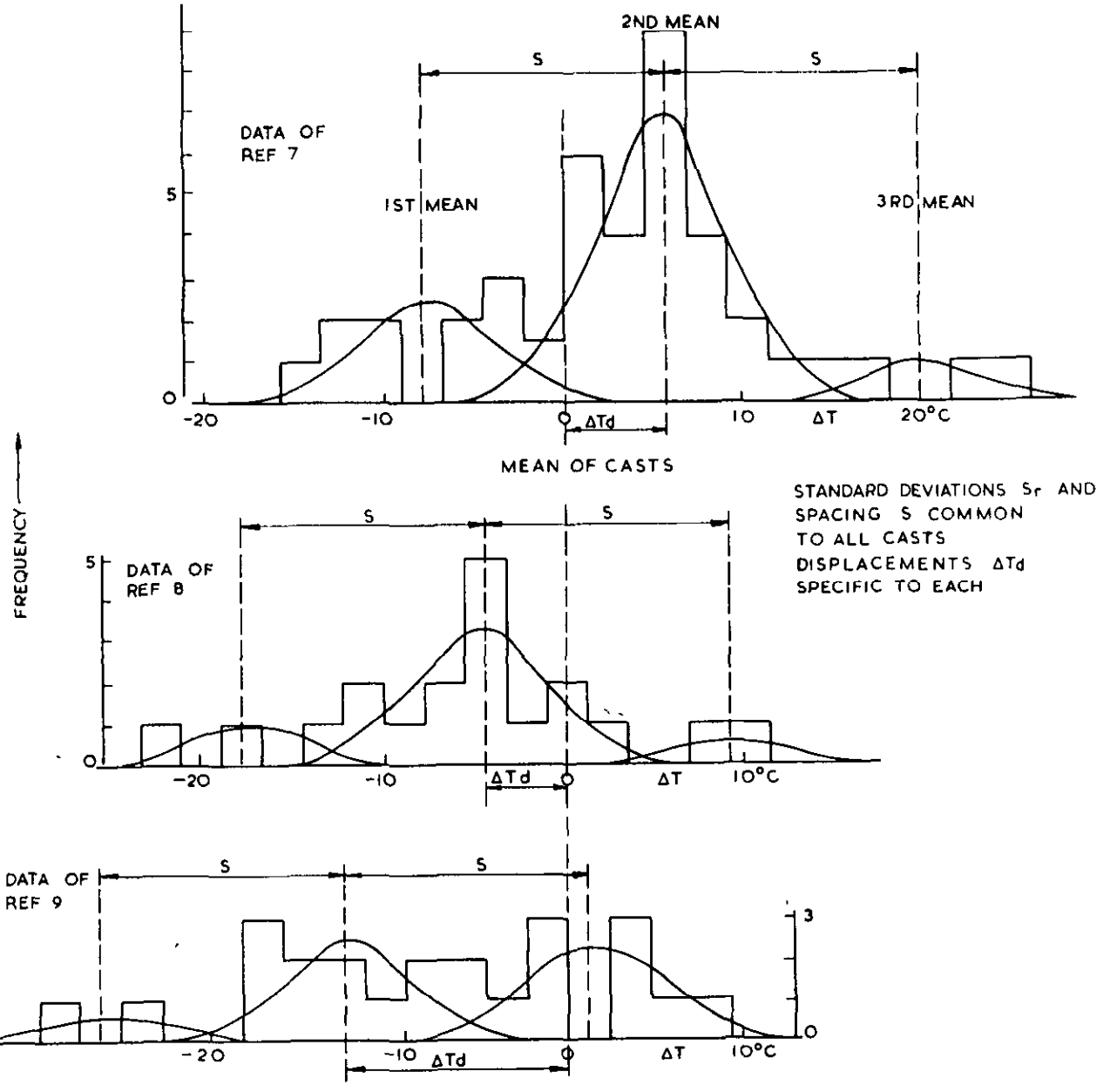

SCHEME OF REGULARITIES IN A GROUP OF SETS OF DATA FOR A SINGLE ALLOY

FIG. 10

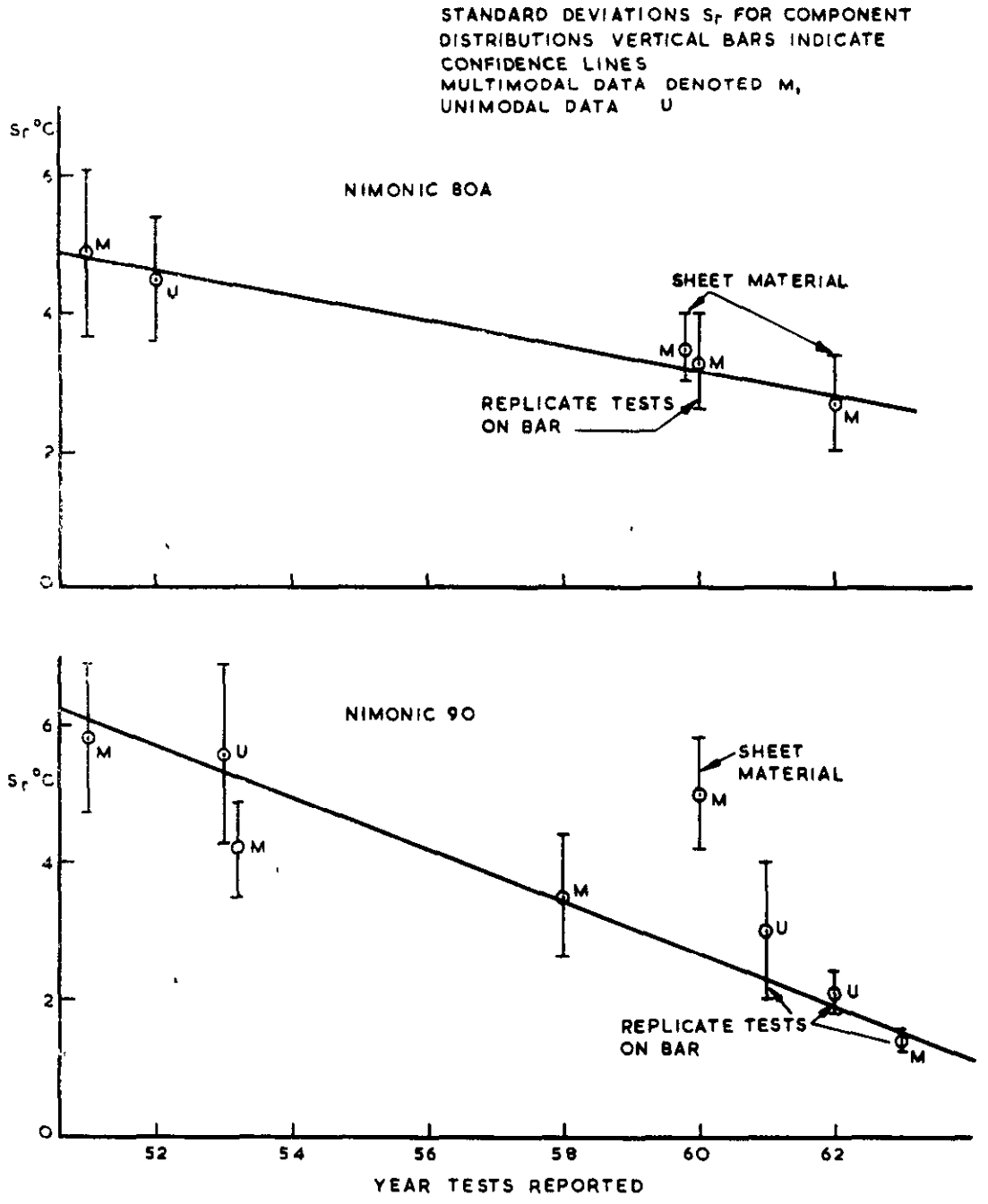

STANDARD DEVIATION OF NIMONIC RUPTURE DATA vs DATE OF TESTING.

FIG 11

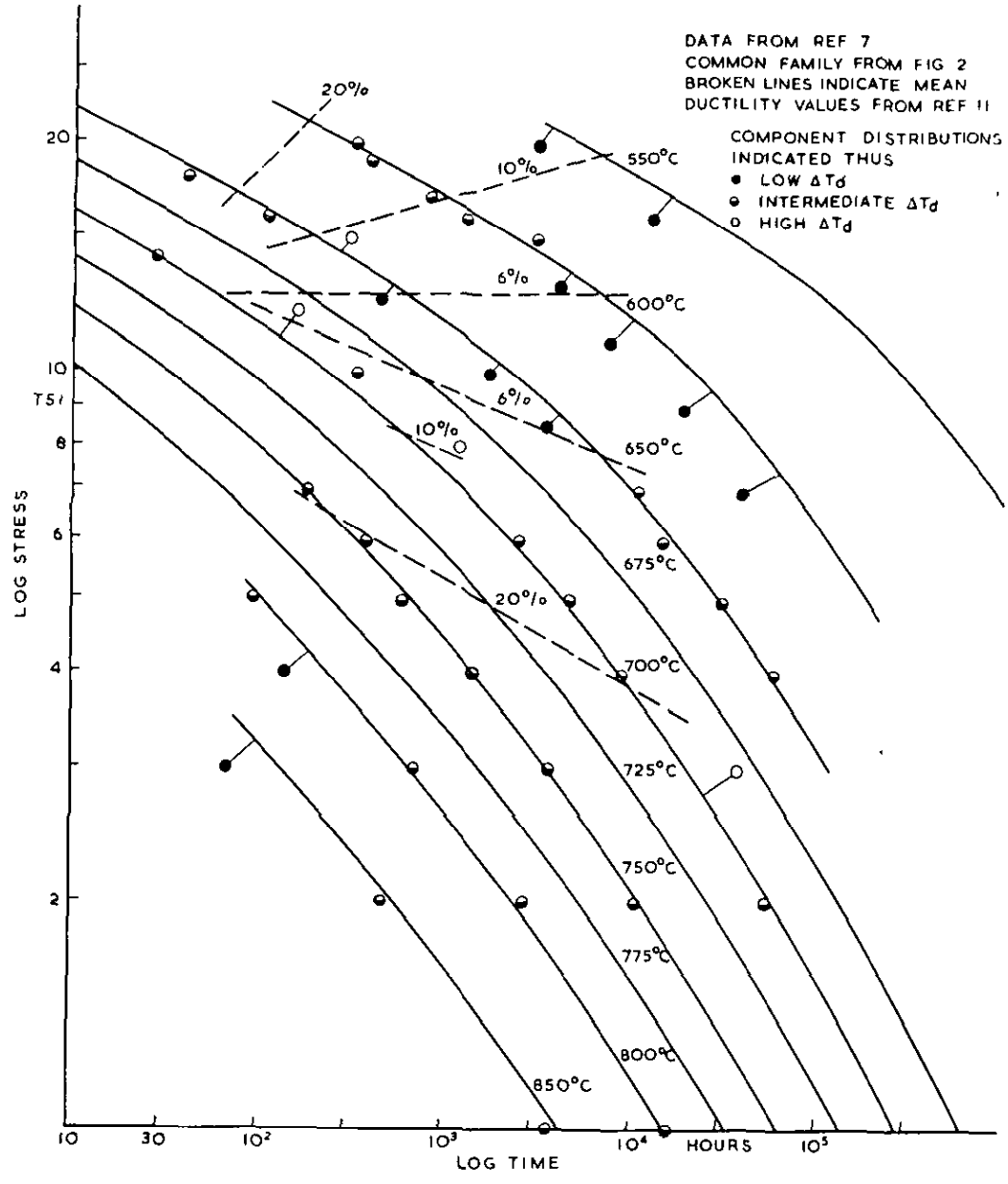

RUPTURE DATA FOR SINGLE CAST OF 18-12-Nb STEEL SHOWING EFFECT OF STRESS AND TEMPERATURE ON SCATTER

FIG. 11 (a)

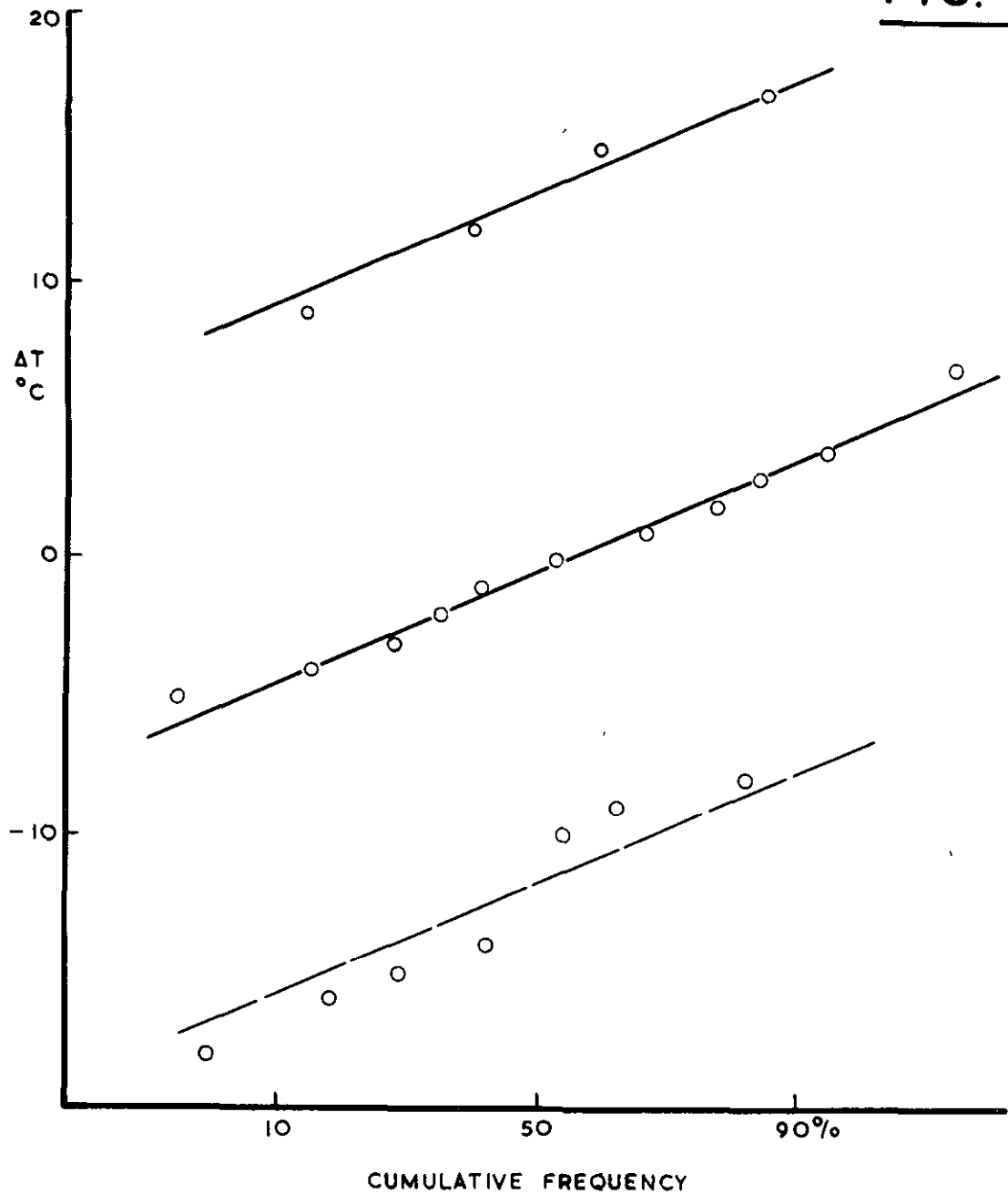

OGIVE OF SCATTER IN FIG. 11.

FIG 12

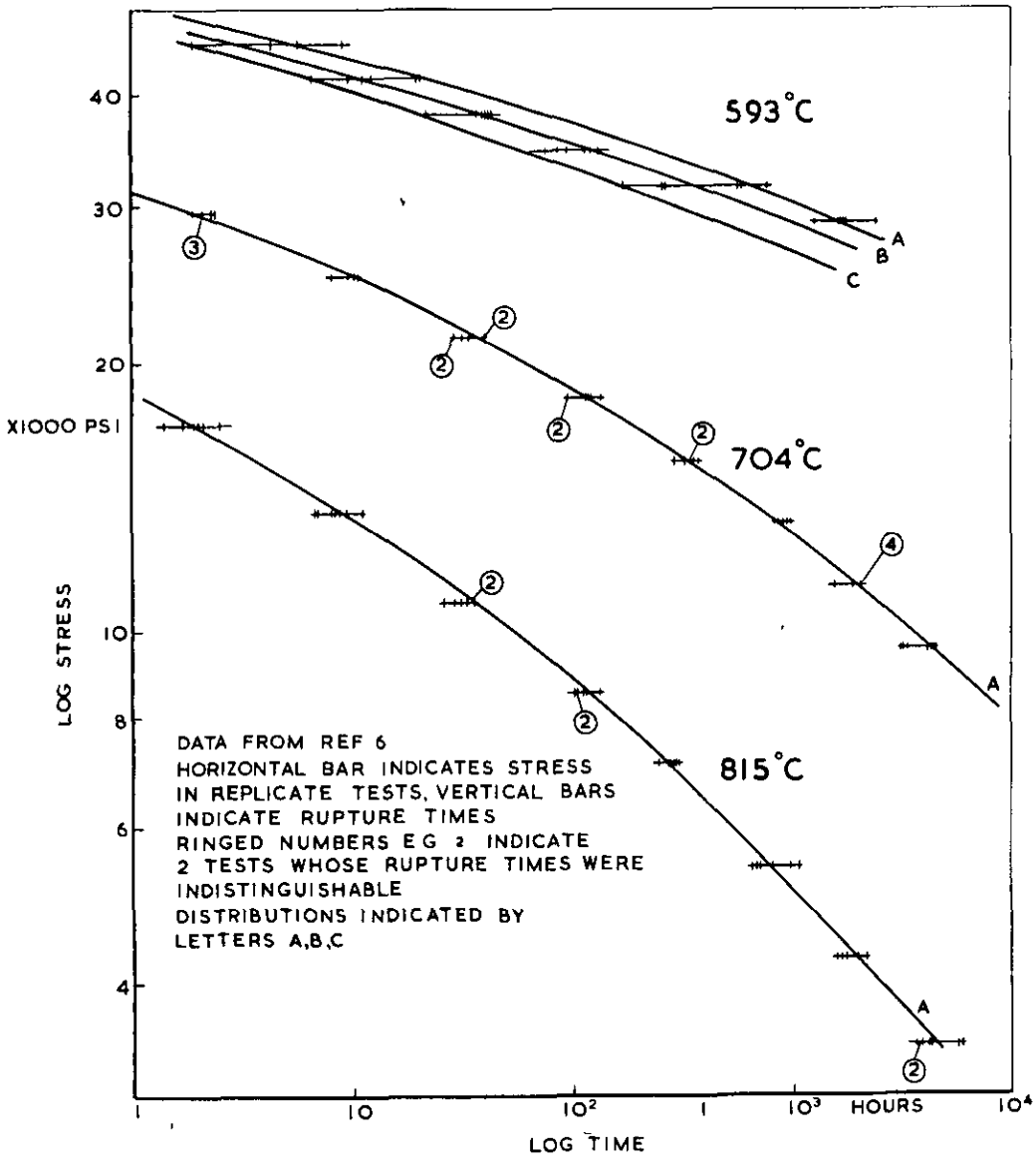

RUPTURE DATA, INCLUDING REPLICATE TEST RESULTS, FOR SINGLE CAST OF 18-12-Mo STEEL

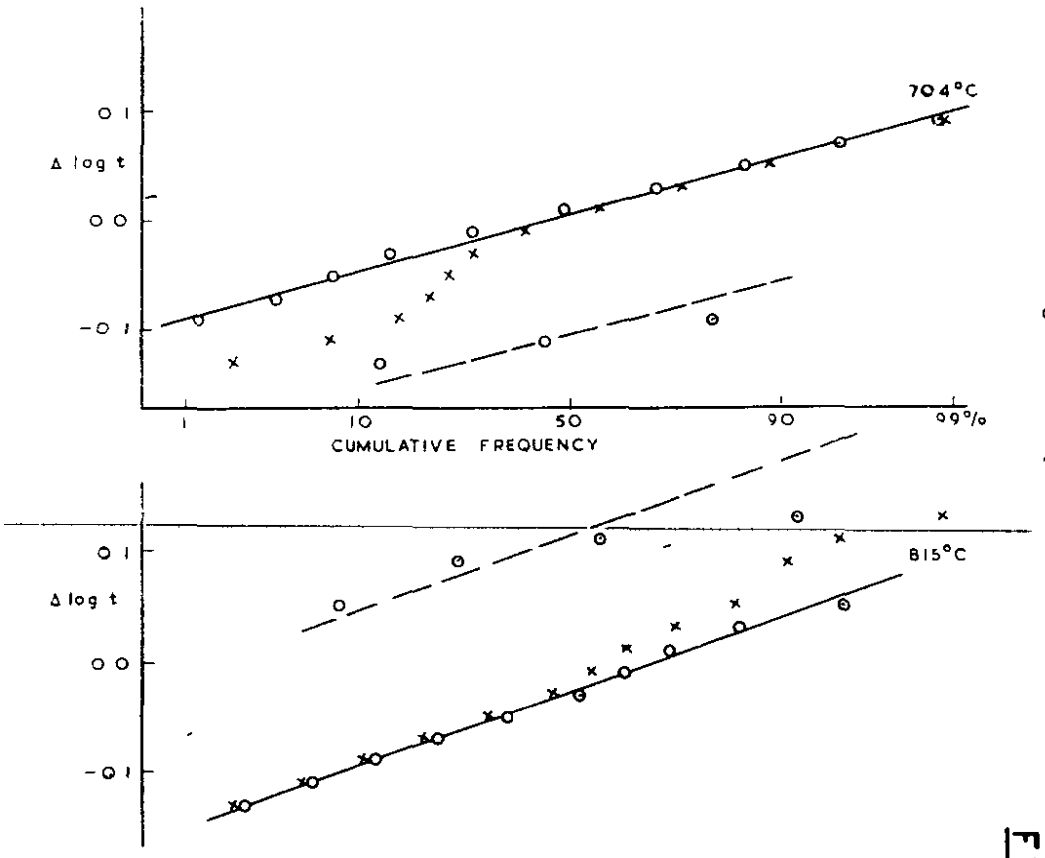

OGIVES OF SCATTER IN FIG. 12 AT 704°C AND 815°C.

FIG. 12 (a)

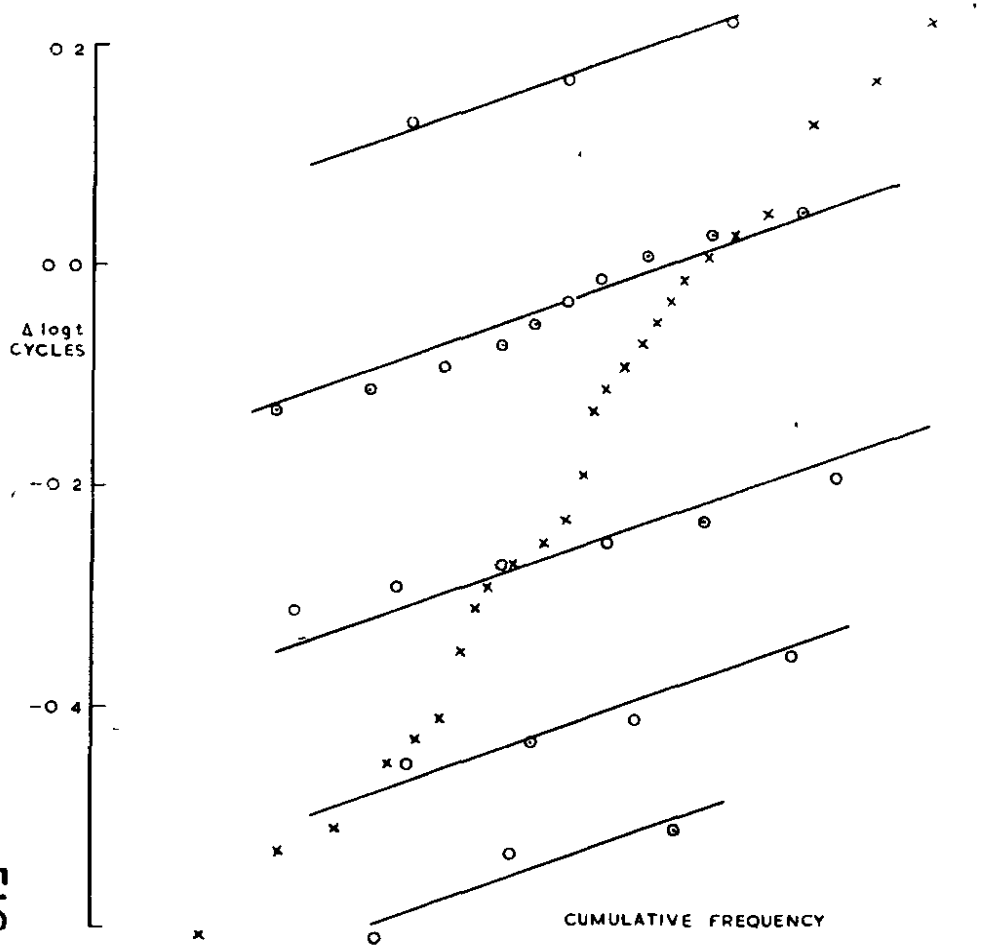

OGIVE OF SCATTER IN FIG. 12 AT 593° C.

FIG. 12 (b)

FIG 13

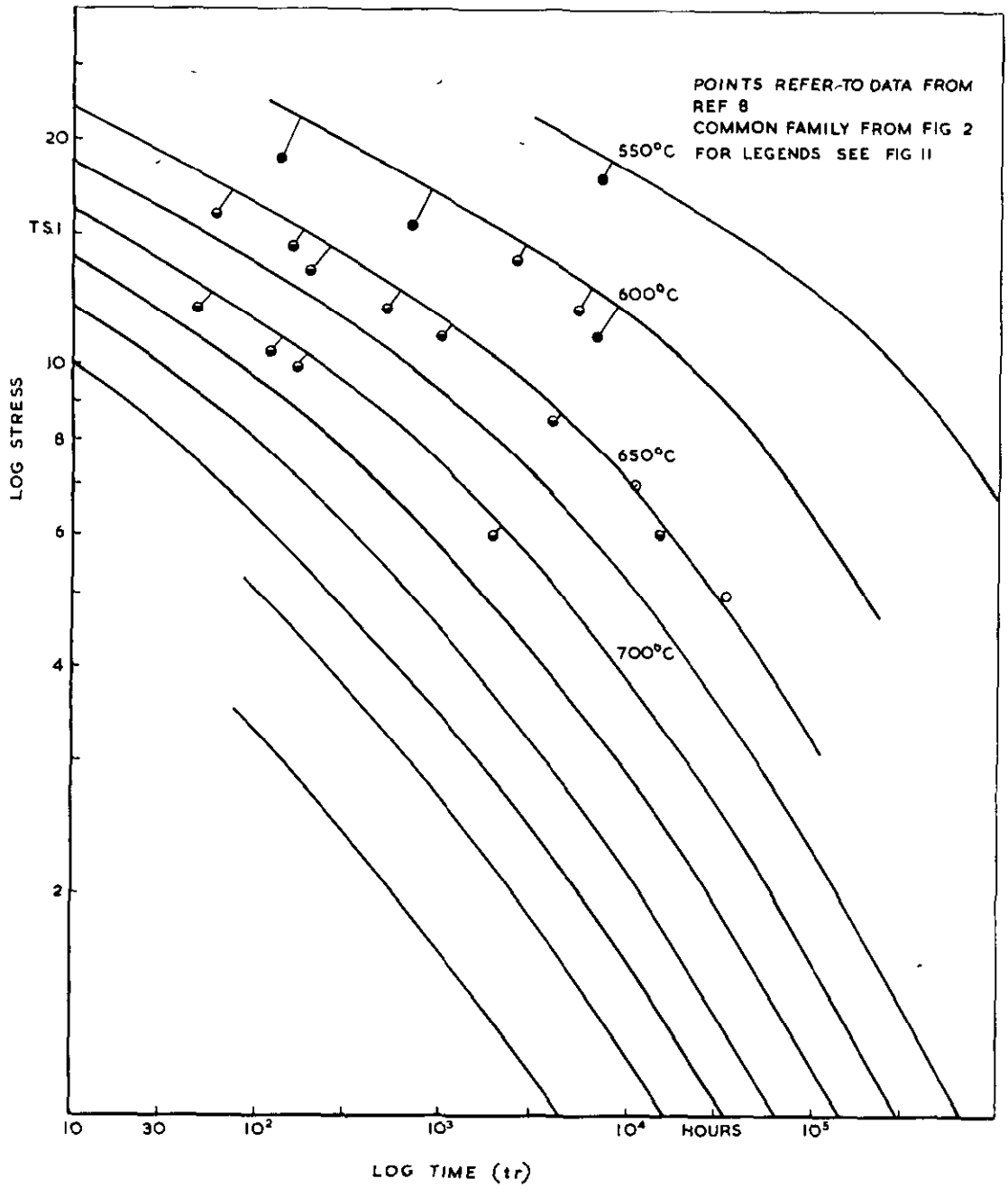

RUPTURE DATA FOR SINGLE CAST OF 18-12-Nb STEEL (REF. 8)

FIG. 13(a)

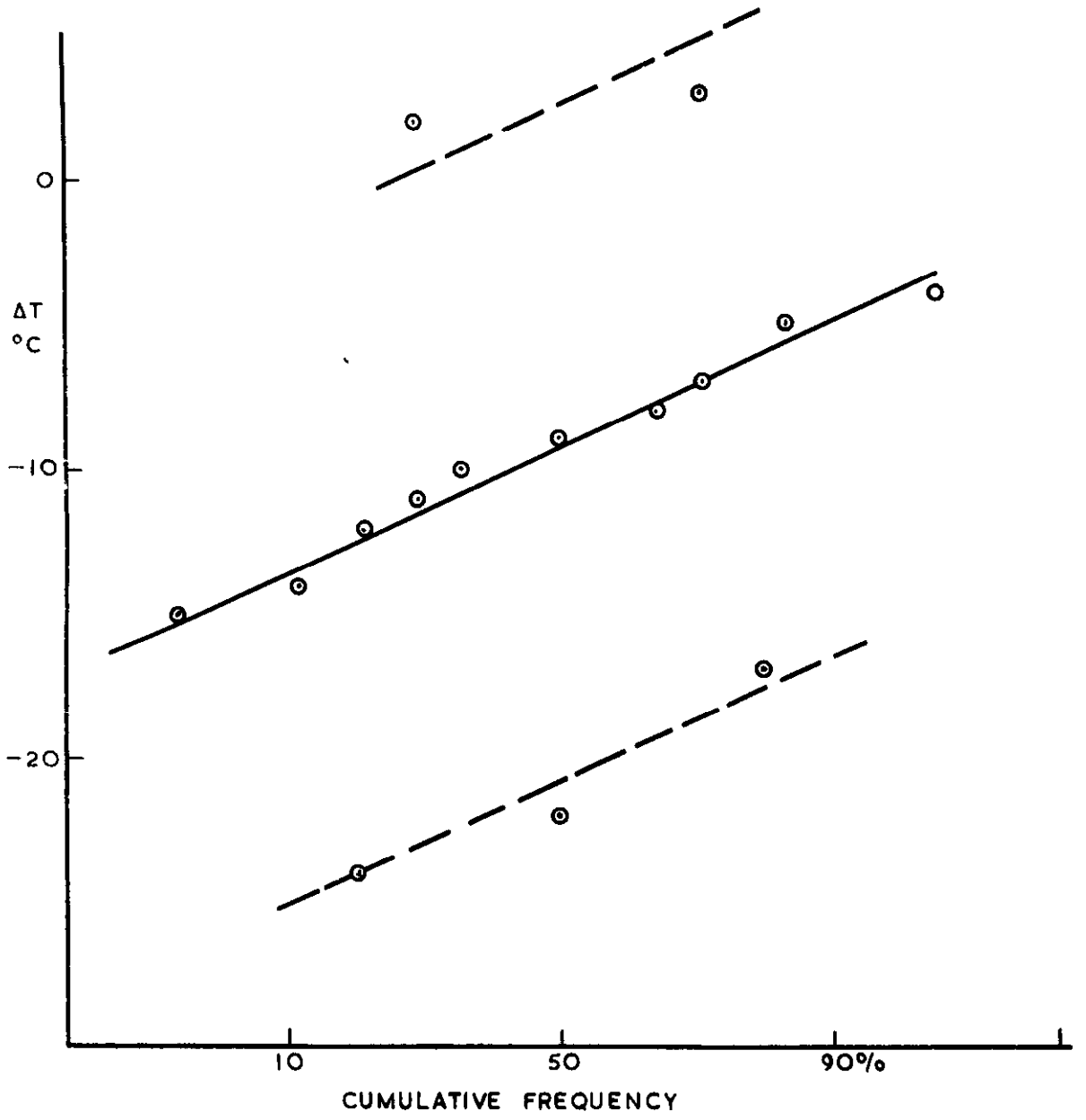

OGIVE OF SCATTER IN FIG. 13

FIG 14

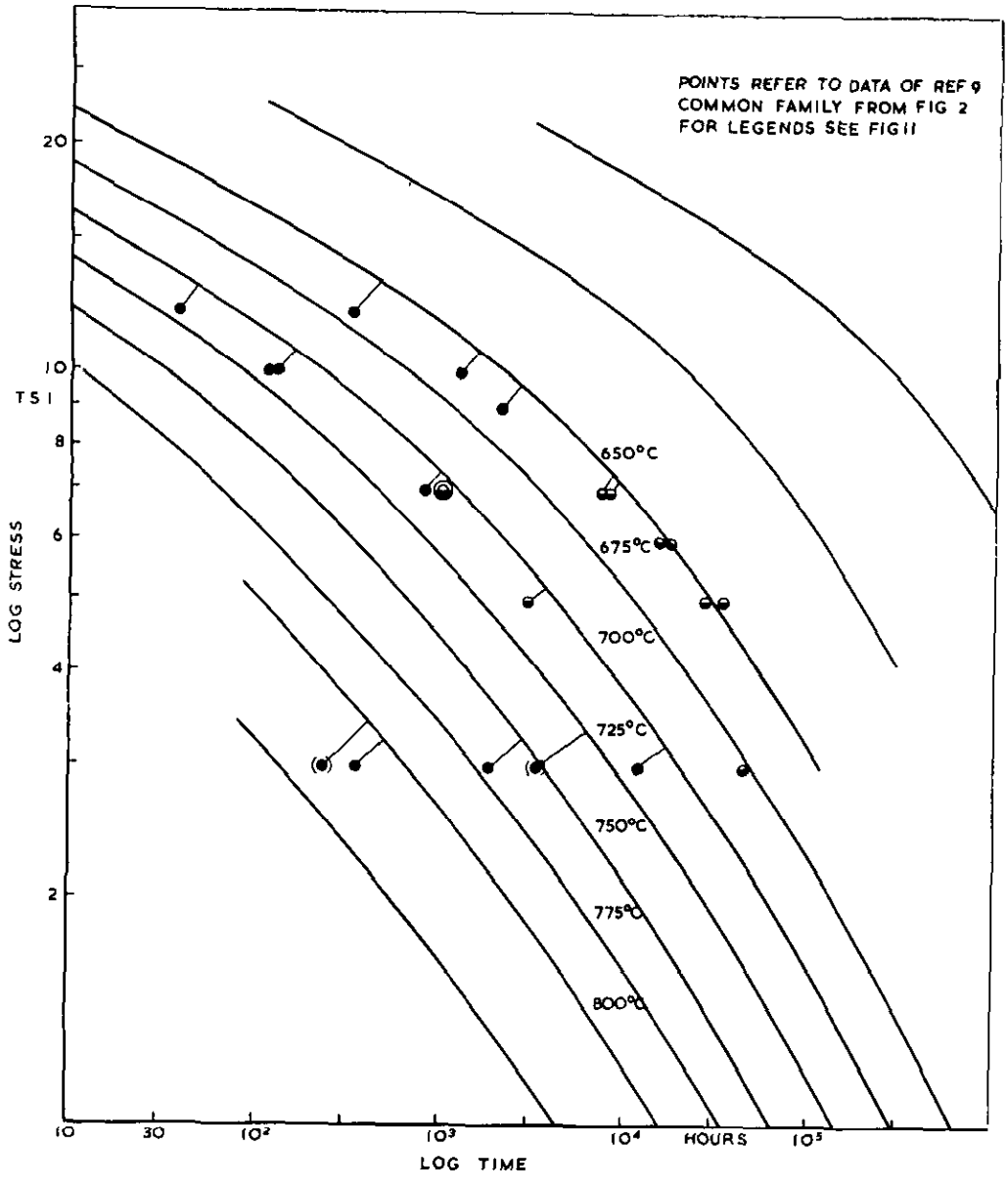

RUPTURE DATA FOR SINGLE CAST OF 18-12-Nb STEEL IN FORM OF SUPER HEATER TUBE

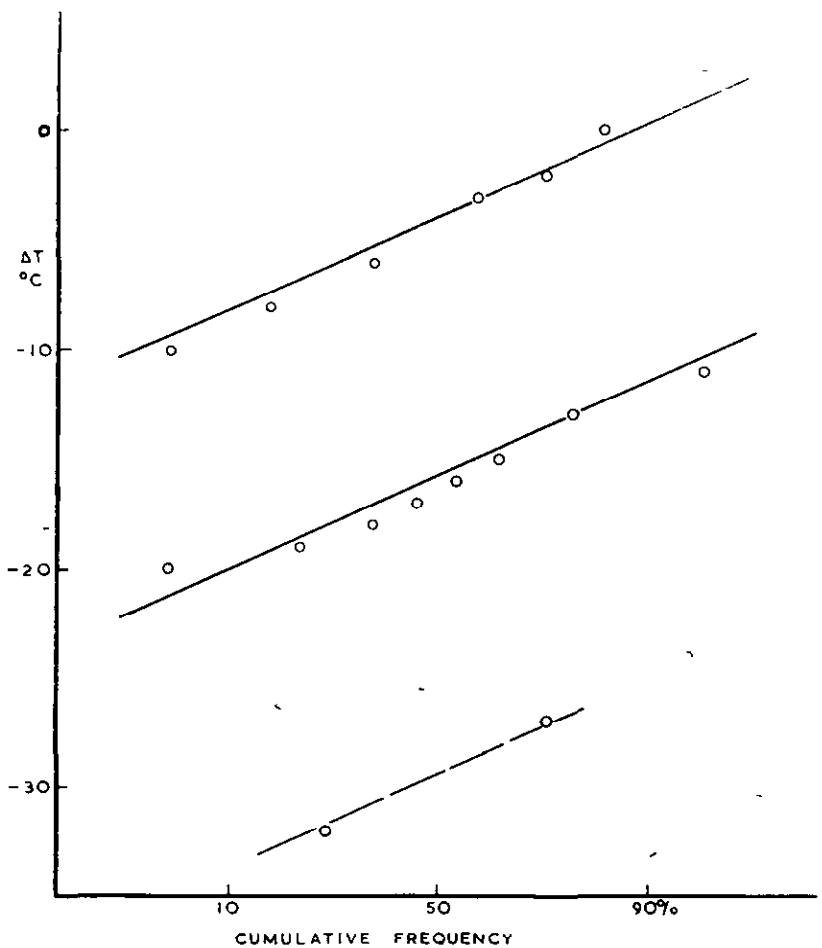

OGIVE OF SCATTER IN FIG 14.

FIG. 14 (a)

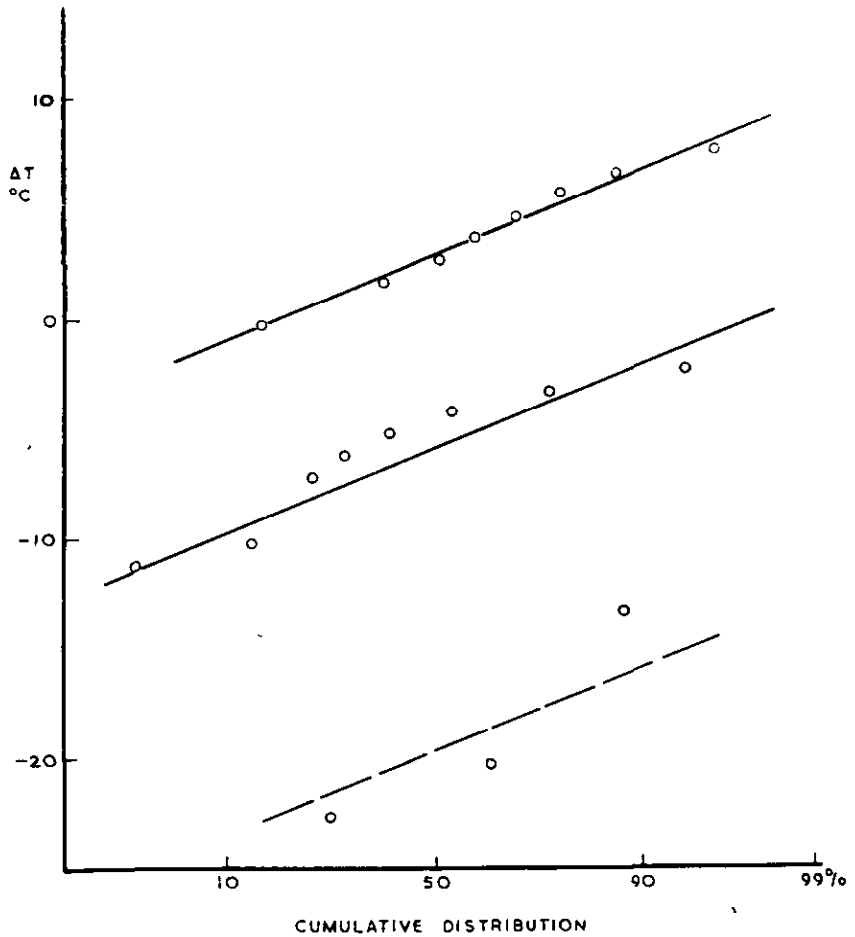

OGIVE OF SCATTER IN FIG. 15.

FIG. 15 (a)

FIG. 15

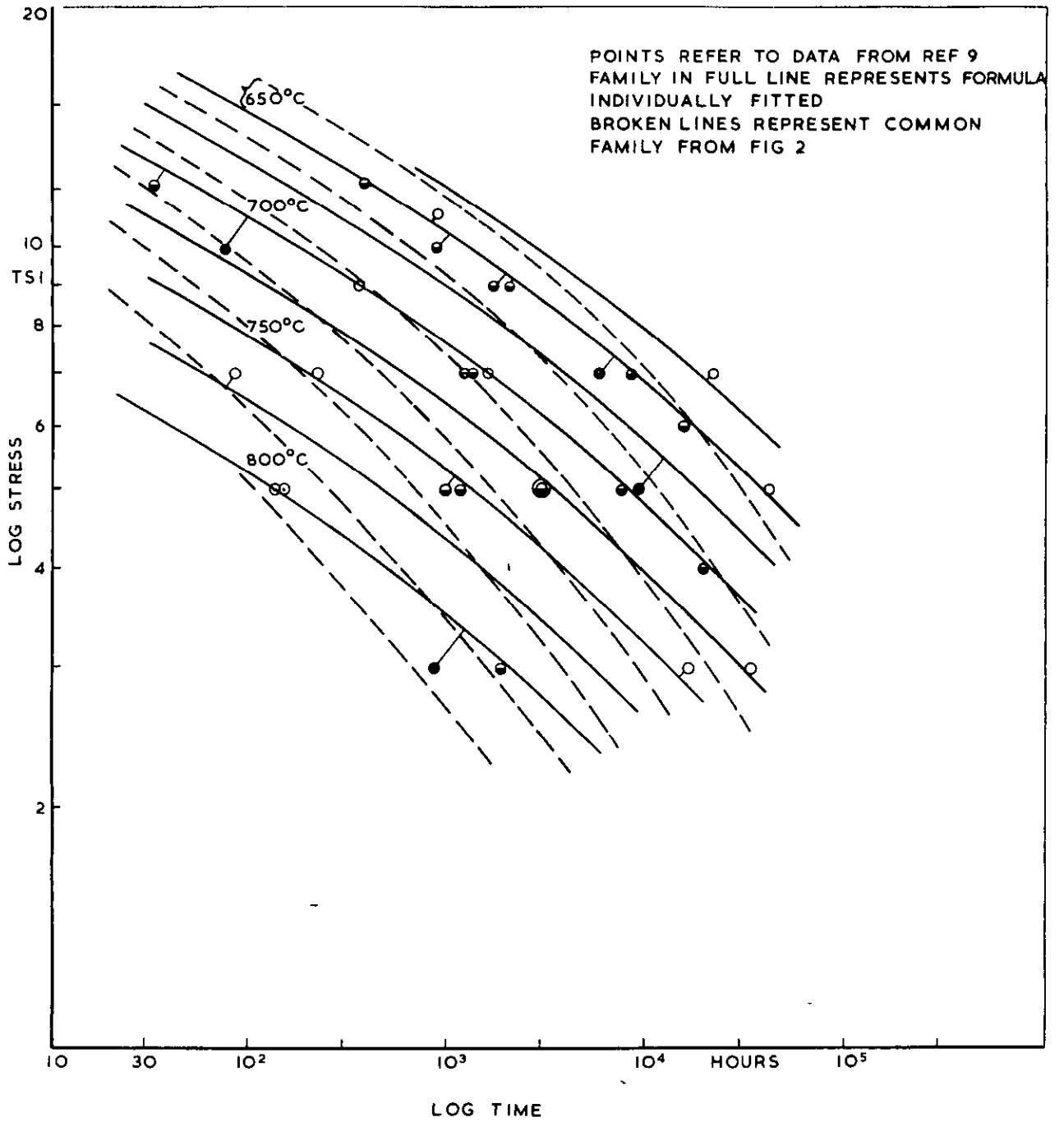

RUPTURE DATA OF REF 9 FOR 18–12–Nb IN FORM OF STEAM–TUBE.

FIG 16

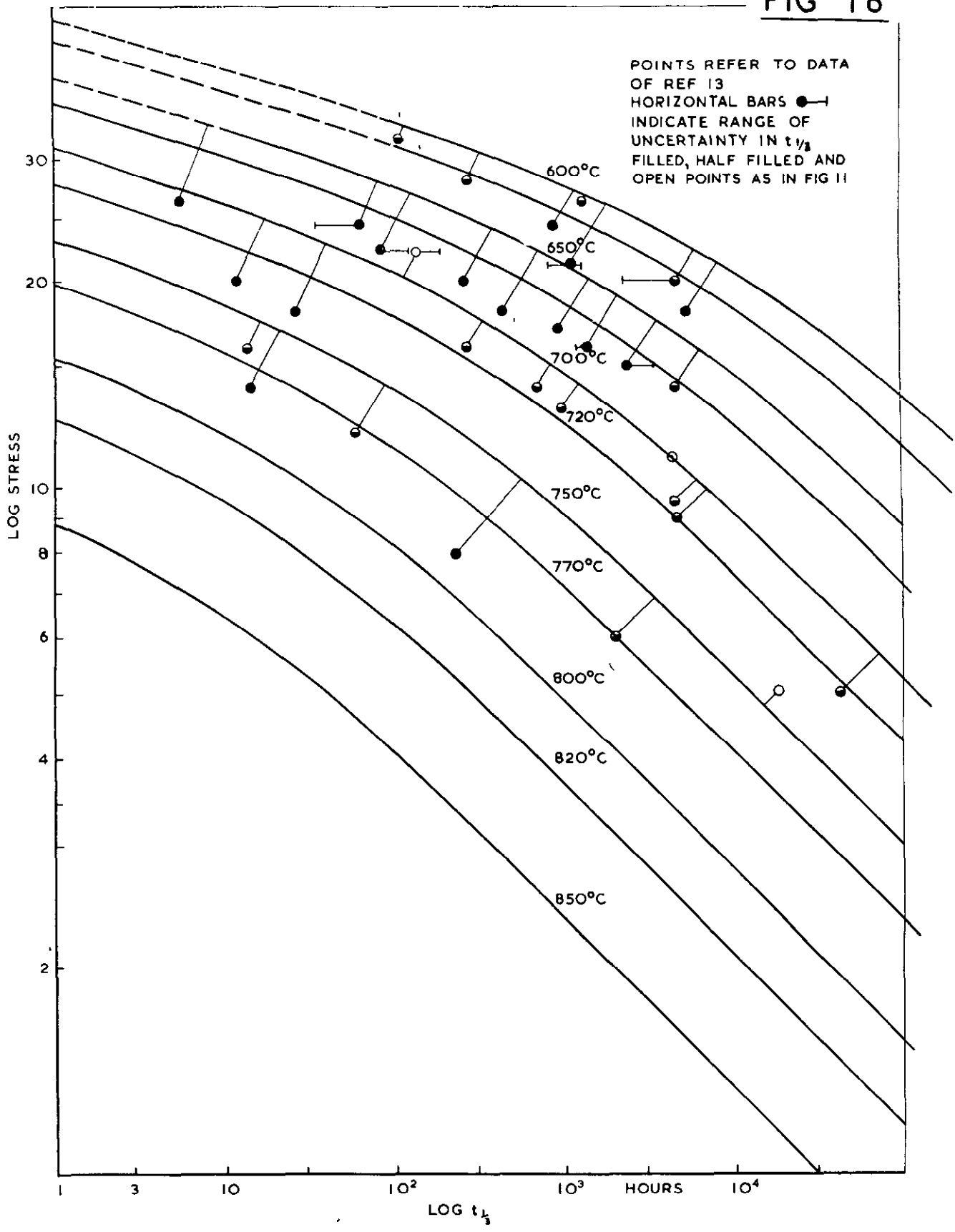

COMMON LOG STRESS vs LOG $t_{\frac{1}{3}}$ FAMILY FOR

NIMONICS 80 AND 80A

FIG. 17

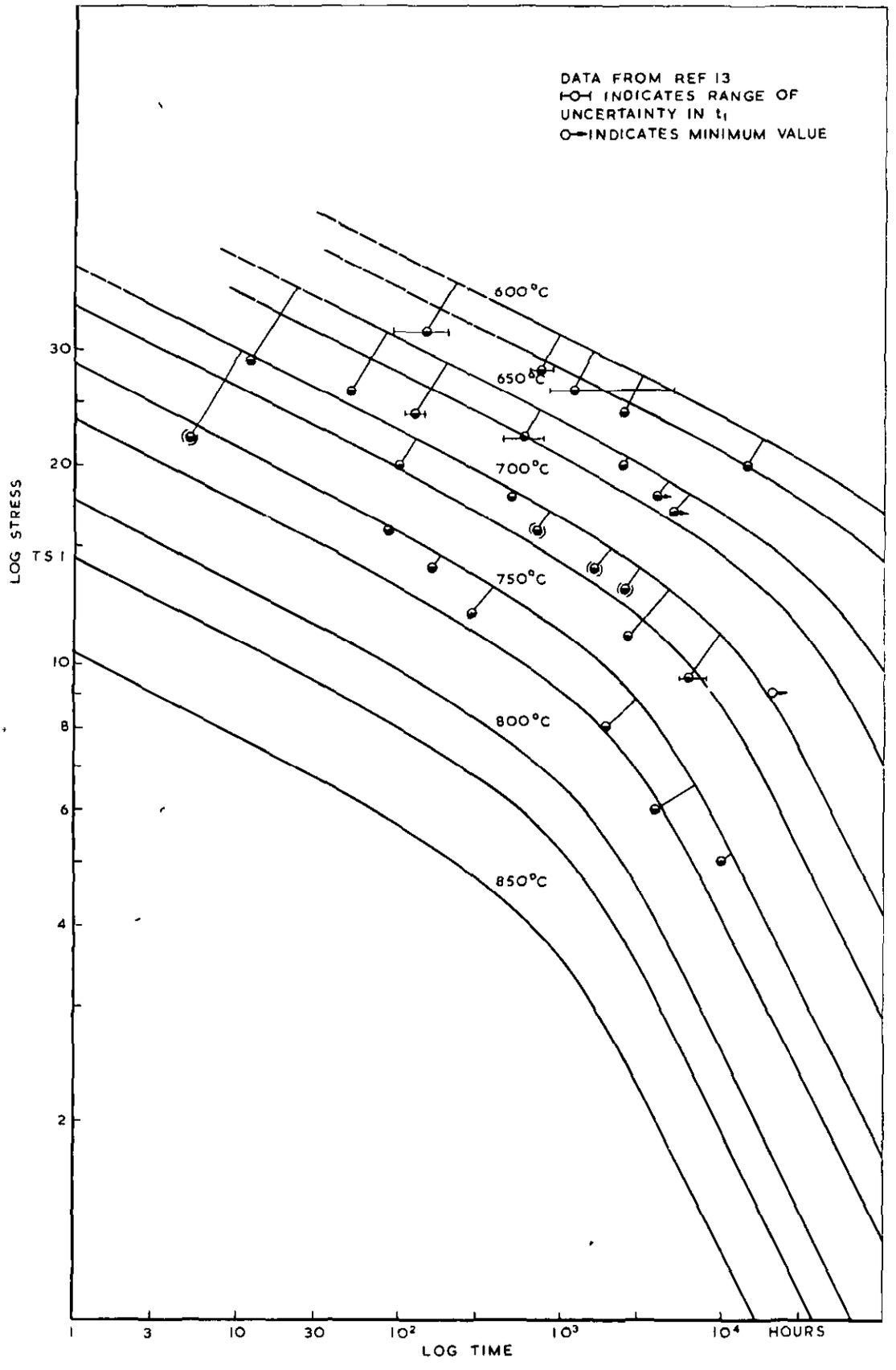

COMMON LOG STRESS vs LOG t, FAMILY FOR

NIMONICS 80,80A.

FIG. 18

DATA FROM REF 13

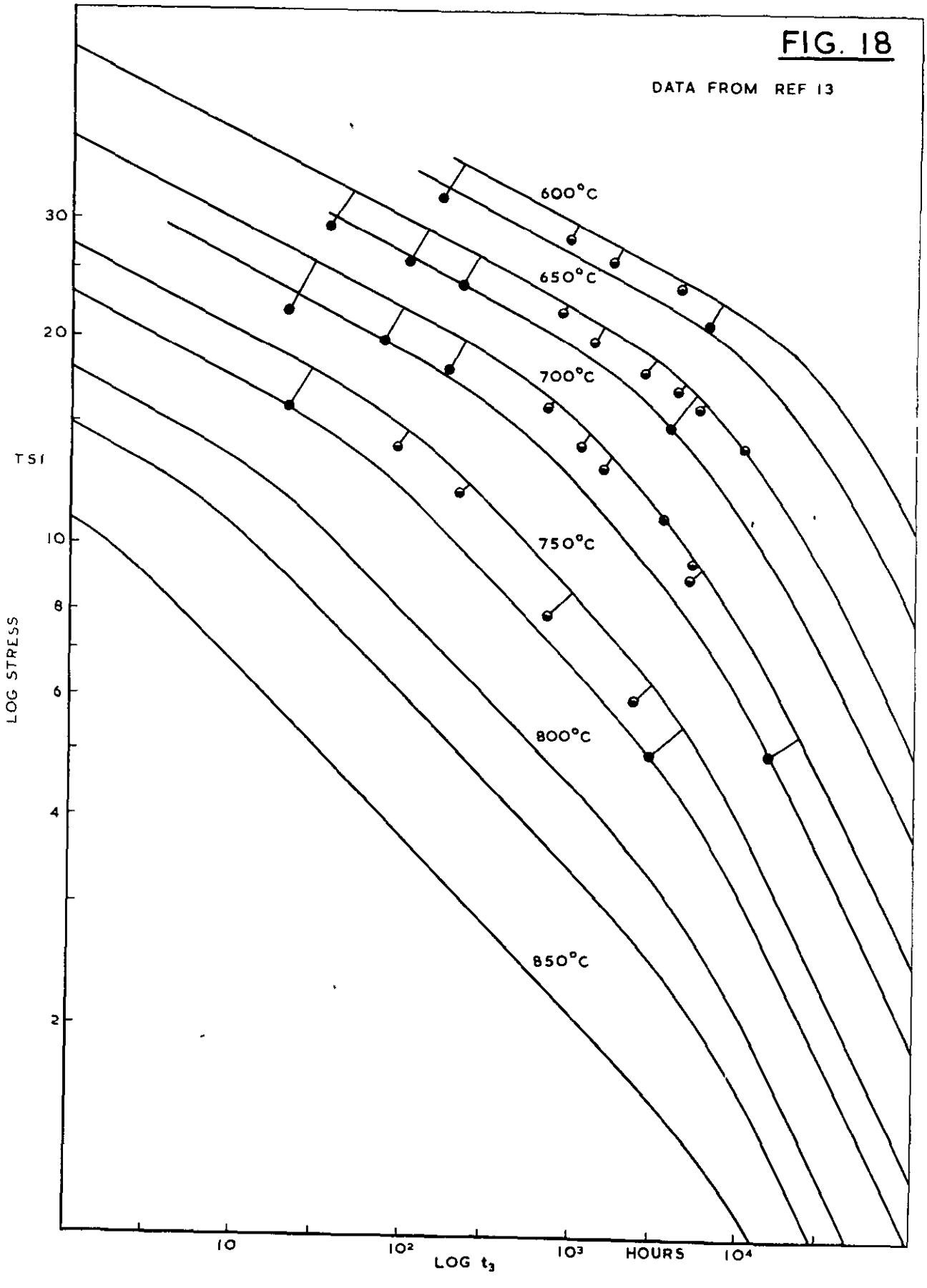

COMMON LOG STRESS vs LOG t_3 FAMILY

FOR NIMONICS 80, 80A

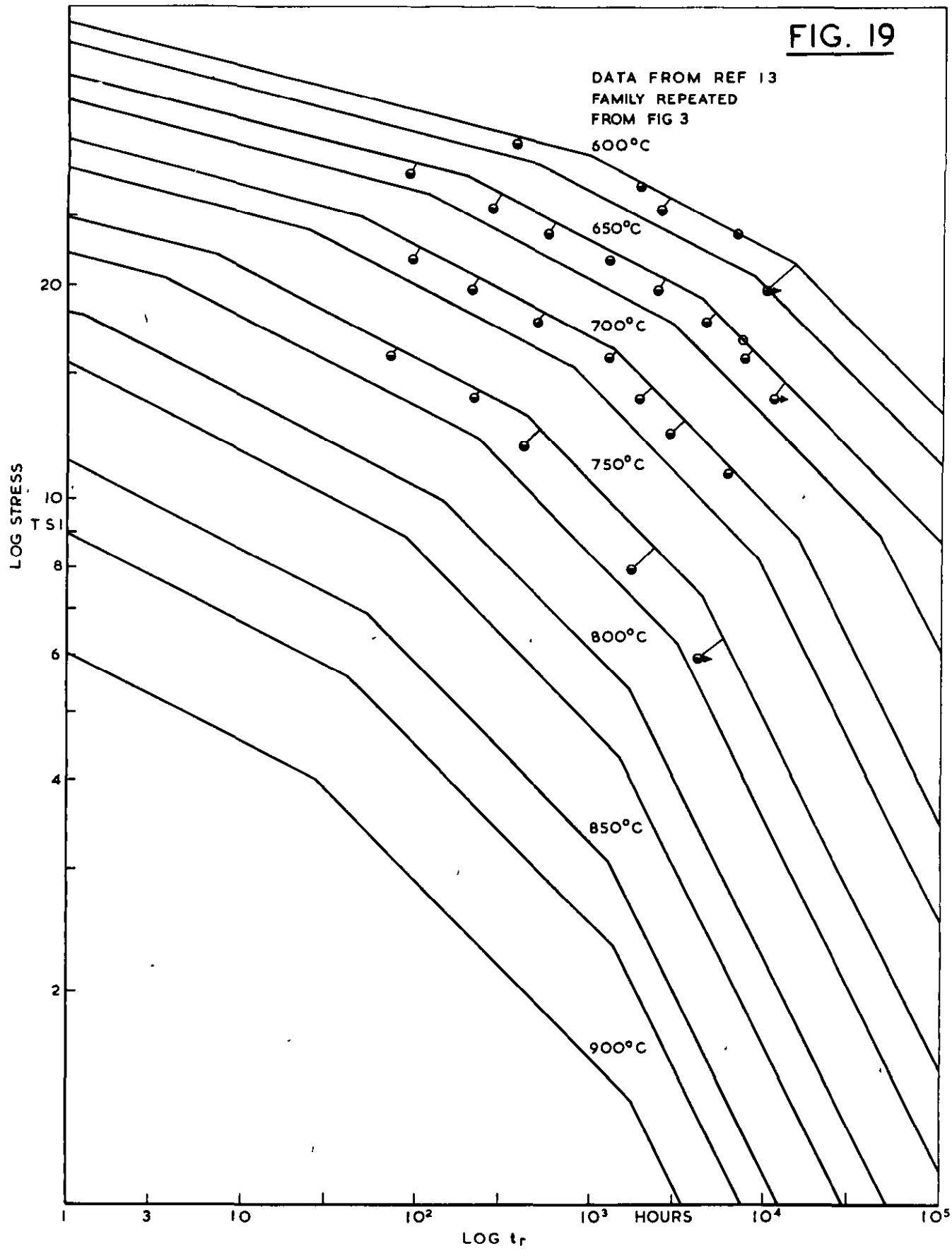

COMMON LOG STRESS vs LOG t_r FAMILY

FOR NIMONICS 80 AND 80A.

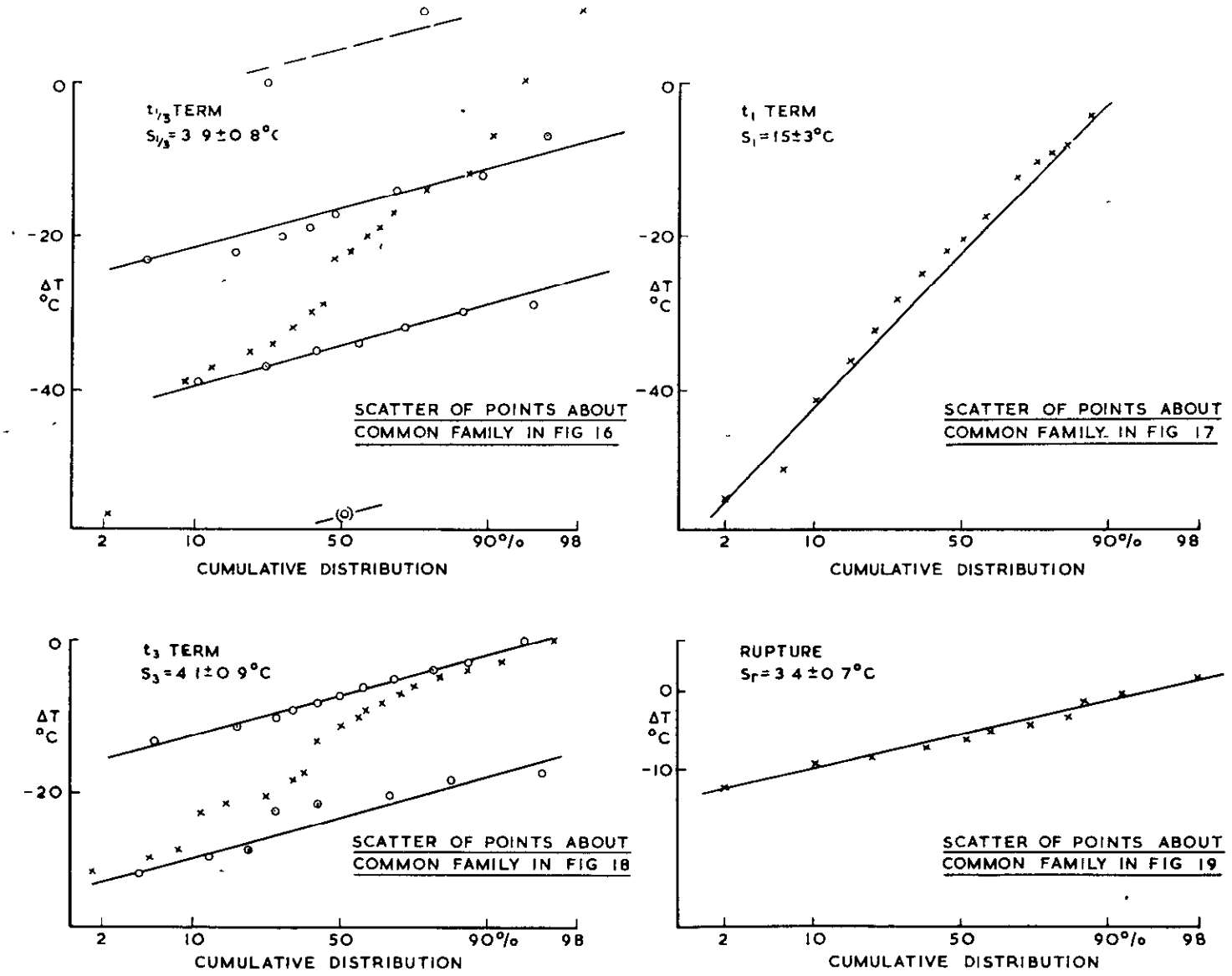

DISTRIBUTION OF SCATTER IN CREEP AND RUPTURE TIMES FOR ONE CAST OF NIMONIC 80 ABOUT COMMON FAMILIES

FIG 20

FIG 21

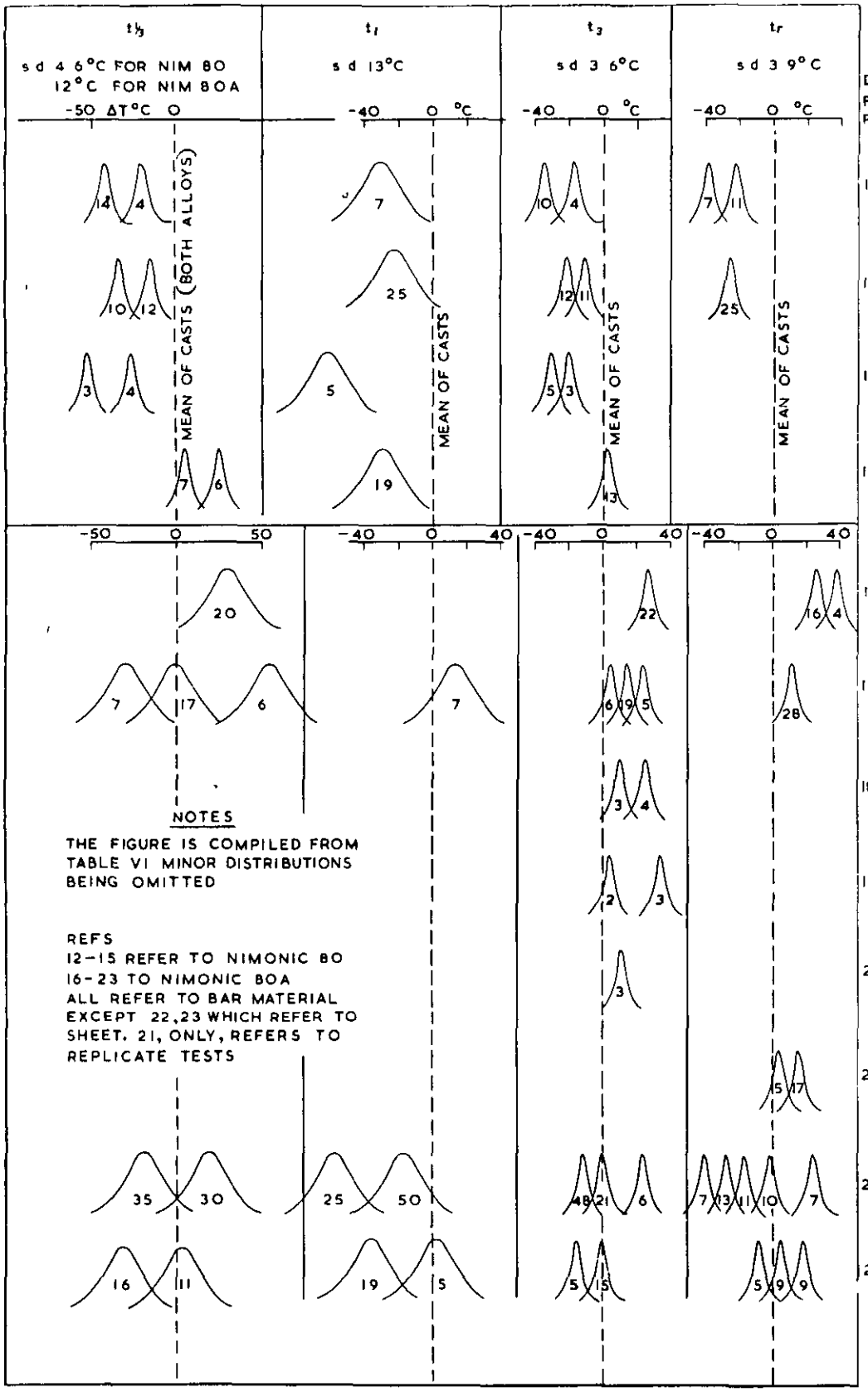

ABSCISSA DEVIATIONS IN TEMPERATURE TO SCALE
ORDINATE : FREQUENCY OF OCCURENCE SCHEMATIC
NUMBERS UNDER CURVES INDICATE NUMBER OF TEST RESULTS IN CORRESPONDING COMPONENT

DIAGRAMMATIC SUMMARY OF SCATTER OF NIMONICS 80 & 80A

ABOUT COMMON FAMILIES

FIG. 22

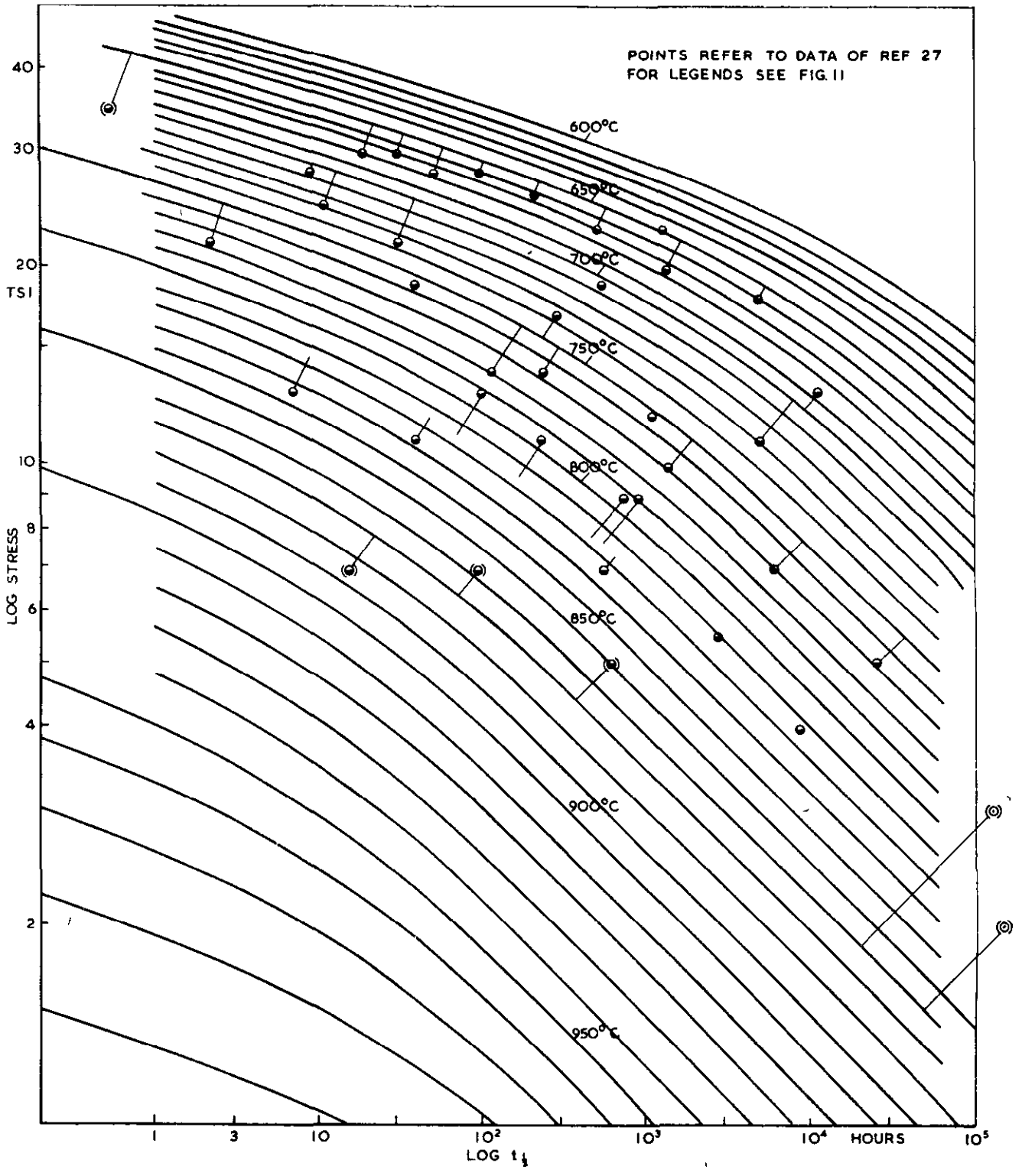

COMMON LOG STRESS vs LOG $t_{\frac{1}{2}}$ FAMILY FOR NIMONIC 90

FIG 23

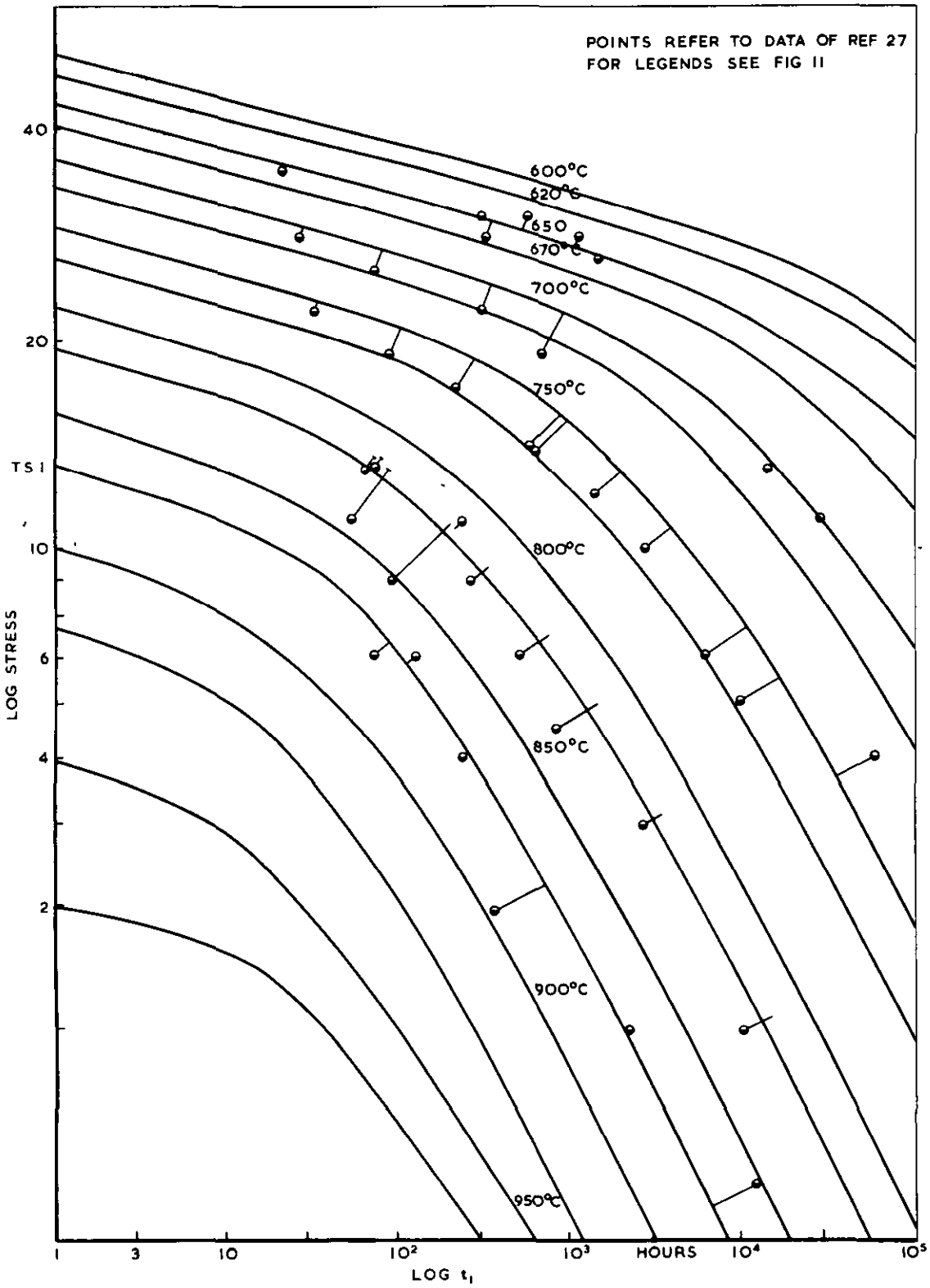

COMMON LOG STRESS vs LOG t_1 FAMILY FOR NIMONIC 90

Fig.24

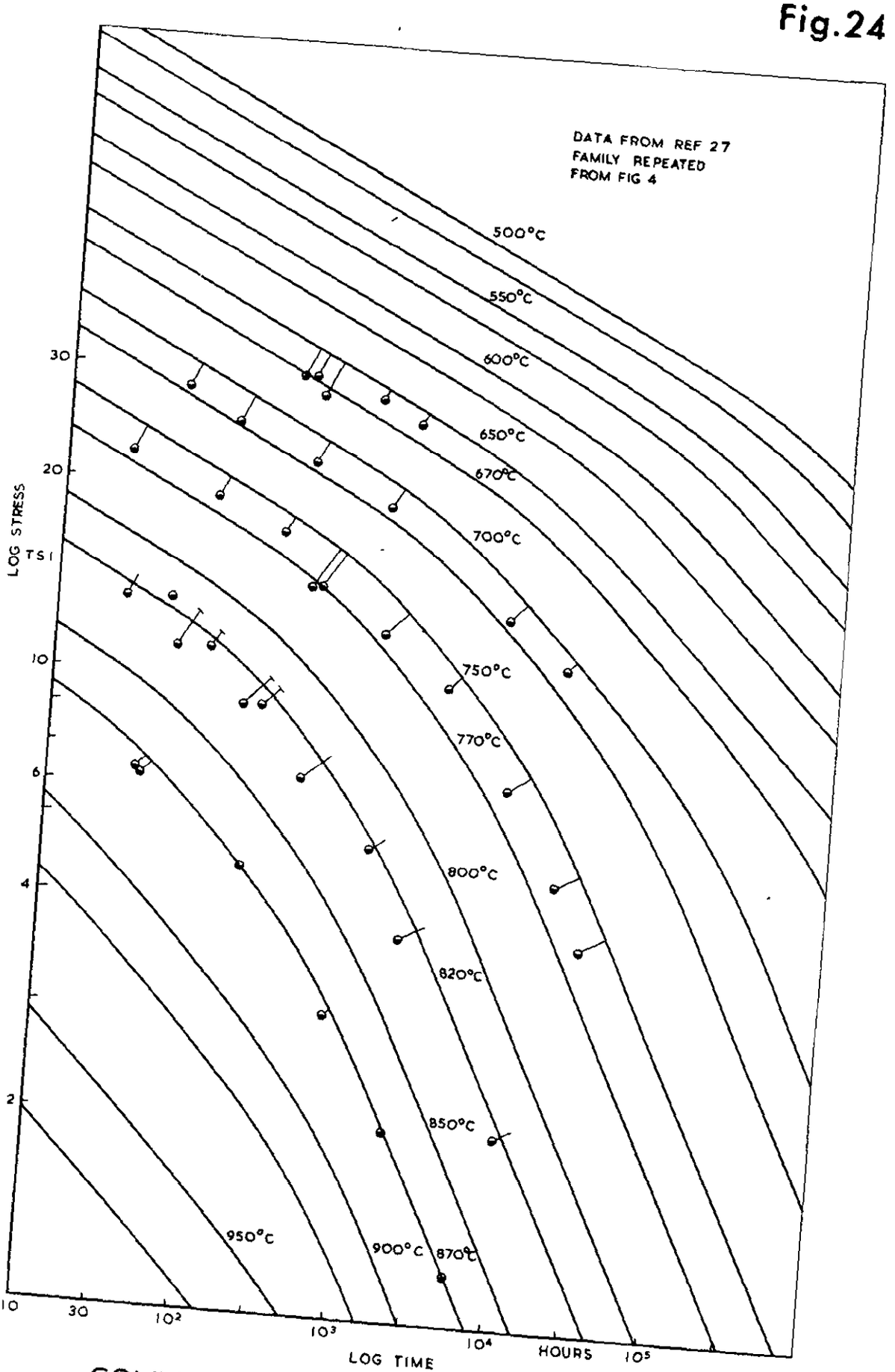

COMMON LOG STRESS vs LOG t_3 FAMILY FOR NIMONIC 90.

FIG. 25

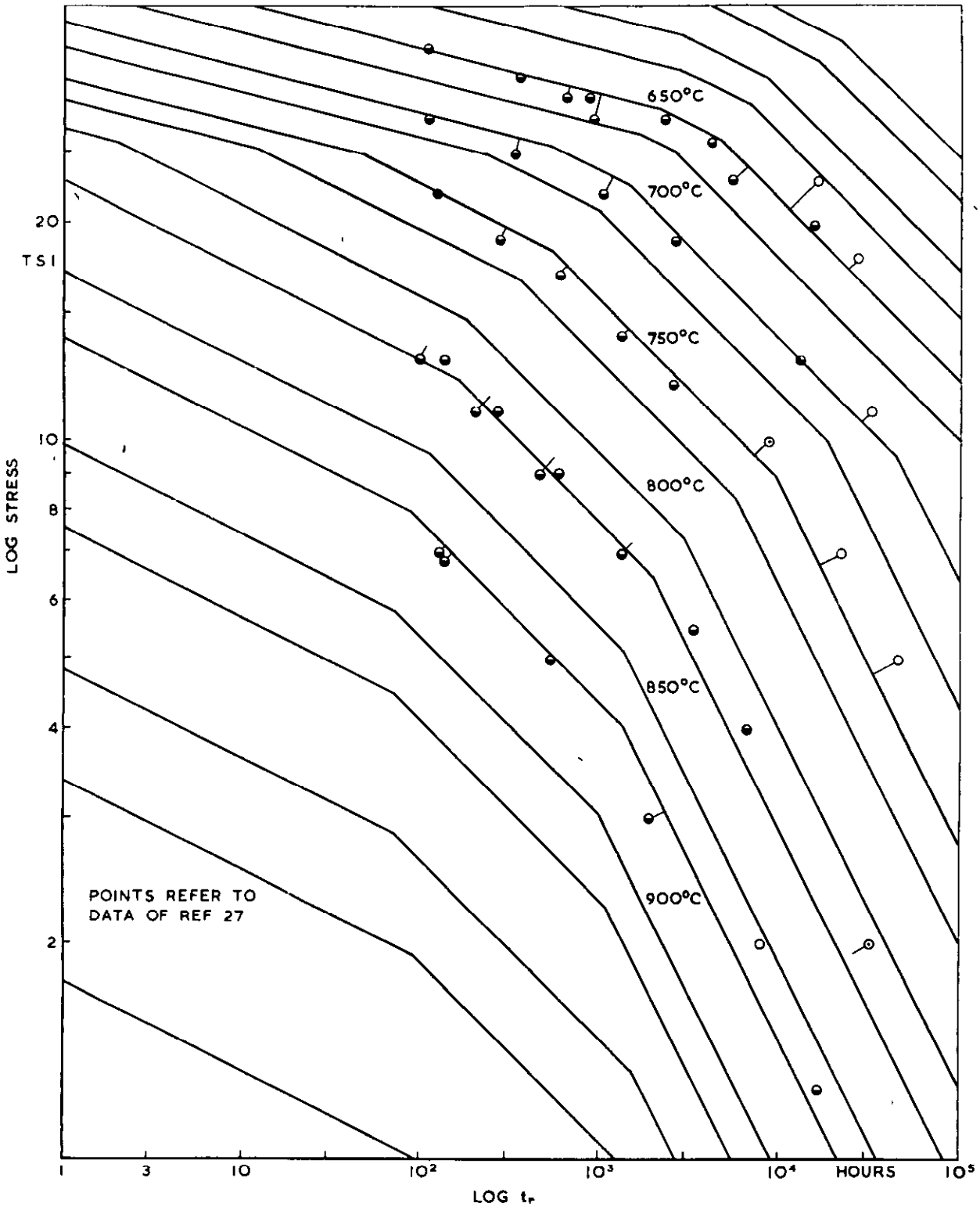

COMMON LOG STRESS vs LOG t_r FAMILY FOR NIMONIC 90

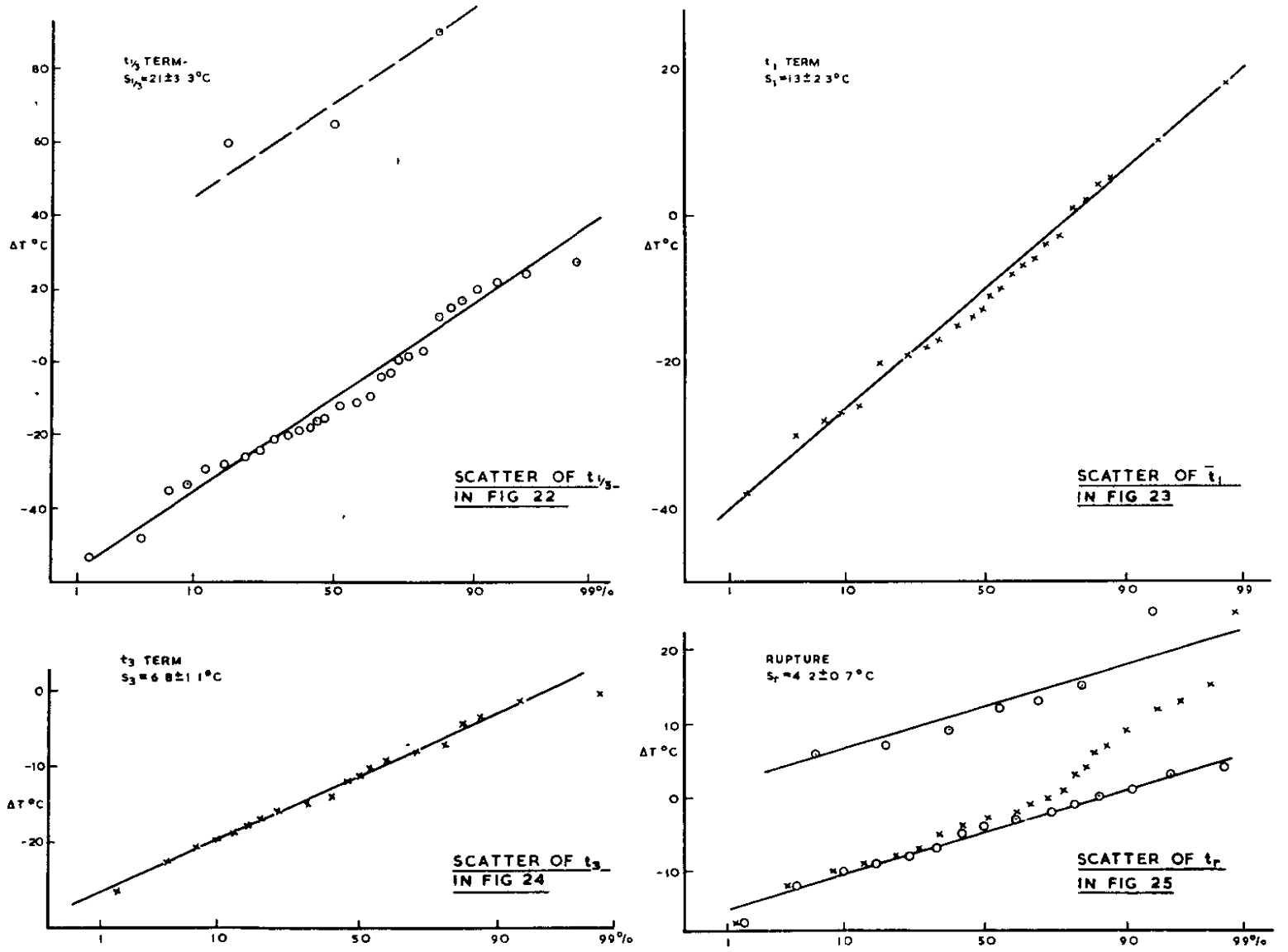

DISTRIBUTION OF SCATTER IN CREEP AND RUPTURE TIMES FOR ONE CAST OF NIMONIC 90 ABOUT COMMON FAMILIES

FIG. 26

FIG 27

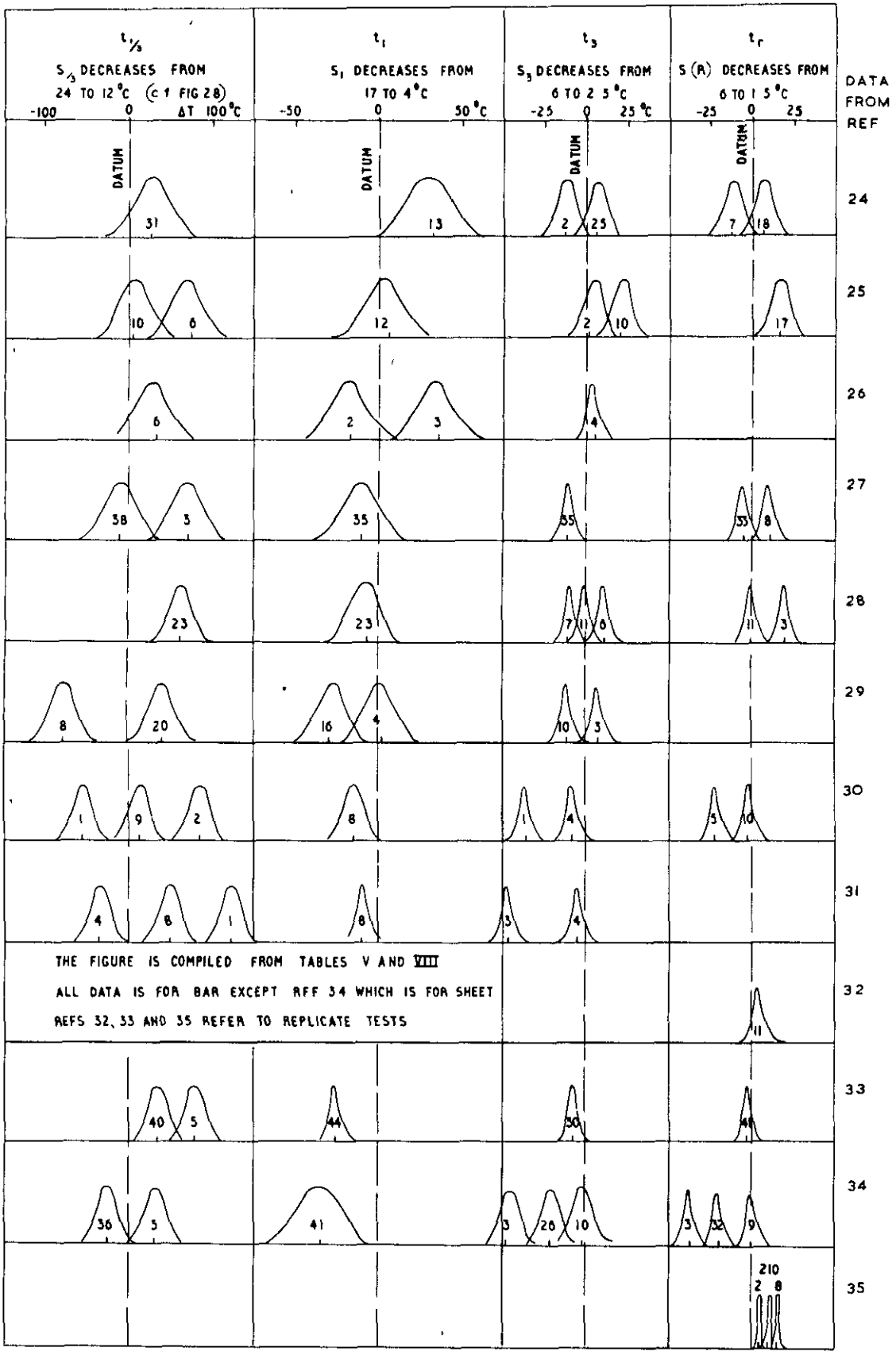

ABSCISSA DEVIATIONS IN TEMPERATURE, TO SCALE
ORDINATE. FREQUENCY OF OCCURENCE, SCHEMATIC
NUMBERS UNDER COMPONENT DISTRIBUTIONS INDICATE
NUMBER OF VALUES IN THAT COMPONENT

DIAGRAMMATIC SUMMARY OF SCATTER OF NIMONIC 90

ABOUT COMMON FAMILIES

FIG 28

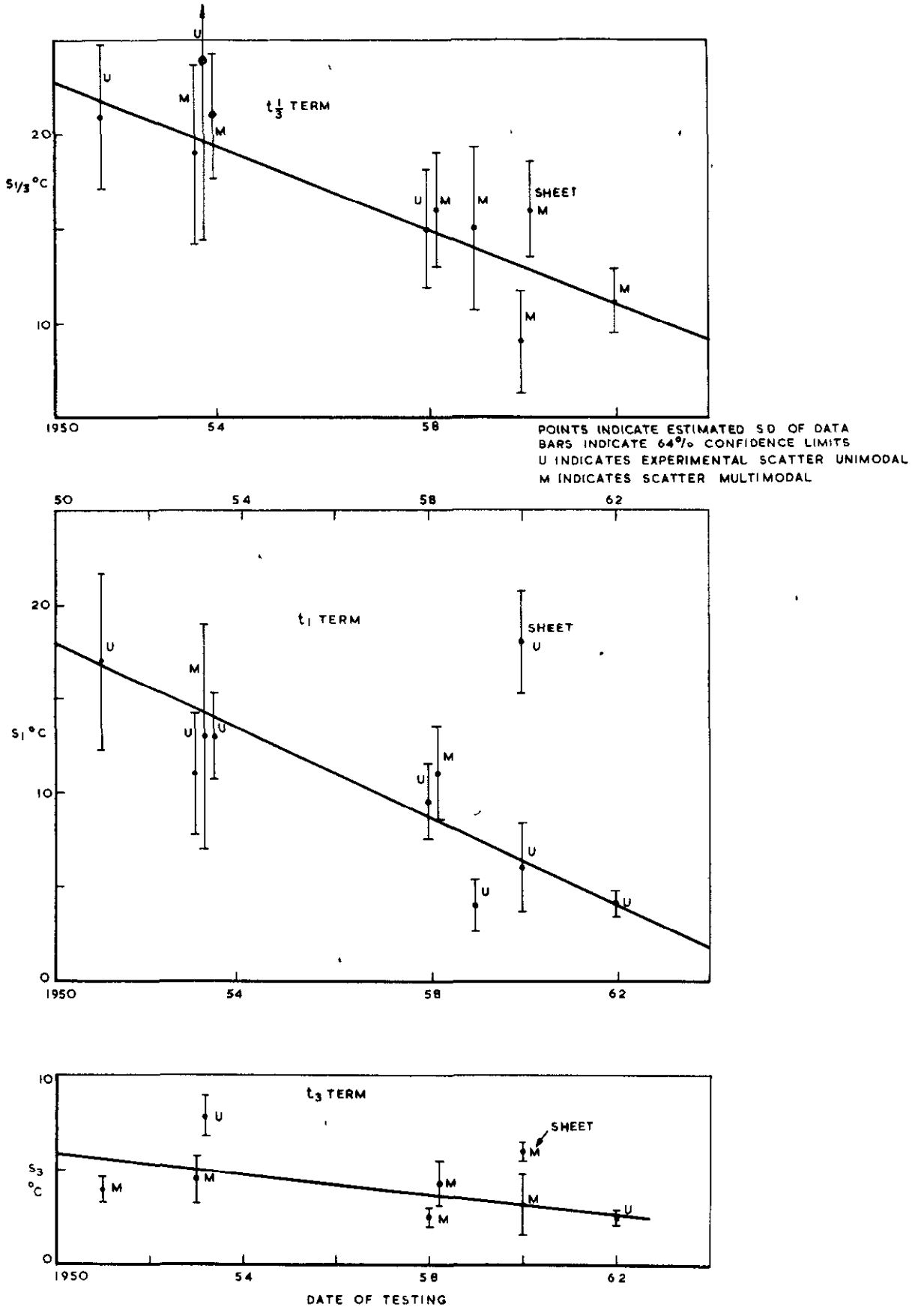

S.D OF NIMONIC 90 CREEP VS DATE OF TESTING.

FIG 29

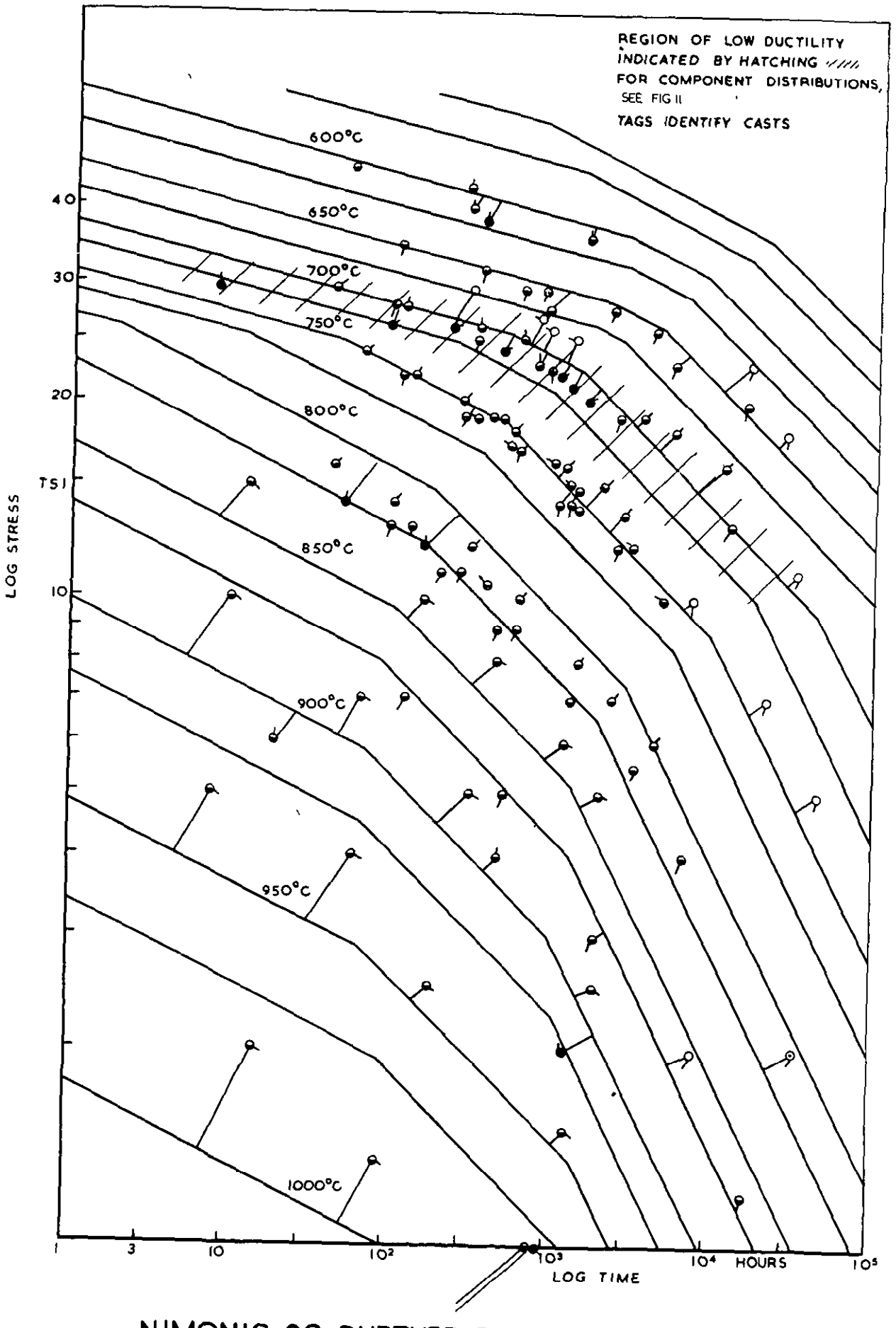

NIMONIC 90 RUPTURE DATA FOR FIVE CASTS

INDICATING DISTRIBUTION OF TRIMODAL CREEP

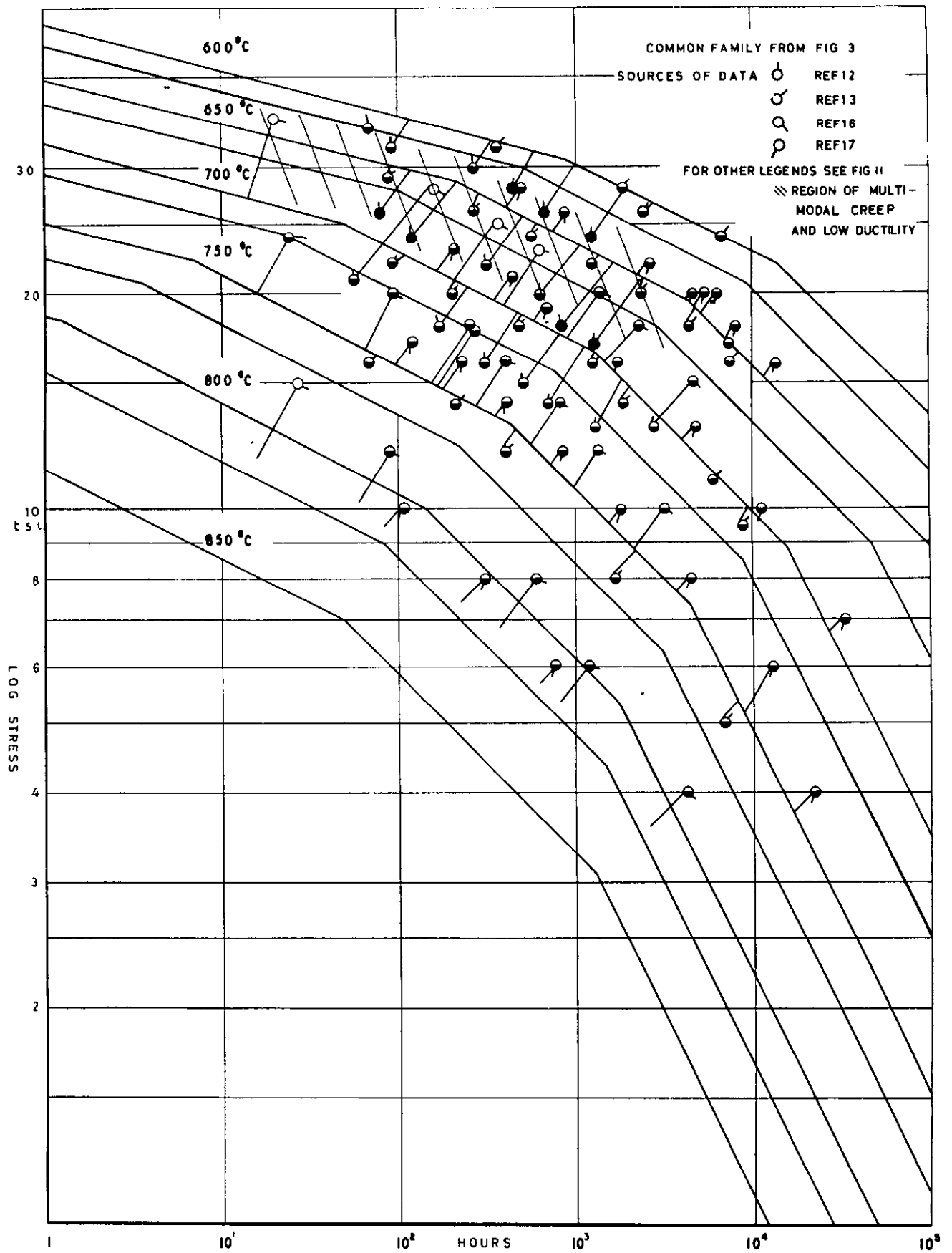

NIMONIC 80-80A RUPTURE DATA FOR FOUR CASTS INDICATING DISTRIBUTION OF TRIMODAL CREEP IN BAR

FIG. 31

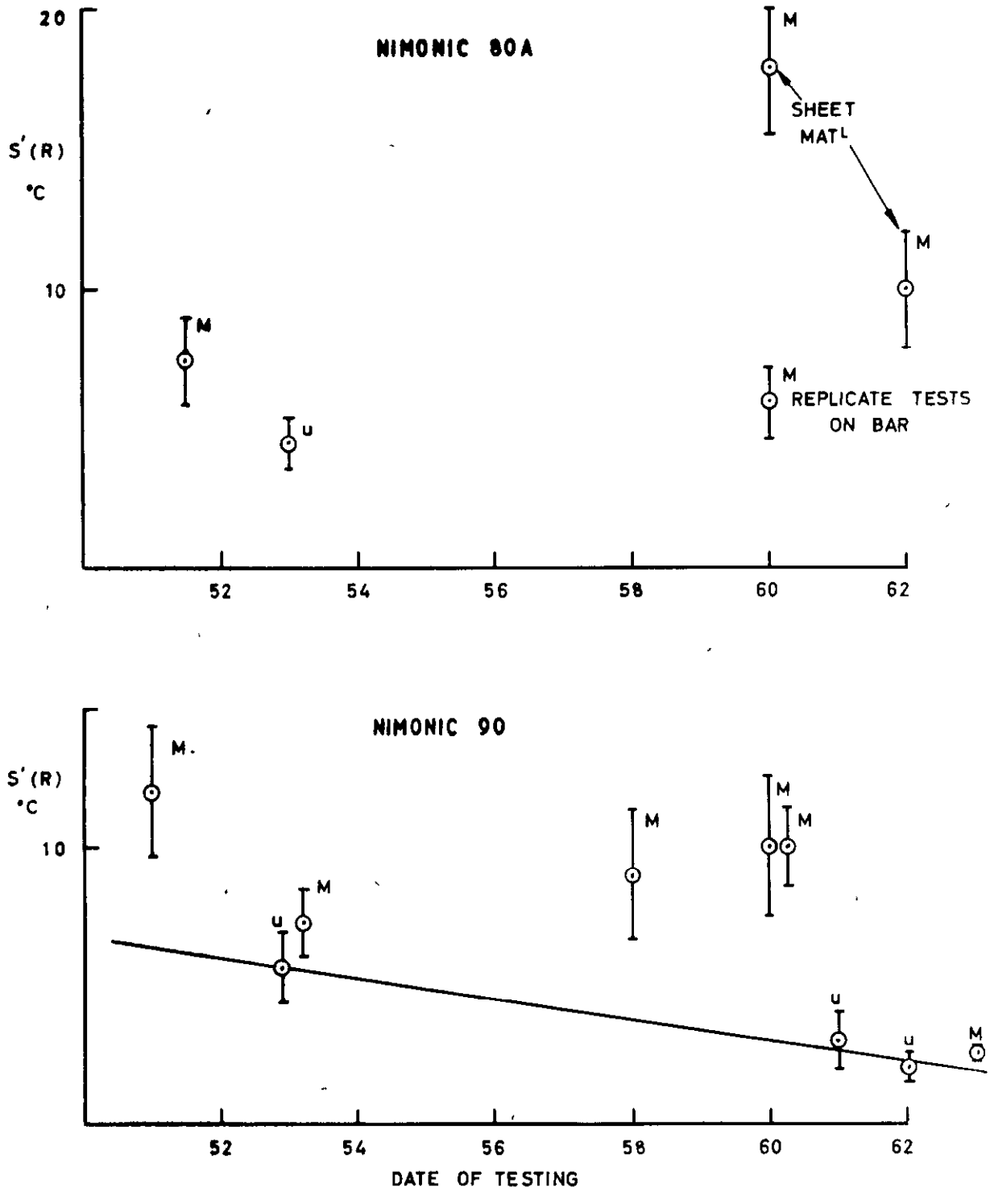

OVERALL STANDARD DEVIATION OF NIMONIC RUPTURE DATA vs DATE OF TESTING

FIG 32

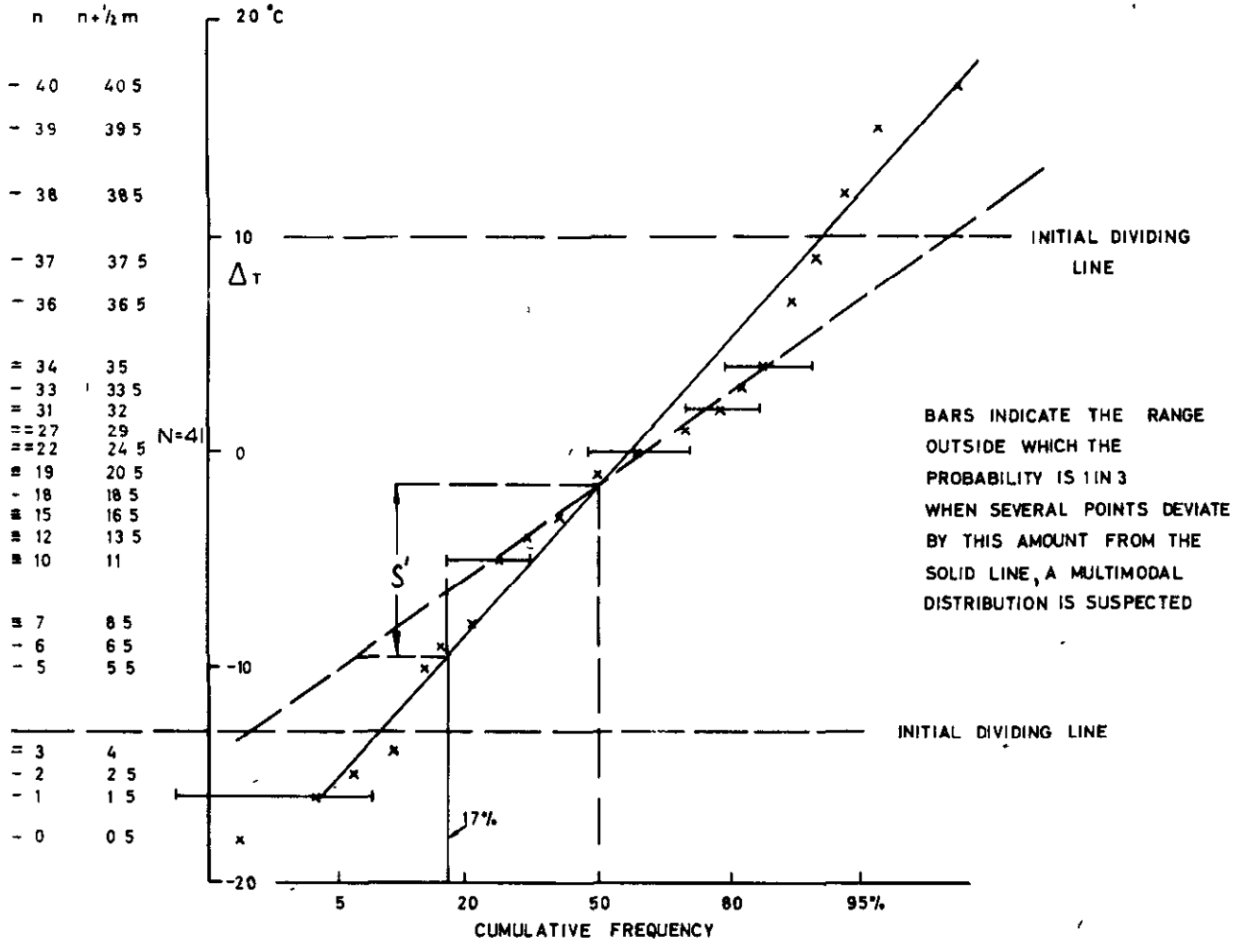

FIRST EXAMPLE-DIRECT PLOT OF SCATTER DATA

FIG 33

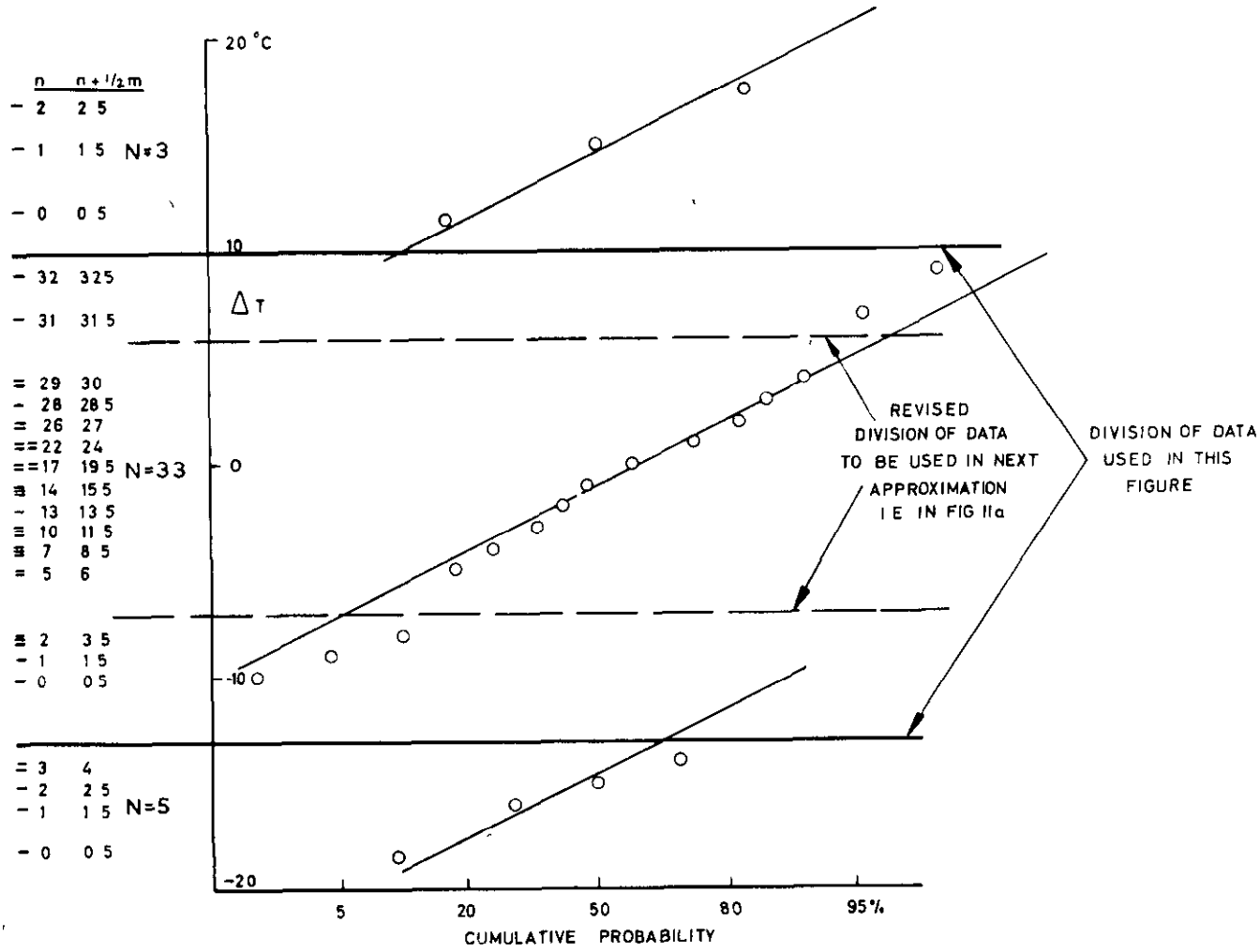

FIRST EXAMPLE - INITIAL DIVISION OF DATA INTO COMPONENTS

FIG 34

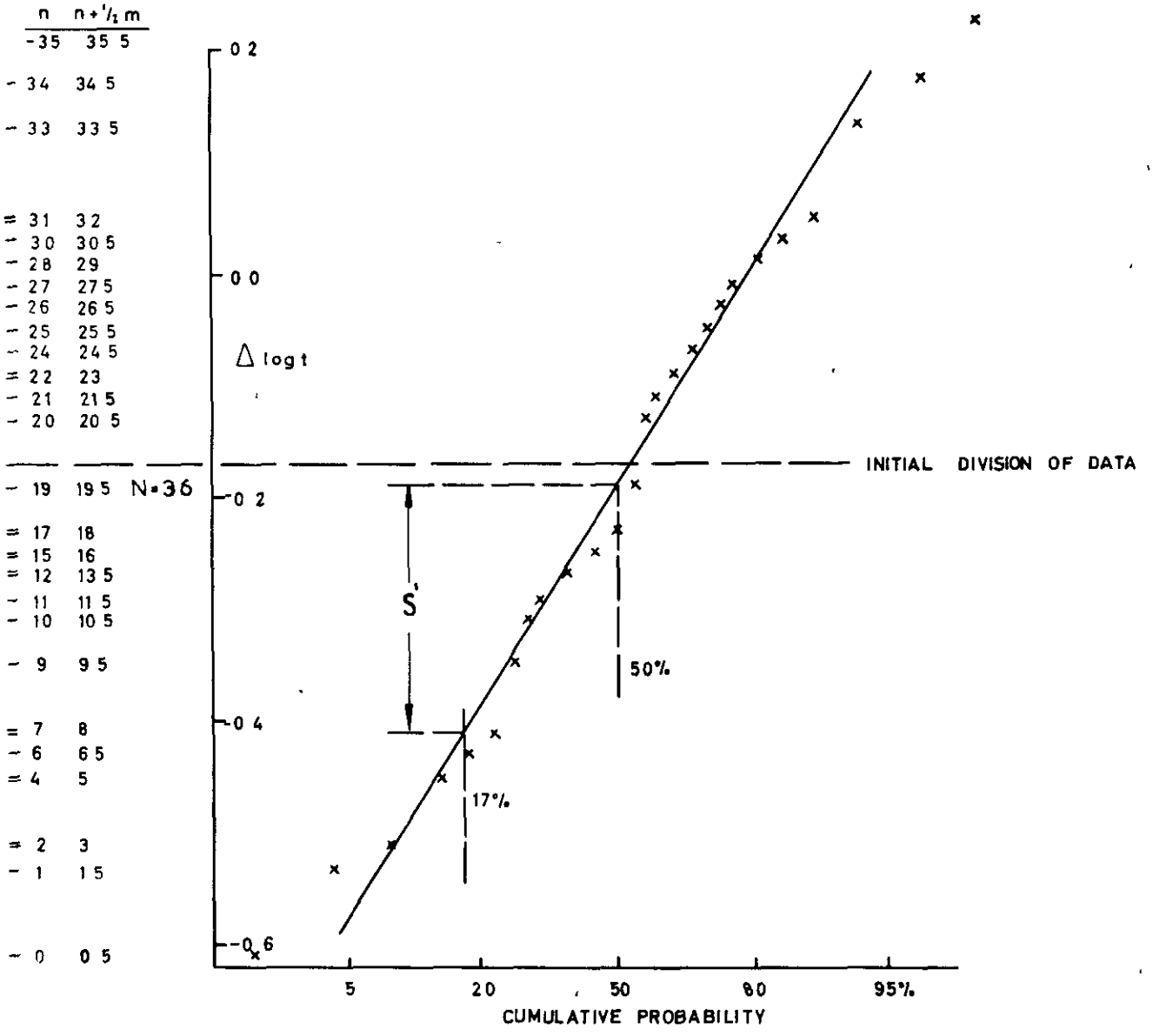

SECOND EXAMPLE-DIRECT PLOT OF SCATTER DATA

FIG 35

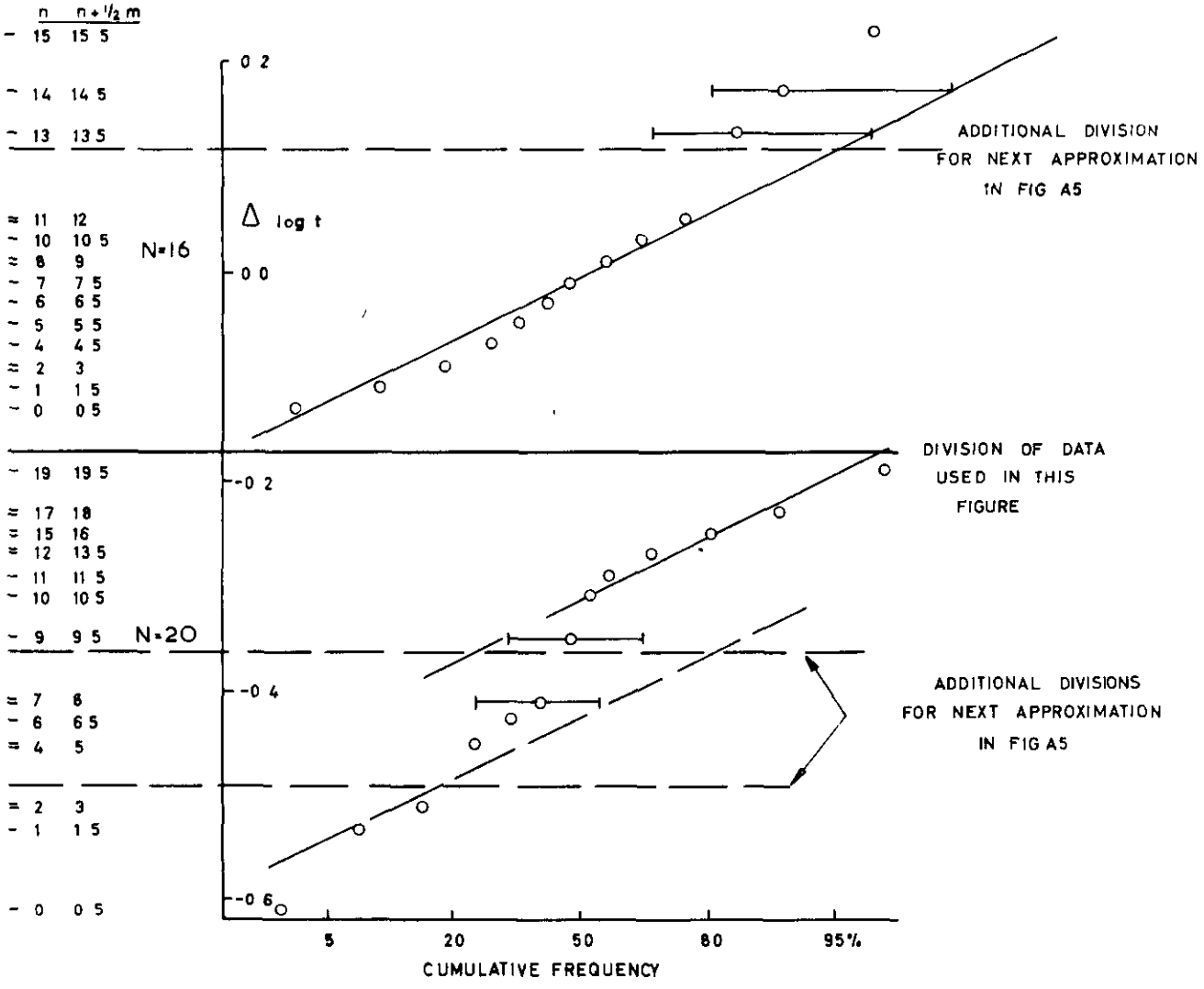

SECOND EXAMPLE - INITIAL DIVISION INTO TWO COMPONENTS

FIG 36

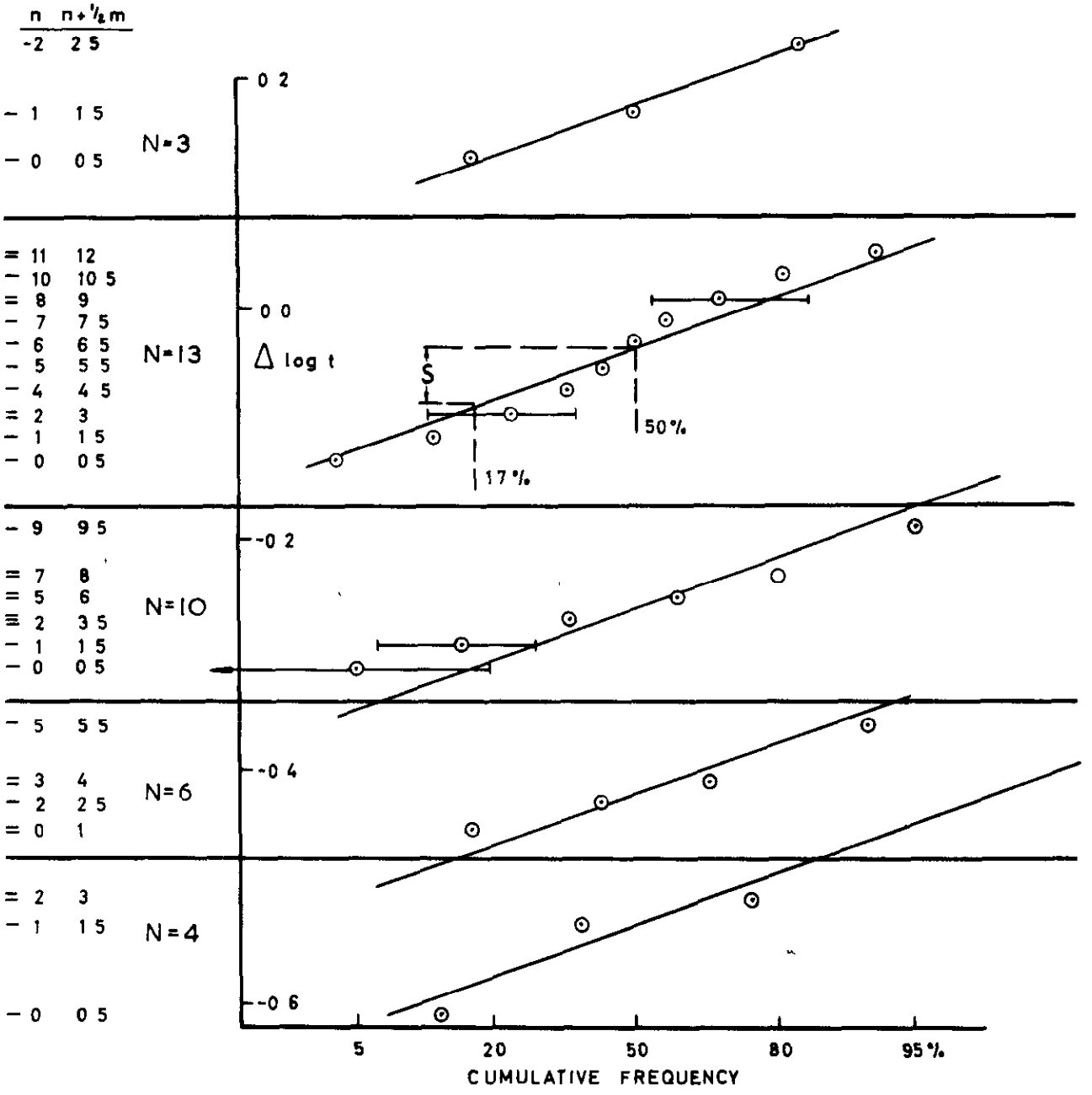

FINAL DIVISION INTO FIVE COMPONENTS

Printed and published by
HER MAJESTY'S STATIONERY OFFICE

To be purchased from
49 High Holborn, London W C 1
423 Oxford Street, London W 1
13A Castle Street, Edinburgh 2
109 St Mary Street, Cardiff
Brazennose Street, Manchester 2
50 Fairfax Street, Bristol 1
35 Smallbrook, Ringway, Birmingham 5
7 - 11 Linenhall Street, Belfast 2
or through any bookseller

Printed in England

S O Code No. 23-9017-35